Faculty of Science and Technology

MASTER'S THESIS

Study program/ Specialization: Petroleum Technology	Spring semester, 2011 Open access
Writer: Steven Ripman	………………………………………… (Writer's signature)
Faculty supervisor: Kjell Kåre Fjelde External supervisor(s): Jan Helge Haugen, Statoil	
Titel of thesis: Casing Wear in Multilateral Wells	
Credits (ECTS): 30	
Key words: - Actual Wear vs Simulated Wear - MLT Wells - Wear Factor - Maximum Scenario	Pages: ………101………… + enclosure: ………9… Stavanger …15.06/2011…… Date/year

Acknowledgement

The work done in this report, which is a result of my diploma thesis, concludes the 5'th and final year of my Masters degree in Petroleum Engineering at the University of Stavanger.

The thesis has been accomplished in collaboration between the Institute of Petroleum Technology at the University of Stavanger and Statoil with the contribution of the drilling engineers at Grane who discussed and suggested the thesis subject.

I greatly appreciate the help of my supervisors Kjell Kåre Fjelde at UiS and Jan Helge Haugen at Statoil who have given me feedback and kept me focused in my research. I would also like to express the importance of the good working environment experienced at the Grane department which has made a huge difference in terms of accessibility of the staff, and their willingness to engage in dialogue with a student. In short, the experience has been nothing but positive.

I hereby declare this work to be solely my own and in accordance to the regulations of UiS.

UiS, Stavanger, June 2011-06-09

Steven Ripman

Figure List

Table List

Summary

According to the engineering community at Statoil it's a big challenge to simulate the correct wear in a well prior to it being drilled based on the simulation program DrillNet [1] (formerly known as Cwear). Wear factors have repeatedly shown to correlate poorly with actual wear seen in the well after it's been logged. With today's tools and practice, it's very difficult to assess how far it's possible to operate within acceptable casing wear, especially in MLT wells. It is therefore a need to systemize the available data and drilling parameters. DrillNET can simulate casing wear based on real data and thereby back calculate a wear factor by adjusting it to fit the actual wear seen on the USIT log. Even though this is a time consuming task it may alter the intended casing program to a more simplified outcome or on the other hand it might point out a section of casing which needs to be strengthened based on the simulation results.

DrillNET has a database of wear factors which propose to use a value of 5 for the P-110 steel casing, which covers most of the interval of interest with regards to casing wear on Grane, and 25 for the chrome intervals which are added where corrosion might be an issue. After having simulated and back calculated the wear factor for four different MLT wells, the database value of 5 for the P-110 steel might not always be adequate while the value of 25 for the chrome sections seems to be sufficient.

When looking at the actual and simulated wear one can clearly see that the simulated wear is dictated by the peaks of the actual wear graph. These peaks may appear unpredictable where there is no increase in the dogleg severity or other parameters which might indicate increased wear. This makes it hard to account for when simulating in the planning process and it might push the wear factor up to a conservative value if there aren't any high value wear peaks. Another observation is made when evaluating the amount of time the bit has been rotated down hole inside the casing which is the most crucial wear parameter. Well G-13 has almost twice the amount of rotational hours compared to well G-07 even though they are approximately the same length. Since the wear factor controls the wear efficiency the initial idea was that G-13 would have a higher wear factor than G-07, which proved to be untrue in this case. The fact that the wear decreases with a bigger wear groove due to a larger contact area may help to explain why the additional hours of rotation seem to affect the wear less.

The interval found in this thesis suggests that the wear factor lie between 1,6 and 6 for the P-110 steel casing and between 7 and 21,5 for the chrome intervals. The specific value to choose in these intervals when doing a simulation is strongly dependent upon the individual wells and the somewhat unpredictable wear peaks.

Introduction

More and more wells are now drilled in the ERD (extended reach drilling) category and wellbore trajectories often follow highly-deviated, S shaped, horizontal, short radius and multilateral paths. The number of rotating hours required to drill these wells has risen as measured depths have increased and well paths have become more complicated. The use of top drive systems and the ability to back ream while rotating is now common practice, and the search for oil and gas has also moved into ever deeper waters. As all these conditions became more common, operators began to notice unacceptable levels of wear on casing or even experiencing holes worn through the casing.

Operators, recognizing the operational threat to the integrity of their wells and the associated economic and environmental impact, have started studying casing and riser wear issues [2]. There is potential for significantly reducing the risk and cost of high-angle and horizontal wells through the development of casing wear computer models which accurately predict casing wear in these wells. But like for any other computer model the output is only as good as the input which means that the research done on beforehand has to be accurate and able to represent the scenario at hand.

The computer model which is to be used in this thesis is DrillNet which is based on the work done by Maurer Engineering and their DEA-42 project called "Casing Wear Technology". There are certain things a computer model cannot take into account, amongst them the rate at which the steel is worn away, more commonly known as the wear factor. Even though this DEA-42 project has the most extensive database (which is available in DrillNet) of wear data available within the industry, it does not mean that specifying a specific casing type implies a specific wear factor.

Because the wear factor for a given well tends to be unique since no two wells are alike, the motivation behind this thesis is driven by the uncertainty in what wear factor to apply and how this can be investigated.

The thesis can be divided into three parts with regards to the actual simulation work;

1. Pre-simulation - Gathering all the input and developing a workflow
2. Simulation - Performing the simulation and producing both the actual and simulated wear plot.
3. Post-simulation – Extracting information from the simulation results and discussing the observations seen from the results and its implications.

1. Background on Wear

1.1 Definition of Wear and Casing Wear

This chapter defines the mechanical action of wear and describes how a model can help to simulate expected casing wear in a well that is planned to be drilled.

In material science, wear is the erosion of material from a solid surface by the action of another surface. It is related to surface interactions and more specifically the removal of material from a surface as a result of mechanical interaction wear. This definition along with the model used in this thesis does not include the reduction in dimension when plastic deformation occurs and impact wear where there is no sliding motion. It also fails to include cavitation and corrosion which will give an additional degree of wear. If this needs to be included it can be combined with separate calculations that consider these issues.

In directionally drilled holes the drillstring tension forces the rotating tool joints against the inner wall of the casing for extended periods of time. As the rotating tool joints grinds against the casing wall, erosion of both the tool joints and casing creates material from the solid surfaces. The wear grade will be influenced by a number of different factors such as RPM (especially the total number of revolutions), mud properties, load variations, dogleg severity and so on [2]. These different parameters and additional ones will be discussed later in this chapter.

1.2 The Effect of Casing Wear and its Consequences

Although casing wear has been a problem for many years, published literature on the subject isn't abundant. Therefore the consequences may not be well documented and the risk may well be neglected at times.

As a result of the erosion of the casing wall, the geometry of the casing tubular will change accordingly. When the axial force experienced by the drillstring holds the rotating tool joints against the inner wall of the casing, the erosion will reduce the wall diameter.

Different aspects that affect the consequences include:
- Integrity of the well
    - Depending on how large the reduction in wall diameter is, both burst pressure and collapse pressure will be reduced. Depending on the severity of the pressure rating reduction, the well may be abandoned, either by not recognizing the problem before it's too late or by recognizing the problem before a catastrophe might occur [3].

- Well life
  - Wear shortens service life of risers and flex joints and reduces burst and collapse strength of casing strings.
  - Since platforms have limited slots available for drilling it is necessary to re-use slots in order create new sidetracks and multilaterals. For this to be a viable option the amount of casing wear must be considered. When completing drilling a well one must be sure that the amount of casing wear doesn't exceed a certain limit that prohibits the possibility of safely completing a future re-entry.
- Cost
  - The economic loss to the industry is difficult to calculate. Costs might be calculated by adding together the industry-wide cost of early replacement of assets, lost rig time, patching casing, squeeze jobs relating to casing wear, running extra casing strings to seal a wear area and environmental cleanup and well control costs [4].

1.3 Types of Casing Wear

The main wear forms are:
- Adhesive wear
- Abrasive particle wear
- Polishing wear

It's important to recognize that these three wear forms can be present all at once but in different parts of the well.

1.3.1 Adhesive Wear

Adhesive wear can be described as plastic deformation of very small fragments within the surface layer when two surfaces slide against each other [5]. The result is displayed in Figure 1.
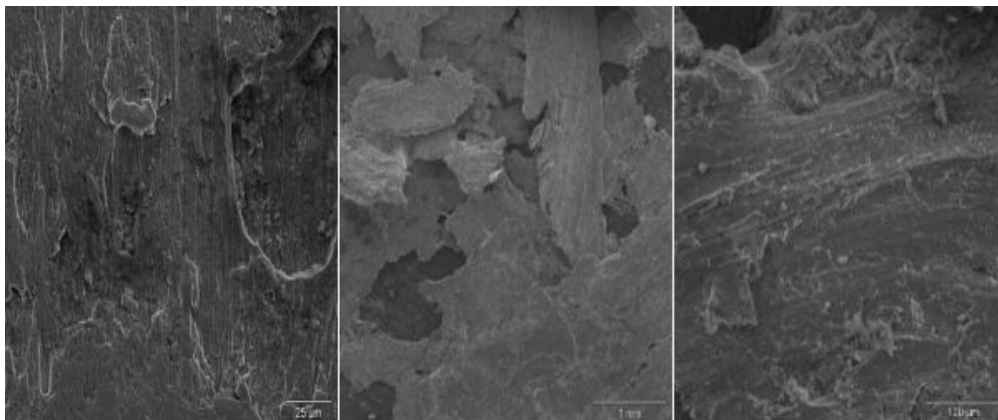
Figure 1. Micro morphology of Adhesive Wear [6]

This wear mechanism is produced by the formation and subsequent shearing of welded junctions between two sliding surfaces and has a threshold pressure of about 200 psi [5]. Lubricating films, oxide films etc. reduce the tendency for adhesion to occur which cause adhesive wear to be a rare phenomenon when drilling with oil based mud. If experienced, the best way to prevent it is by raising the hardness and thereby preventing microplastic distortion of the surface.

1.3.2 Abrasive Particle Wear

Abrasive wear occurs when a hard rough surface slides across a softer surface. There are two types of abrasive wear; two body and three body. Two body wear is referred to as machining wear while three body wear is referred to as grinding wear.

- Machining wear - When sharp particles of crushed tungsten carbide get imbedded in the hardbanding (see chapter 4), machining wear occurs. The casing is prone to machining when [6];

  1. The casing experiences a high lateral force
  2. Surface of tool joints are welded with tungsten carbide (see chapter 4)
  3. There is a non-abrading agent between the tool joints and casing surface

The particles or the opposing surface, act as cutting tools, cutting the metal in long chips as seen in Figure [2].
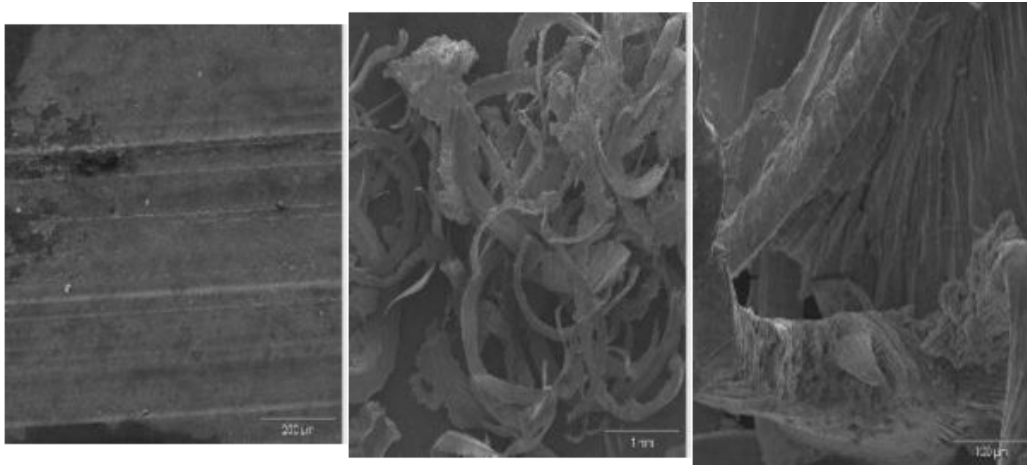
Figure 2. Micro morphology of Machining Wear [6]

- Grinding wear - Grinding wear is a result of solid particles which are found in mud, sand and cuttings, which roll between the casing and the tool joint and create a fine powder of steel particles. The relatively small contact area between the tool joint and casing will cause high contact pressures because of the large lateral force. This

high pressure will cause high contact loads on the abrasive particles, allowing them to exceed the strength of the steel and cause fracturing of the casing surface at localized points [6]. This is illustrated in Figure [3].
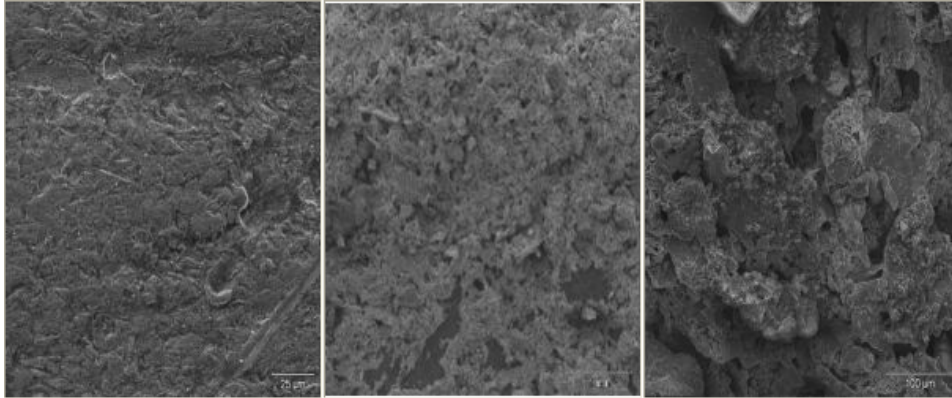
Figure 3. Micro morphology of Grinding Wear [6]

1.3.3 Polishing Wear

When the very fine particles of steel powder is created when rolling between the casing and tool joint it will blend in with softer material and produce a smooth, polished surface. The casing wear rate caused by polishing is very low and happens over a longer period of time [6]. As shown in Figure [4], polishing wear doesn't reveal any clear signs of wear on the casing surface.
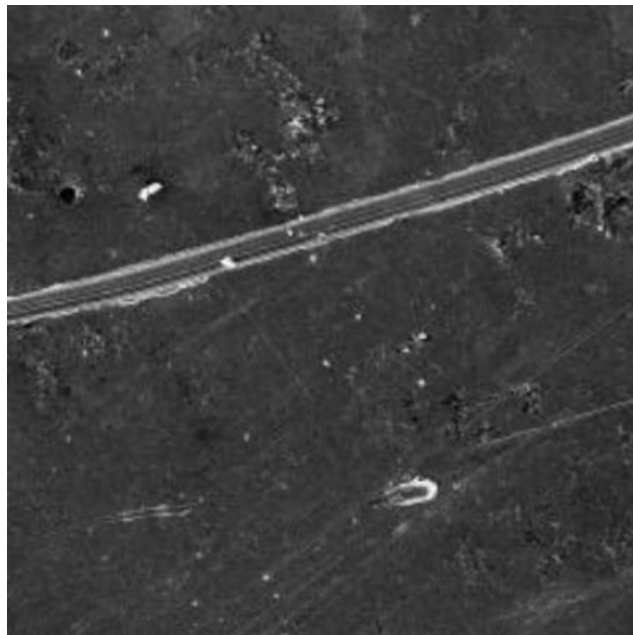
Figure 4. Micro morphology of Polishing Wear [6]

1.4 Wear Debris

In wells where there is a significant amount of wear is expected, magnets are placed in the flow line before the mud passes through the shakers. The debris will then be caught by the magnets and the amount will help indicate the actual amount of wear. There is no guarantee that all the metal will stick to the magnet as it can get stuck in the hole or manage to just flow by it. Some of the metal will not originate from the casing and this will influence the interpretation of the actual casing wear from debris collection. Determining the amount of casing wear is not the only reason to collect the wear debris alone. If the debris is pumped back in the hole it can cause failure of down hole tools when passing through the bottom hole assembly and also cause additional wear of the casing when flowing back up the annulus.

An additional reason for collecting the wear debris is to determine the shape of the metal shavings which gives a good indication of which wear mechanism that has dominated. If shavings are in powder form, as seen in Figure [3] then the wear is attributed to grinding or polishing; if shreds of metal are observed, then the wear mechanism is either adhesive or machining, as seen in Figure [1] and [2]. Adhesive wear gives flakes whilst machining wear gives thinner strands of material.

1.5 Casing Wear by Rotation

Rotation, tripping and wireline running results in the generation of crescent shaped wear grooves (key seating) in the inner wall of the casing as seen in Figure [5]
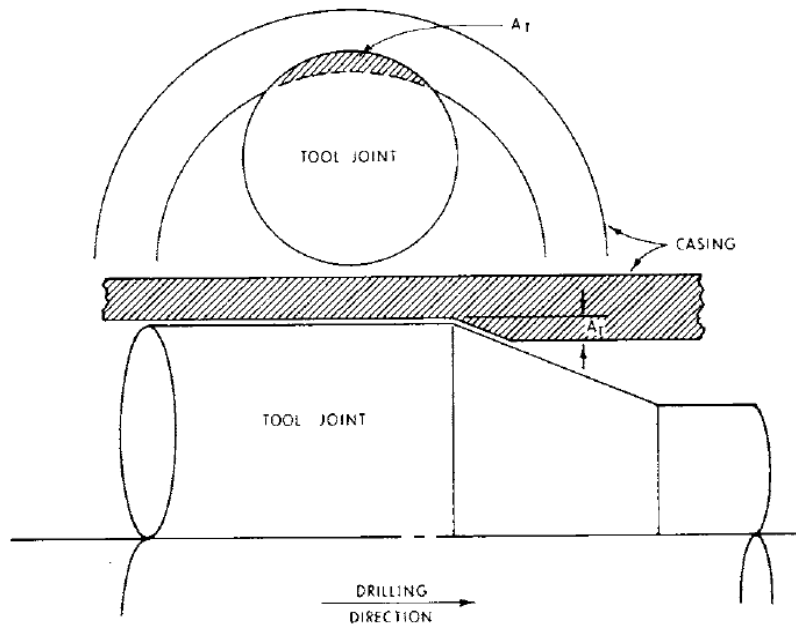
Figure 5. Crescent Wear Groove [3]

The outer curve of the crescent corresponds to the outside diameter of the thickest part of the tool joint.

During initial contact between casing and drill pipe tool joint, the contact area is very small, contact pressures are high, and wear rates (rates of penetration of tool joint into casing) are high. Under these initial conditions with such a high contact pressure and relatively rough surface, the film formation is disrupted which reduces any effect that lubricants are designed for. The high contact pressure gives a high friction coefficient, especially in unweighted and low density mud. When the wear groove starts to take form the friction coefficients stabilizes at a lower value due to a larger contact area [3].

1.5.1 Wear Volume

Models that are being used to predict casing wear by the industry assume that the metal volume which is worn away is proportional to the frictional energy transmitted to the casing by a rotating tool:

Volume removed per foot = Frictional work per foot/specific energy   Eq. 1.1

Specific energy is the energy required to remove one cubic inch of steel.

Frictional work per foot = Lateral load per foot*friction factor*sliding distance   Eq. 1.2

Combining "friction factor" and "specific energy" into a "wear factor":

Wear factor = Friction factor/specific energy   Eq. 1.3

then,

Volume removed per foot = Wear factor*normal force per foot*sliding distance   Eq. 1.4

Here "sliding" distance is the total distance where there is contact between casing wall and either drillpipe collar, coiled tubing or wireline. This distance can be expressed as:

Sliding distance = π * tool joint diameter * rotary speed * tool joint contact time   Eq. 1.5

Where the tool joint contact time is defined as:

Tool joint contact time = (drilling distance * tool joint length) / (rate of penetration * drill pipe joint length)   Eq. 1.6

Combining these equations the volume of casing wall removed per ft (in in.^{3}/ft) in a given amount of time is mathematically expressed as [3], [7], [8] :

$$WV = \frac{WF \times LL_{dp} \times \pi \times D_{tj} \times 60 \times RPM \times t}{ROP}$$

Eq.1.7

Where:

WV = Wear volume [in.^{3}/ft]

WF = Casing wear factor [inch^2 /pound force]

LL_{dp} = Lateral load on the drill pipe per foot [in lb/ft]

D_{tj} = Outer diameter of tool joint [inch]

RPM = Rotations per minute

ROP = Rate of penetration [meters per hour]

t = Rotating time [hours]

Although tool joint loads are around 20 times larger than the drill pipe loads, the tool joint lengths are only 1/20 as long as the drill pipe lengths, effectively cancelling one another out. This defends the fact that wear is calculated using drill pipe lateral load instead of tool joint lateral load.

To use the model to predict casing wear for a drilling operation normal force per foot is computed from the well path geometry, drillstring configuration, and drilling fluid density. Knowing the drilling parameters (ROP, RPM, distance drilled) the frictional work done to each foot of the casing is calculated. Combining this information with the wear factor determined from laboratory tests allows the volume removed per foot to be computed. Knowing the wear volume per foot, the depth of the wear groove can be computed [9] .

1.5.2 Depth of Casing Wear Groove

The relationship between the wear volume, WV, and the wear depth, h, equals [10];

$$WV = 12(\beta r^2 + R(s + h)\sin \alpha - \alpha R^2)$$

Eq. 1.8

Computing the angles α and β can be done with geometry using the dimensions and angles illustrated in Figure 6;
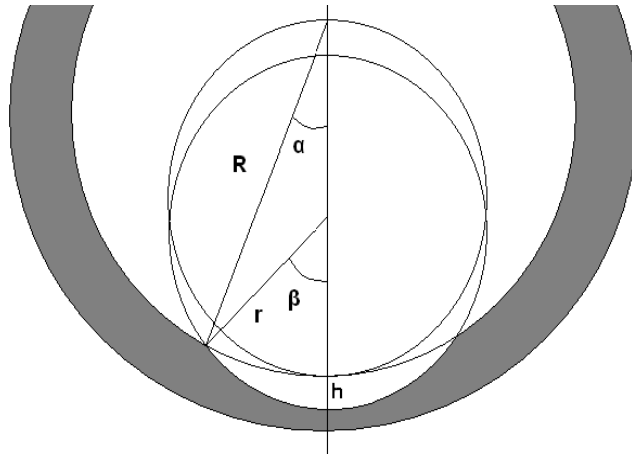
Figure 6. Depth of Wear Groove [8]

Where;

WV = Wear Volume [in.^{3}/ft]
h = Wear Depth [in.]
R = Casing Inner Radius [in.]
r = Tool Joint Outer Radius [in.]
s = Offset Distance = R - r

The angles β and α are in radians and are expressed as:

$$\alpha = \arcsin\left[\frac{1}{2R(s+h))}\sqrt{2\left[R^2(s+h)^2 + r^2R^2 + r^2(s+h)^2\right] - \left(R^4 + r^4 + (s+h)^4\right)}\right] \quad \text{Eq. 1.9}$$

$$\beta = \arcsin\left(\frac{R\cdot\sin\alpha}{r}\right) \qquad \text{Eq. 1.10}$$

2 Casing Wear by Tripping

The drilling activity is the process which accumulates the most wear, by far, compared to the other wear processes which includes tripping in and out of the well with drill pipe, coiled tubing and wireline [3]. Notice that it's only while using drill pipe that a tool joint is involved, both wireline and coil tubing have the same outside work string diameter.

During tripping, when a defined point on the working string slides across the casing wall, there is a frictional work done which is equal to:

$$W = \mu \cdot LL \cdot s \qquad \text{Eq. 2.13}$$

Where:

W = Frictional work per foot [ft-lb]
μ = friction coefficient [dimensionless]
LL = lateral load imposed on the casing wall at the point of wear [lbs]
s = sliding distance [ft]

The wear factor was previously defined as Eq. 1.1;

Volume removed per foot = frictional work per foot/specific energy

This can again be defined with symbols as;

$$WV = \frac{W}{\varepsilon} \qquad \text{Eq. 2.14}$$

Where:

ε = Specific energy [ft-lb/in./ft]
WV = Wear volume [in.^{3}/ft]

The wear factor, $WF = \dfrac{\mu}{\varepsilon}$, can be expressed as $\varepsilon = \dfrac{\mu}{WF}$ so that the wear volume becomes;

$$WV = \frac{\mu \cdot LL \cdot s}{\dfrac{\mu}{WF}} = LL \cdot s \cdot WF \qquad \text{Eq. 2.15}$$

3 Field-Measurable Parameters Affecting Casing Wear

To predict the rate of casing wear it is necessary to express the rate of wear in terms of field-measurable parameters. These parameters include [2]:

- Lateral load
- Well Survey - Dogleg severity
- Mud composition
- Drill pipe wearing capability
- Casing wear resistance
- Accumulated rotating time and RPM (rotations per minute)

3.1 Lateral Load

Computing the normal force per foot is the key to successful prediction of casing wear. This is evident from looking at the equation for wear volume, Eq. 2.15. Normal force per foot is the product of twice the drillstring tension load and the sine of one half of the dogleg severity (section 3.2), in degrees per foot [9] . The forces in this equation are illustrated in Figure 7.
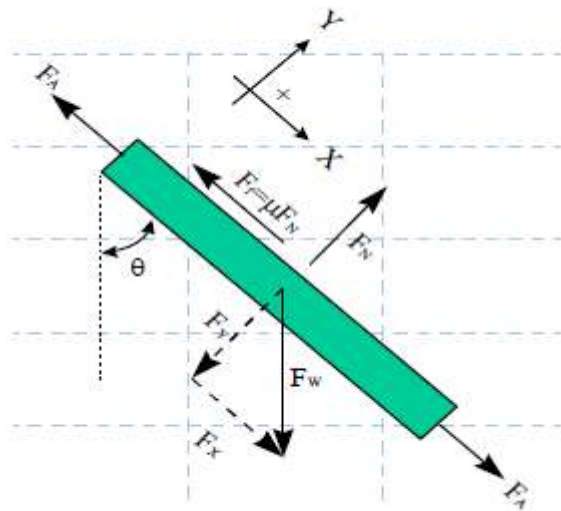
Where:

F_n = Normal force

F_y = Forces in y-direction

F_w = Gravitational force

F_A = Axial force

F_r = Frictional force

Figure 7. Forces acting on the drillstring [11]

Casing wear predictions usually start with a measured or expected dogleg, and for a given dogleg the lateral load is, as stated above, defined as;

$$LL = 2T \sin\left(DLS/2\right)$$
<div align="right">Eq. 3.16</div>

Where:

T = Buoyed weight of drillstring load below point of wear [lbs]
DLS = Dogleg severity [degs./ft]
LL = Lateral load [lbs]

When drilling there is a weight on bit, WOB, applied and the drillstring load must be corrected for it by subtracting the WOB. The drillstring tension at the wear point, disregarding the friction, then equals:

$$T = \left(w_{DS} - WOB\right)\sin\gamma$$
<div align="right">Eq. 3.17</div>

Where:

w_{DS} = Buoyed weight of drillstring below wear point [lb]
γ = Deviation Angle from Vertical

Since the tension of the drillstring is at its highest at the surface, the effect of a shallow dogleg is then much more severe than a deeper one.

3.2 Well Survey - Dogleg Severity

Since the normal force per foot has such an impact on the prediction of casing wear it's crucial that the dogleg severity calculations are as accurate as possible since they directly impact the normal force calculations (see Eq. 3.16).

While drilling, a survey is usually taken at each stand which means around every 30 meters. A survey includes inclination and azimuth data for the given survey point. At each of these points, or survey stations, the direction of the actual well path being drilled is specified by an inclination and an azimuth angle of the tangent to the well path at that station. The well path is assumed to consist of a series of circular arcs or straight lines, depending on the method of calculation, and successive survey stations are connected by one of these arcs or straight lines. When there is a change in direction (azimuth or inclination) and a survey is performed, the dogleg angle between the two survey stations can be calculated by the directional angles shown in the coordinate system, Figure 8, below [9];
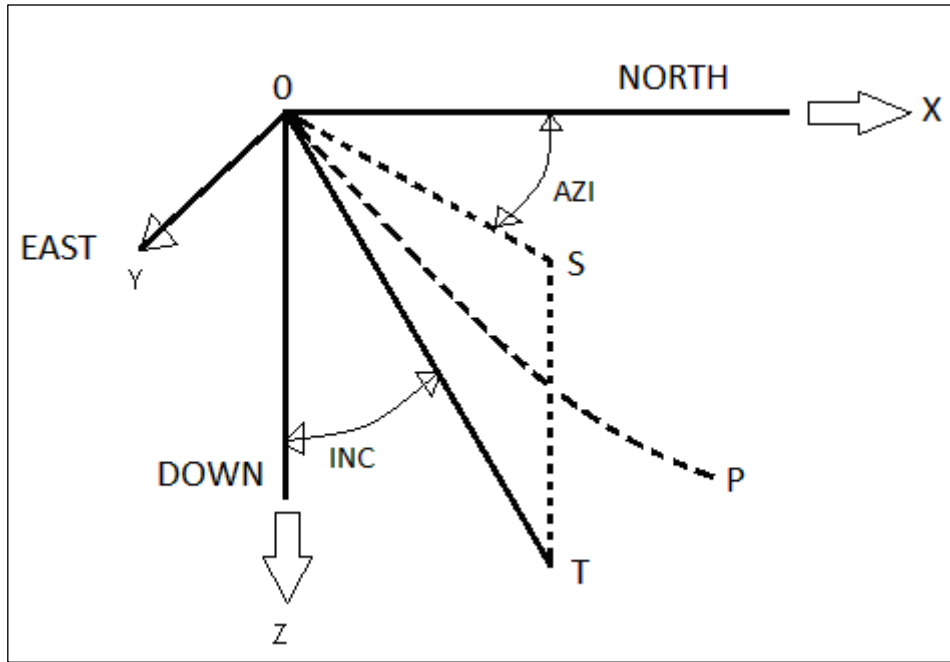
Figure 8. Well Survey – 3D Coordinate System and Direction Angles

The segment of the well path, OP, passes through the origin and the straight line, OT, is tangent to the well path at point O. The angle between points ZOT is the inclination angle, INC, and is defined as the deviation angle from vertical. AZI is the azimuth angle and is defined by the points SOX. It represents the deviation angle from true north with a clockwise positive value. The direction cosines η, ψ, and ω, of the tangent OT are defined as:

$$\eta = \cos(\angle TOX) = \sin(\angle INC) \cdot \cos(\angle AZI)$$
Eq. 3.18

$$\psi = \cos(\angle TOY) = \sin(\angle INC) \cdot \sin(\angle AZI)$$
Eq. 3.19

$$\omega = \cos(\angle TOZ) = \cos(\angle INC)$$
Eq. 3.20

Now the difference in direction, $\Delta\phi_{i,j}$, between the two survey points, i and j, along the well path can be defined in terms of the direction cosines of the tangents at these survey points;

$$\cos(\Delta\phi_{i,j}) = (\eta_i \cdot \eta_j) + (\psi_i \cdot \psi_j) + (\omega_i \cdot \omega_j)$$
Eq. 3.21

The dogleg severity can then be computed as shown in Eq. 1.13 by dividing the difference in direction, $\Delta\phi_{i,j}$, by the measured depth distance between the two survey points.

$$(DLS)_{i,j} = \frac{100}{L_{i,j}} \Delta\phi_{i,j}$$
Eq. 3.22

Where:

$(DLS)_{i,j,a}$ = Apparent (measured) dogleg severity between stations i and j [deg./100 ft]

$L_{i,j}$ = Measured depth from station i to station j [ft]

$\Delta\phi_{i,j}$ = Difference in direction from station i to station j [deg.]

As seen from Eq. 3.22 it's important that the measured depth from station i to station j is as correct as possible. If there is an offset between the measured depth of the actual dogleg interval and the apparent dogleg interval, the correct value of the dog leg severity is obtained by utilizing the ratio between the two intervals, with the apparent dogleg interval as the denominator, and multiplying this with the original Eq. 3.22 [9] . The difference of these two well paths is illustrated in Figure [8] and in the example below;
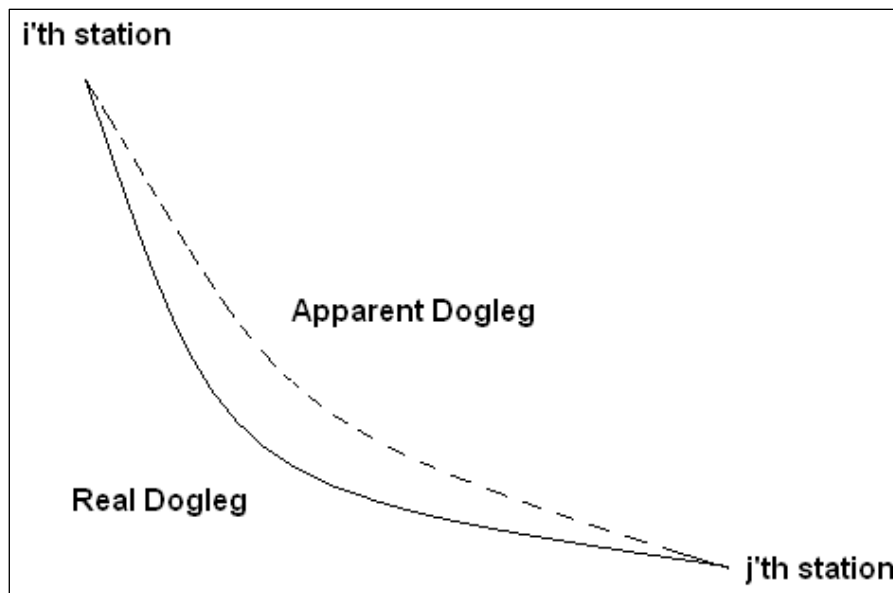
Figure 9. Real Dogleg versus Apparent Dogleg [9]

For example, if $\Delta\phi_{i,j}$ = 6°, $L_{i,j}$ = 100 ft, and the actual length of the dogleg section is 80 ft, then;

$$(DLS)_{i,j,a} = 6°/100\,ft \text{ , and } K = \frac{100}{80} = 1,25$$

And the real dogleg severity, $(DLS)_{i,j,r}$, becomes;

$$(DLS)_{i,j,r} = 1,25 \cdot 6 = 7,5°/100\,ft$$

The value of the K factor will never be below 1,0 since the apparent dogleg severity is always equal to or less than the real dogleg severity, it will always be equal to or less than the real dogleg severity, making the predicted/simulated wear less or equal to the actual wear. If the correct wear factor is used, the casing wear is proportional to the dogleg severity which means that the calculated value will never be greater than the observed value. When the correct wear factor is used, apparent dogleg severity is the only value an engineer has available to make casing wear predictions, but it's only after the well has been logged and real dogleg severity has been calculated and compared, that the effect of the predictions can be compared to the actual outcome [9].

There are two types of doglegs [10], either a gradual type or an abrupt type. In gradual doglegs only the tool joints contact the casing and the wear is uniformly distributed along the dogleg as drilling progresses. An abrupt dogleg is characterized by both tool joint and drill pipe contact along a short length because of an abrupt change in inclination and/or azimuth. The latter type of dogleg is the most critical and can often go undetected if survey measurement points down along the well are spaced to far apart.

There are many methods used calculate the well path trajectory and dogleg severity from well survey data, the dogleg severity determined by the method above assumes that direction change is uniformly distributed along the path from station i to j

3.3 Mud Composition

Wear and friction are the result of a complex tribological process that takes place when there is contact between the drill pipe tool joint and the casing, with mud as the intermediate medium. The two types of drilling fluids, water and oil based, yield a significant difference with respect to lubricity and protection against casing wear. The properties of the oil in the oil based mud causes the two steel surfaces to be separated by an oil film and thereby reducing the torque and drag observed. This makes the oil based mud the obvious choice when drilling a high angle, long reach well.

Various mud composition factors that affect casing wear includes; mud density, type of weighting material and the addition of several mud additives and salts, lubricants, and sand and silt. In an SPE paper [12] conducted by Shell E&P, these different factors have been discussed on the basis of thorough laboratory experiments. Results from small-scale tests have shown to be non-representative and so Shell has conducted them in full scale test machines. The general outcomes will be summarized below;

3.3.1 Effect of Weighting Material Type

The results of tests with various weighting materials show removal of casing tool-joint material (tests done on rough tool joints, i.e. not smooth) by particles present in the contact area. The

rapidness of casing tool-joint removal increases with particle hardness in the series barite, iron oxide, and quartz. Since chalk and drilled solids have relatively small particle sizes compared to the weighting materials, it reduces the film thickness which acts as a protective layer between the tool joint and casing, thereby increasing adhesive wear. All weighted mud tested clearly showed less severe wear compared with unweighted mud. When using mud with the weighting material barite with densities ranging from 9.2 to 19.2 lbm/gal (1000 to 2300 kg/m^3), the unweighted mud was found to cause severe adhesive damage. The reason for this is that barite forms a protective layer between the two steel surfaces.

3.3.2 Effect of Additives

Different types of additives were added such as lignosulfonate, starch, CMC, sulfonated lignite, salts and various types of lubricants, to both weighted and unweighted mud. For the weighted mud there was no evidence of change in wear by either additives or lubricants. The following effects were seen for unweighted mud:

- All the commercially available lubricants tested partially prevent adhesive wear.
- The addition of diesel (10 vol. %) or 1-mm (0.04-in.) diameter glass beads had no effect on wear. Since diesel doesn't contain any reactive components it's unable to create a chemically bound lubricant film. And because of the large size of the glass beads they weren't able to reach the contact area and affect the wear.
- When salt was added there was evidence of reduced casing wear because salt accelerates corrosion. The corrosion creates an outer layer which partially prevents adhesive wear.
- The polymeric mud additives (lignosulfonate, starch, CMC, sulfonated lignite), used to control the viscosity, reduces the casing wear to some extent but is clearly less effective than the lubricants.
- G-Seal was primarily designed to act as a bridging and sealing agent in permeable formations. Its coarse sized is able to seal off pore throats effectively and its spherical form acts as a bearing on the low side of the hole which the drillstring can rotate on, instead of the casing. The rotational energy exerted by the drillstring onto the casing is then instead absorbed by the graphite spheres and distributed among them and their rolling reaction, reducing the torque, drag and wear. The size of these graphite spheres depend on the pore throat size and can range from around 40 to 2000 microns.

3.3.3 Effect of Sand and Silt

Minimal or no wear was observed when small quantities of sand and/or silt (2 to 4 vol. %) was added to the weighted mud. The reason for this is that it gets diluted in the weighting material and loses its effect. In unweighted mud an occasional increase in the friction factor was observed when sand reached the contact area but no overall wear rate was observed.

4 Hardbanding of Drill Pipe Tool Joints

Hughes Tool Company introduced hardbanding into the industry as early as the 1930's [13]. As with casing, the drill pipe also experiences excessive wear by rotation. Originally, hardbanding was introduced to limit the wear of drill pipe and other down hole tools from abrasive wear [14]. This has been an area of interest for many engineers, especially since wells are getting longer and more complex, giving a rise in the required rotating hours.

The cost of new drill pipe has been, at times, above US$100/ft. Combine this with increased drilling activity and a delivery time of up to a year; the cost of pipe is suddenly a significant part of the expenses. As a result of this, concerned pipe owners, drilling contractors and tool companies wanted to prolong the life of down hole equipment and pipe, which lead to the application of tungsten carbide as the most common method of hardbanding tool joints. This solution proved to be a concern with regards to casing wear [2]. As the length of the wells increased, the evidence of casing wear increased with it. Because of this, new hardbanding materials were created and tested but without big success up until 2000, which made the tungsten carbide the preferred hardbanding method until then [13].

The first hardbanding that was developed in the 1930's was created primarily to protect the drill pipe tool joints from wear in open hole drilling. Sintered tungsten carbide particles were dropped into the heated liquid metal that forms the tool joint and applied in a raised condition to prevent that the entire tool joint contacts the casing or open hole. For a period of time this was a successful way of dealing with drill pipe wear but as the wells became deeper and more complex, the metal matrix holding the tungsten carbide particles got worn away and as such exposed the particles to the casing. This led to excessive casing wear and the industry was now forced to look at new ways of hindering this wear and experimented with different shapes and sizes of tungsten carbide particles, but with no success [14].

Hughes Tool Company then developed a tool joint that had a groove machined into it so that the hardbanding could be applied flush with the rest of the tool joint which seemed to improve the amount of casing wear considerably. But, as the previous solution, this only lasted until the wells evolved into even deeper and more complex holes and the effect of having a longer contact length became evident in the amount of torque and drag experienced. Hughes Tool Company then tried to machine an even deeper groove into the tool joint so that two layers could be applied, one layer of tungsten carbide hardbanding and a second layer of mild steel on top, flush with the tool joint O.D [14]. This worked until the soft layer of steel got worn away and the tungsten carbide was exposed. Since hardbanding with tungsten carbide was such a failure with regards to casing wear, the use of it was abandoned altogether and drill pipe with no hardbanding at all became the preferred option. What the industry did not realize at the time was that a drill pipe without any hardbanding caused as much casing wear as the tool joint with tungsten carbide. This severe adhesive wear, which occurs when to surfaces with similar

hardness slides against each other, was enough to wear out the drill pipes at an alarming rate. Even though the price of drill pipe was low and the delivery time short at that time, it forced the industry into developing new ideas and different types of alloys was the answer. The evolution of different alloys is still an ongoing process and as long as wells become longer and longer it will continue to evolve.

The standard today is to make us of so called "casing friendly hardbanding" which typically protects the casing more than it protects the drillstring. This kind of hardbanding reduces the friction coefficient which effectively reduces the amount of wear and at the same time significantly reduces the drag and torque while drilling and tripping in and out of the hole [13].

There are now many different types of hardbanding materials on the market but there are only a few that sufficiently protects the casing and the drill pipe at the same time [14] . Statoil has co-operated with Trio Oiltec Services in developing new alloys such as OTW-12 and OTW-16 which are now approved and used in many Statoil wells. This alloy produces a microstructure which exerts an overall resistance to combined wear by gouging, abrasion, erosion, heavy impact and pressure at ambient temperatures.
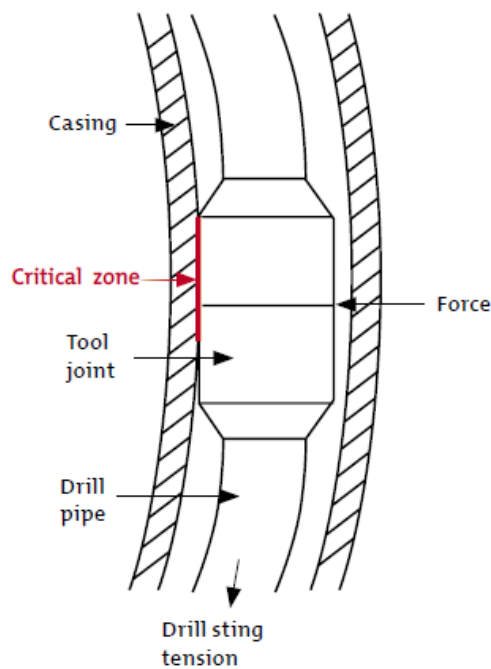
Figure 10. Critical Zone of Wear [15]

5 Casing Design in Multilateral Wells

How a well is designed with respect to the casing and its weight, section length and pressure rating greatly impacts the amount of wear that can be tolerated. Whenever wear is present it will reduce the initial pressure rating of the casing because of the wall thickness reduction. Because of this it's important to have done calculations on worst case scenarios regarding burst, collapse and tensile forces so that the right design can be applied.

The wells considered in this thesis consist only of multilateral wells that have a 9 5/8" x 10 3/4" liner section with a 10 3/4" tieback as illustrated in Figure 10. This liner section, along with the tieback, represents most of the wear since this is where the build-up section starts and the amount of rotation seen is high compared to the other casings. Every reservoir section (every multilateral) is drilled inside this casing. Since the production tubing is placed inside the 9 5/8" x 10 3/4" liner and tieback, it's defined as the production liner/casing and needs to be designed with respect to that and what requirements that is typical for this.
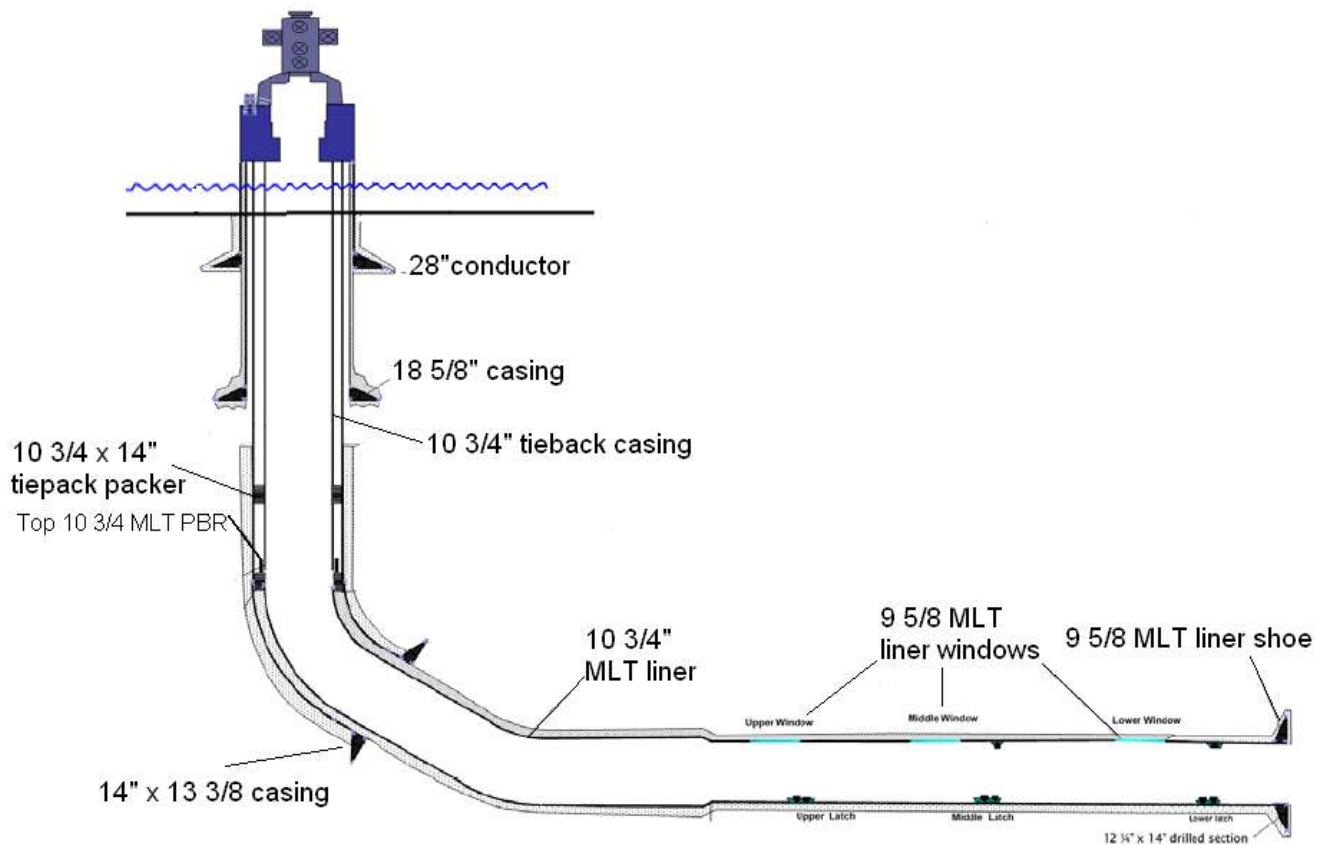
Figure 11. Schematic of casing design.

Casing design is more or less a stress analysis procedure where the goal is to engineer a tubular which can withstand a variety of both external and internal pressures along with thermal fluctuations, self weight loading, wear and corrosion. All components of the casing string including connections, circulation devices and landing string shall be subject to load case verification and the weakest points in the string with regards to burst, collapse and tensile strength rating shall be clearly indentified as stated by [16].

Design of the casing is often done with economics as one of the key drivers because casing makes up a considerable part of the total well cost, often reaching 20%, depending on the material quality chosen/needed [17].

The ability of the casing to withstand both internal pressure (burst) and external pressure, (collapse), is effectively reduced by a diminishing wall thickness. It is therefore important to correctly estimate these reductions in order to do a safe casing design and to determine if additional casing needs to be set to cover a worn casing before further drilling operations commence [18].

As there is little point in designing for loads that are not encountered in the field, or in having a casing that is disproportionally strong in relation to the underlying formations, there are four major elements to the design process [19]:

- Definition of the loading conditions likely to be encountered throughout the life of the well
- Specification of the mechanical strength of the pipe
- Estimation of the formation strength using rock and soil mechanics
- Estimation of the extent to which the tubular will deteriorate through time and quantification of the impact that this will have on its strength

Since knowledge of all the anticipated forces regarding the design process has to be determined or to some extent predicted, some risk is involved and the introduction of a design factor is necessary. This factor should be a compromise between a safety margin and economics and address all the uncertainties involved [17]. It's important not to confuse the term "design factor" with "safety factor". When using a safety factor it implies that the forces affecting the casing are known and that a specific margin is allowed for safety purposes [19].

The three basic wellbore conditions concerning forces are burst, collapse and tensile forces which will be discussed in the following sections along with a general outline of how to evaluate an intermediate casing design procedure. The first load consideration should be the burst condition since this will be the basis for most of the casing string design. Next, the collapse load should be considered and adjustments made if necessary. Then, when the weights, grades and section lengths have been evaluated and deemed satisfactory to withstand the burst and collapse criteria's previously considered, the tension load is assessed. The last step is to check the bi-axial and tri-axial reductions in burst strength and collapse resistance caused by compression and tension loads, respectively [20].

5.1 Casing Design Criteria

When designing a well there are certain design criteria which have to be followed. The worst case collapse, burst and tension scenario creates this basis and has to be accounted for in the design process. In order to be able to differentiate the worst case scenario from all the other scenarios which create a significant force on the casing, a thorough investigation of these will have to be done with calculations of forces acting on the casing for each relevant scenario. The relevant scenarios on Grane are tabulated below and are used as a basis for every well there.

Table 1: Casing Design Criteria

Casing String	Collapse	Burst	Tension
Surface	Full/Partial evacuation of well Lost Returns with mud drop Cementing	Displacement to gas Pressure test Green cement pressure test Gas kick (4m3)	Running in hole Green cement pressure test Service loads Overpull load Pre-cementing static load
Intermediate	Full/Partial evacuation of well Lost Returns with mud drop Cementing	Pressure test Green cement pressure test Displacement to gas Gas Kick (8m3)	Green cement pressure test Service loads Running in hole Overpull load Pre-cementing static load
Production liner	Full evacuation Full/Partial evacuation Above/Below packer Lost returns with mud drop Cementing	Pressure test Green Cement pressure test Tubing leak Injection down casing Gas Kick (8m3) Displacement to gas	Green cement pressure test Service loads Running in hole Pre-cementing static load
Production tie-back	Full evacuation	Pressure test Tubing leak	Service loads Overpull load Running in hole

5.2 Burst

Burst loading on the casing is induced when the internal pressure exceeds the external pressure. The most conservative design for burst assumes the gradient of dry gas inside the casing, the pressure of which equals the formation pressure of the lowest zone from which the gas may have originated or, alternatively, the fracture pressure of the open hole below the shoe. This loading condition, with dry gas in the well, will necessarily be provided by kick conditions. Since there are many factors affecting the design when considering burst, many of the operating companies modify this basic "dry gas" design concept according to a number of other influences which amongst others include that there usually is a combination of gas and mud when taking a kick along with the presence of casing wear [19].

As seen in Table 1 there are numerous situations where pressure conditions arise that can result in a burst pipe. Even though there are many situations, they can be categorized into the following main categories [21];

1. *Gas-filled casing.* As mentioned above, a design that assumes a gradient of gas inside the casing is a conservative design. The inside pressure below the wellhead consist of the formation pressure minus the hydrostatic weight of the fluids behind the casing string. The difference between these two curves represents the load on the casing string which is illustrated in Figure 12.
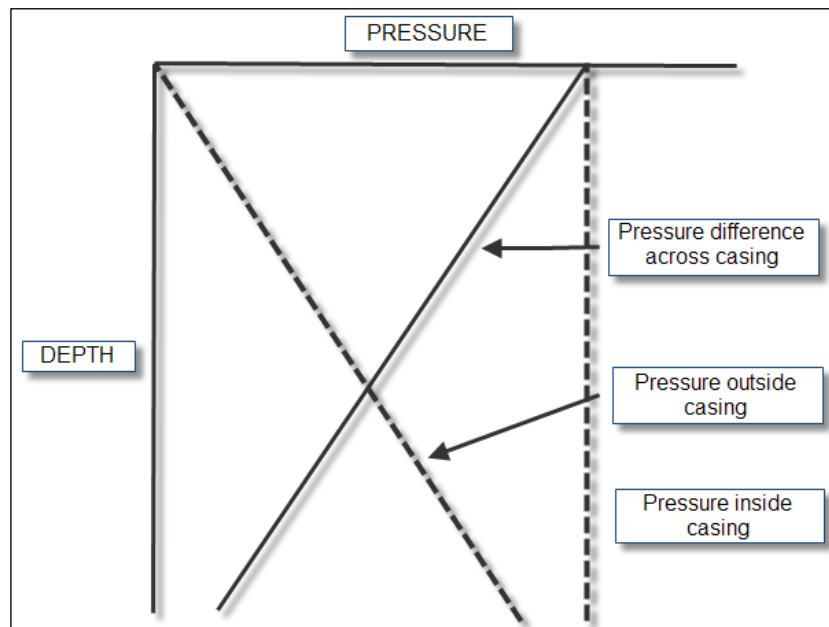
Figure 12. Gas-filled Casing Scenario [21]

2. *Leaking tubing criterion.* If a leak occurs at the top of the production tubing during well testing or production it will be superimposed on top of the casing/tubing annulus. Usually there's a production packer installed at the bottom of the production string which isolates the annuli above and below. With the gas superimposed on top of the annulus fluid a significant pressure arises above the packer which becomes a critical element under these circumstances.

3. *Maximum gas kick.* This scenario takes into account the largest volume of gas influx which can protrude into the wellbore at the next casing setting depth and be circulated out without fracturing the formation at the previous casing shoe. Here a maximum kick volume must be chosen which is based on the kick volume detection accuracy; how big of a volume that goes undetected into the well before circulation starts. When the kick volume is chosen the depth of the next casing shoe is used to determine the pressure at the previous casing shoe.

All likely scenarios must be considered and the most realistic scenario must be established. The design has to be able to take into account several criteria.

5.3 Collapse

Collapse loading on the casing is induced when the external pressure exceeds the internal pressure. There are several situations which can lead to a casing collapse but the most severe situation arises when there is a loss of circulation in the well which results in a reduced internal pressure if the well is not refilled. The casing is also subjected to a collapse pressure when it's cemented in place because of the density difference between cement outside the casing and the mud inside the casing but this isn't as relevant to casing wear as the first scenario. It's important to note that no allowance is given to increased collapse resistance when the casing has been cemented in place. This is due to the fact that the cement won't always set itself up as predicted; mud pockets can occur which will effectively reduce any support the casing would have experienced.

When losing mud to the formation the lowest and most reasonable pressure remaining inside the casing is set equal to a column of seawater as it is improbable that the remaining pressure will be lower than this. The maximum external pressure on the casing is equal to the heaviest mud weight expected. These two pressure gradients are illustrated in Figure 14 and the same logic applies here as with the burst scenario with regards to the design of the casing.
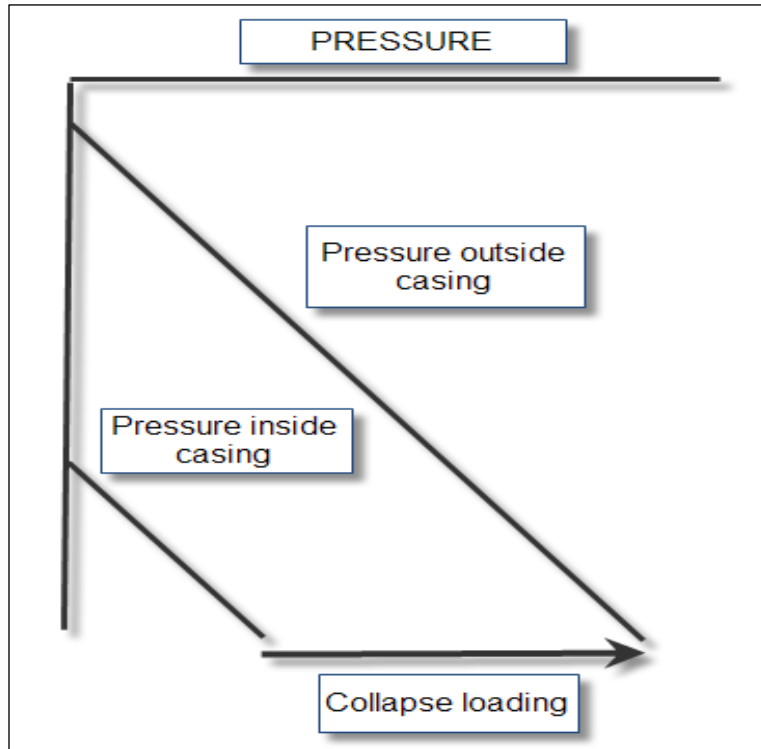
Figure 13. Resultant collapse load line [21]

5.4 Tensile Strength

This is the load imposed by the weight of casing itself plus any additional axial load caused by i.e. dynamic forces or shock loads, movements to free differentially stuck pipe, pressure testing, drag forces and so on. Each joint must be capable of supporting the weight of the string below that point. When the weights, grades and lengths of each section have been through thorough investigation, the tension load can be evaluated. As with burst loading the tension criterion implies that the strongest casing is installed at the top of the string. [17]. When considering the compression and tension load, it's important to include the buoyancy involved. There are two schools of thought concerning buoyancy, namely those who believe in the principle of Archimedes, and those who calculate the hydrostatic forces starting with the bottom surface of the string which is called the piston force approach. The principle of Archimedes is simple and can be expressed as [21];

When a body is submerged into a fluid, the buoyancy force equals the weight of the displaced fluid.

This method considers only the drillstring volume (displacement volume) times the density of the volume displaced, which in most cases will be mud. The result is illustrated on the left hand side in Figure 14 along with a schematic of the drillstring.

The reduction in string weight as a result of the buoyancy experienced is, by the piston force method, determined by the forces acting on all the exposed horizontally oriented areas of the casing string, i.e. where there is a change in diameter. This force is equal to the hydrostatic pressures at the specific depth times the horizontal area exposed [20]. Figure 15 shows the tension load line and how the tension is distributed down along the casing. The string will eventually go over into compression as the buoyancy pressure lifts the string upwards and exceeds the weight of the bottom end of the string up to a certain neutral point. A minimum over pull value is included to allow for pulling on stuck pipe. For comparison, the net force from Archimedes principle is shown.

The weakest part of the casing, regarding tension, is usually the coupling. Therefore the tension design line is primarily used to determine the type of coupling to be used [20].

Both methods are accepted as valid when designing the casing program with regards to tension since both methods give the same surface value. As previously mentioned, the tension criterion implies that the strongest casing is installed at the top of the string. But, since the piston force method only considers the external axial force it should never be used to calculate failure since it neglects that stress is actually a three dimensional state [21].
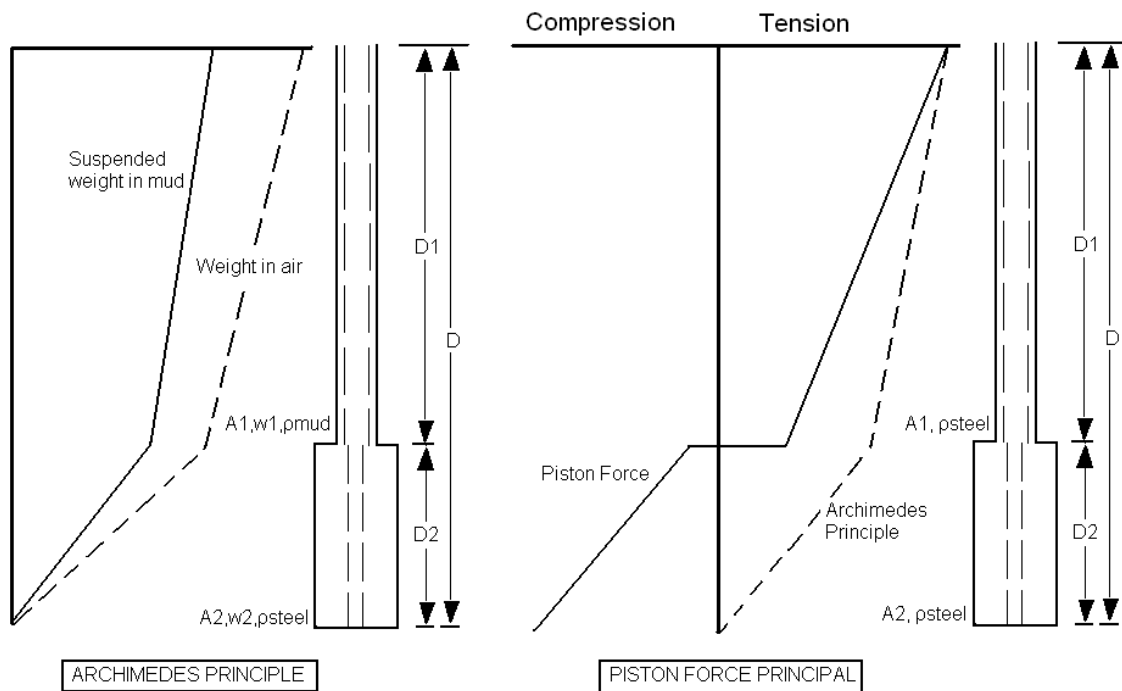
Figure 14. Buoyancy Forces – Archimedes vs. Piston Force Method [21]

Note that Figure 12, 13 and 14 will change according to what scenario which is chosen to be evaluated. Usually all scenarios posing a probability of occurring will be evaluated which will generate a lot of different Figures.

5.5 Failure Criteria Methods

There are different methods on how to enhance the characteristics of materials so it will withstand forces beyond the limits of regular steel but, as with everything else, it's a question of cost vs. gain.

5.5.1 API Equation – Burst

The common approach of how to estimate burst failure when casing wear has occurred, and a wear groove is present, is to use the American Petroleum Institute (API) equation which is an adaption of the Balow equation [18];

$$P_{API} = 0,875 \frac{2 \cdot \sigma_y \cdot t}{D}$$

Eq. 5.22

Where:

P$_{API, Burst}$ = Bust limit of tubular [psi]
σ_y = Yield strength of casing material [psi]
 t   = Casing wall thickness [in.]
 D   = Casing outside diameter [in.]

This formula relates the internal pressure that a tubular can withstand with regards to its dimensions and the strength of its material. The factor of 0.875 is to account for the API pipe wall thickness tolerance of 12.5% less than the nominal wall thickness. API specifies that steel which is used for production of tubular goods has a tensile strength required to produce a total elongation of 0.5 to 0.6 percent of the gauge length[1].

When determining the reduced casing burst strength on a crescent worn casing, the minimum wall thickness is used as the overall wall thickness so that it theoretically becomes a uniform worn casing [18]. This is illustrated in a Graph 1 showing the casing wall burst strength as a function of casing wall thickness and how a reduction in the wall thickness affects the burst pressure.

---

[1] Gauge length - Original length of the portion of a specimen measured for strain, length changes, and other characteristics [22]

When the 9 5/8" P-110 casing wall is worn down from an initial casing wall thickness of approximately 0.75 inches, to 0.5 inches, the corresponding reduction in casing burst pressures is 5000 psi, from 15 000 to 10 000 psi. This method of calculating the burst pressure is debated as being over-conservative and may result in a higher casing cost.
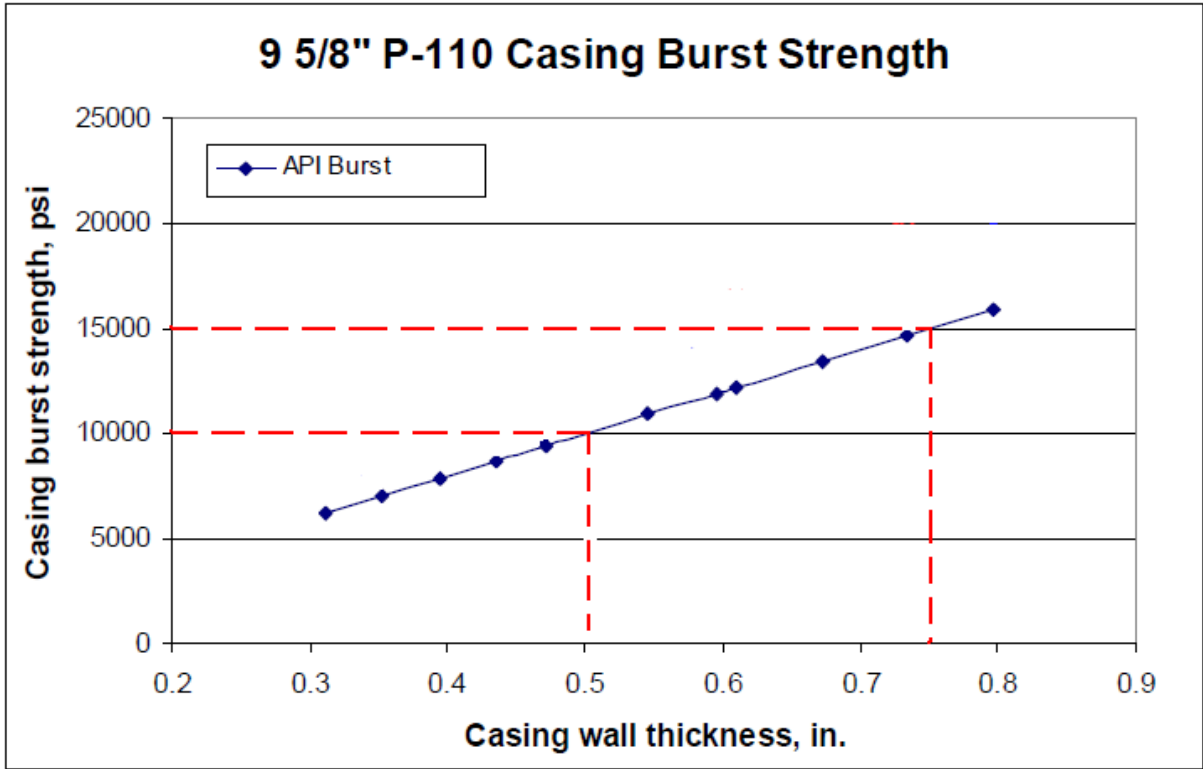
Figure 15. Burst strength as a function of casing wall thickness [18]

5.5.2 API Equation – Collapse

The derivation of the API collapse equation is a time consuming task and will not be focused on in this thesis. The equation is as follows [21];

$$P_{Collapse} = \frac{2CE}{1-v^2} \left\{ \frac{1}{\left(\frac{D_o}{t}-1\right)^2 \cdot \frac{D_o}{t}} \right\}$$

Eq. 5.23

Where:

P$_{collaps}$ = The pressure at which the casing collapses
C = Constant
E = Young's modulus [bar]
v = Poisson's ratio
D$_o$ = Outer diameter of casing
t = Casing wall thickness

The constant C is found by inverting Eq. 5.23 and solving for C when using the P$_{collapse}$ value given by the manufacturer. This equation is valid for large D/t ratios and is called the elastic collapse approach. For lesser D/t values there are other collapse types.

Both equations 5.22 and 5.23 can be used to determine a how casing wear affects the burst and collapse resistance by adjusting the casing thickness value, t. But this doesn't take into account that the wear is in the shape of a groove with only a small section of the circumference being affected with regards to the thickness. This is discussed in the end of section 5.5.3.

5.5.3 Von Mises

Another accepted failure criteria method is the Von Mises approach. This condition is commonly used to describe the yielding of steel under combined states of stress. The combination of the three principle stresses; axial, radial and tangential, makes up the bases for the initial yield limit [23]. In a body that is elastic and under the influence of loads in 3 dimensions a complex system of stresses arises. At any given point the magnitude and direction of the stresses may change. The Von Mises criterion is a method to decide whether or not any combination of the three principal stresses may lead to a tubular failure. Even though none of the principal stresses, individually, exceeds the yield limit, the right combination with regards to magnitude and direction, may cause failure. The different forces are illustrated Figure 17 and will be defined in the following section.
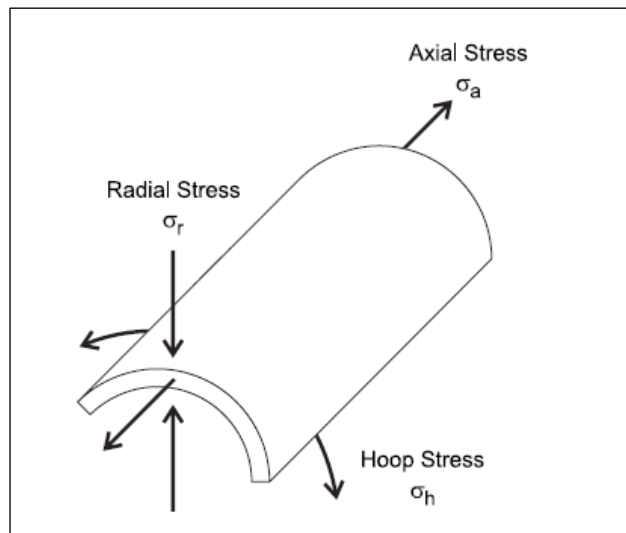
Figure 16. The three principal stresses σ_a, σ_r, σ_t [23]

The three principle stresses are determined by the geometry of the tubular along with the geometry of the well, plus the three variables [23]:

- Internal pressure - P_i [psi]
- External pressure - P_o [psi]
- Axial force - F_a [in.]

In order to find the axial stress,

$$\sigma_a = \frac{F_a}{A_s},$$
<div align="right">Eq. 5.24</div>

when the tubular is in tension, one must first find the correct axial force, F_a.

The axial force is a measure of the real force as measured with a strain gauge at the top. It is important to be aware of the effects of added pressure and fluid when determining this value. So, the equation for the real axial force consists of the weight of the tubular plus the difference between the inside and outside pressure of the tubular multiplied with the cross sectional area of the steel, A_s (buoyancy effect), as written below.

$$F_a = F_e + (P_i - P_o) \cdot A_s \qquad \text{Eq. 5.25}$$

As seen by Eq. 5.25, the real axial force, F_a, can be either lower or higher than the weight of the tubular alone, F_e, depending on the inside and outside pressure.

The radial stress, σ_r, and the tangential stress, σ_t, are defined by Lame's equations and are shown as follows;

$$\sigma_r = \frac{\left(p_i \cdot r_i^2 - p_o \cdot r_o^2\right)}{r_o^2 - r_i^2} + \frac{\left(p_o - p_i\right) r_o^2 \cdot r_i^2}{\left(r_o^2 - r_i^2\right) r^2} \qquad \text{Eq.5.26}$$

$$\sigma_t = \frac{\left(p_i \cdot r_i^2 - p_o \cdot r_o^2\right)}{r_o^2 - r_i^2} - \frac{\left(p_o - p_i\right) r_o^2 \cdot r_i^2}{\left(r_o^2 - r_i^2\right) r^2} \qquad \text{Eq. 5.27}$$

Where:
r_i = Inside radius of tubular
r_o = Outside radius of tubular
r = Point of interest in tubular wall

The axial stress can also be written as:

$$\sigma_a = \frac{\left(p_i \cdot ri^2 - p_o \cdot r_o^2\right)}{r_2^2 - r_1^2} + \frac{F_a}{\left(r_2^2 - r_1^2\right)\pi} \qquad \text{Eq. 5.28}$$

The three principal stresses can be put together in the von Mises yield criterion which is expressed mathematically as:

$$\sigma_y^2 \geq \left[(\sigma_t - \sigma_r)^2 + (\sigma_t - \sigma_a)^2 + (\sigma_a - \sigma_r)\right]^2 \cdot \frac{1}{2} \qquad \text{Eq. 5.29}$$

The right side of Eq. 1.22 is compared to the yield strength of the steel, σ_y, which determines how much stress the casing can withstand before it fails. If the yield strength is higher than the

right side of the equation the steel will theoretically not fail. There will always be a safety factor included in this equation, normally as a percentage of the upper limit in yield strength.

When using the Von Mises formula to compute a pressure rating reduction because of wear one has to assume an average increase of the entire inside circumference around the casing, which effectively reduces the entire wall thickness. This is illustrated in Figure 17 below;
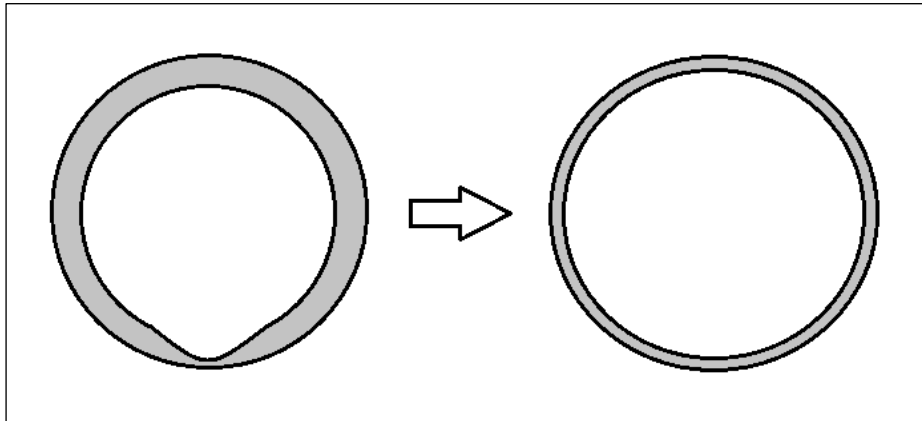
Figure 17. Converting a Wear Groove to an Average Thickness

This will underestimate the pressure reduction due to wear since the wall thickness reduction in the wear groove is averaged out over the entire inside circumference as illustrated above. After having logged the wall thickness reduction in a well with an ultrasonic tool (see chapter 9) it's possible to retrieve the information as this average thickness, illustrated in the right side of Figure 17. But it's the minimum wall thickness which is of interest when calculating a pressure rating reduction due to wear and it can be incorporated by the use of equations developed by Oil Technology Services [OTS] [24]. There are different calculation methods to choose from when performing a simulation in DrillNET, but the OTS equations have been used in this thesis (in DrillNET). A detailed review of these equations is beyond the scope of this thesis and the reader is referred to the reference [24]

6 Effect of Buckling on Casing Wear

Buckling is a big problem in the industry. Knowledge of how to avoid this may prevent costly affairs of dealing with stuck pipe, not being able to pass an internal diameter restrictions, weakened tubulars etc. Casing buckling can cause increased casing wear due to "doglegs" produced by the buckled casing, this will

Buckling is defined as a collapse due to instability under compressive stress [25] . Two types of buckling exist, either a helical (right figure) or sinusoidal (left figure) configuration as depicted in Figure 16. Both configurations depends on the pipe stiffness, weight and hole diameter but the axial force required to force the tubular into sinusoidal buckling is less than for helical buckling. In most cases helical buckling follows sinusoidal buckling as the axial force increases [26]. Buckling will however not necessarily occur at the same time in the entire string. The axial force acting on each point of a long string is different throughout the string which makes it possible to have a string which is only partially buckled and furthermore, different stages of buckling along the length of the string.
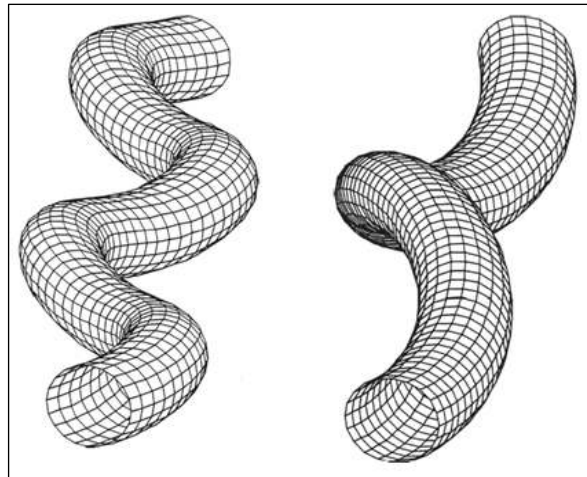
Figure 18. Sinusoidal (left) and Helical Buckling (right) [27]

In highly deviated wells tubulars contact the borehole wall and create a significant drag friction coefficient which may lead to buckling and sometimes a condition called lock-up. Lock-up restricts the tubular in moving any further down into the well because of the extremely high lateral force transfer from the tubular to the casing or the open borehole wall so that no additional weight can be transferred from one point to another down the string.

The longer the horizontal departure (HD) is, compared to the vertical depth (TVD), the more critical the axial force transfer becomes. When the HD/TVD ratio exceeds approximately 4, the

axial force transfer becomes critical and operations such as mud motor sliding, tubulars and completion running, or transferring weight on bit while drilling, become very difficult.   [28]. The critical angle (Inc$_{gravity}$) for a given friction coefficient (μ) where a tubular string can no longer move down into the well due to its own weight is defined as:

$$Inc_{gravity} = \tan^{-1}\left(\frac{1}{\mu}\right)$$

Eq. 6.30

This means that if a friction coefficient of 0,25 is used, the critical angle becomes around 76 degrees. An inclination above these 76 degrees requires a push force from the surface. The basis for the design of drill strings and completion running are torque and drag simulations with special attention on buckling. These simulations determine if the string can be run in the hole or not [28].

6.1 Casing Buckling

Buckling of the casing when trying to land it at the bottom of a drilled well or after it's been cemented in place (high external pressure), may cause problems with casing wear when drilling recommences. This is due to local doglegs that are produced when the casing gets buckled [5]. During buckling, if enough force is applied, the casing will have contact with the borehole wall along the entire length of the casing, so called helical buckling as previously mentioned. When these local doglegs appear they will absorb a lot of the lateral force from the drill pipe when drilling of the next section starts, thereby not uniformly distributing the force throughout the casing.
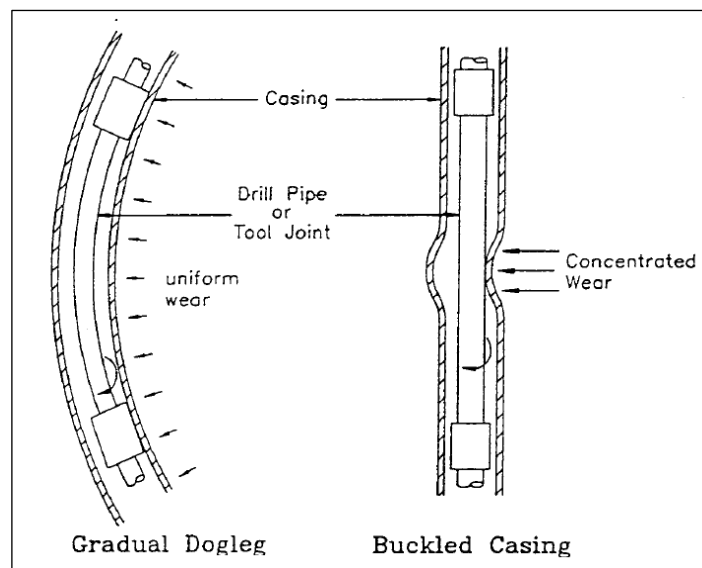
Figure 19. Gradual Dogleg vs. Buckled Casing Dogleg [10]

These local doglegs, created during casing buckling, acts as a starting groove for further casing wear by drill pipe.

A high angle and a large friction factor combined with an obstruction in the well when running the casing to target depth may cause it to buckle, depending on the axial force applied and the compressional force experienced by the casing. Even though the casing has been cemented in place there is still a risk for it to buckle [5].

6.2 Drillstring Buckling & Whirl

Common practice to avoid buckling when drilling vertical wells is to use drill collars having a weight that exceeds the weight on bit (WOB). In doing so, the drill pipe can be put in tension and thereby avoiding the prerequisite for the initiation of buckling, namely compression. Wells that are drilled deviated generate less gravity force on the bit because of the friction between the drillstring and the borehole wall which implies that a bigger section of the drillstring is in compression to achieve WOB. This makes it more challenging with regards to buckling even though heavy weight drill pipe (HWDP) is used to add weight in the BHA area. When the drillstring buckles in a cased hole it will convert some of the axial load into a lateral load and exert it onto the casing wall. Depending on how large this lateral force becomes, it can leave a wear scar on the casing wall.

Friction is an important parameter for buckling to occur, the more friction, the higher the axial load applied on the drillstring while applying weight on bit. In extended reach wells, ERD wells, this may be a limiting factor of how far a well can be drilled. The longer the well the more contact the drillstring has with the casing and/or open hole which gives more friction which again can lead to buckling of the string.

Whirl is categorized as lateral vibration which is defined as a non-central rotation of the bit, and/or BHA, causing lateral impacts with the sides of the wellbore. Continuous rotation of the drillstring generates and maintains this motion. This off centre rotation creates an imbalance which generates torsional, axial and lateral vibration. The lateral vibration can be categorized as;

- **Bit Whirl** – Off-centre bit rotation, especially common with PDC bits
- **Forward BHA Whirl** – Off-centre clockwise BHA rotation
- **Backward BHA Whirl -** Off-centre anti-clockwise BHA rotation

The backward BHA whirl occurs where the borehole wall friction causes the centre line rotation to become anti-clockwise which is in the opposite rotational direction of the drillstring rotation.

Drillstring whirling occurs mainly in the BHA since it's mostly under compression and therefore susceptible to buckle and whirl, but sometimes it can happen in the drillstring.

The initiation of lateral vibration require load and stress values which are higher than what is necessary to induce torsional or axial vibrations and can eventually become more destructive than both of them. But whirl gets harder to initiate as the deviation angle of the wellbore increases due to the effect of gravity.

Problems which are associated with whirl include;

- Reduced ROP
- Premature bit wear
- Uneven string/stabilizer wear due to impacts against the wellbore or casing
- BHA washouts and twist offs
- Borehole enlargement, hole instability and casing damage
- Lateral impacts inducing other vibrations

Casing wear occurs when there is whirl above the bit in the BHA or at the bit when drilling out from a newly set casing (bit inside casing).

A critical form of whirl arises when the drillstring has the same contact point as it wonders around inside the casing as shown in Figure 18.

The Figure illustrates how the drillstring rotates from point A to point B with the same contact point with regards to the drillstring. This forces all the drill pipe wear to the contact point instead of evenly distributing it along the entire circumference of the drillstring as it rotates relative to the casing. It's important to monitor the down hole conditions so that excessive wear can be avoided.
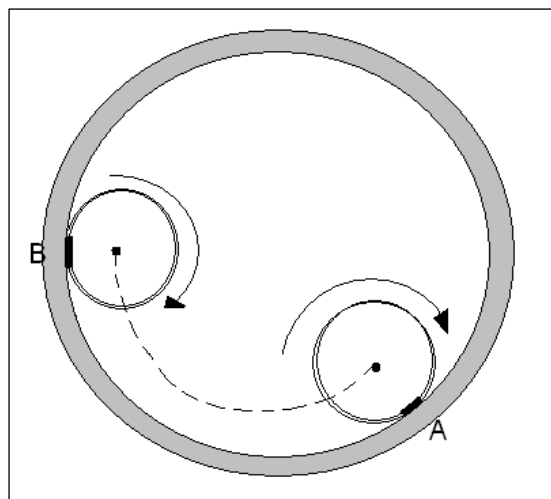
Figure 20. Whirl

7 How to Plan for Expected Casing Wear

Historically, solutions for drillstring and casing wear problems have been addressed through the application of hardbanding. There are a few other methods for reducing casing wear which can be planned and applied before drilling starts. Such strategies include protection material and applying non-rotating drill pipe protectors. All factors that influence casing wear that have been mentioned can of course also be adjusted to reduce the wear to a level which doesn't compromise any crucial baseline of parameters.

7.1 Casing Coating

There have been conducted various tests [5] of different types of internal casing coating which has shown that chrome is the most effective protection material. The other materials tested include Armacor-M, a coating from BP, Stellite and Colmonoy. All scenarios studied by Maurer Engineering [5] showed a decrease in wear when there was a chrome coating present in the casing as illustrated in Figure 21.
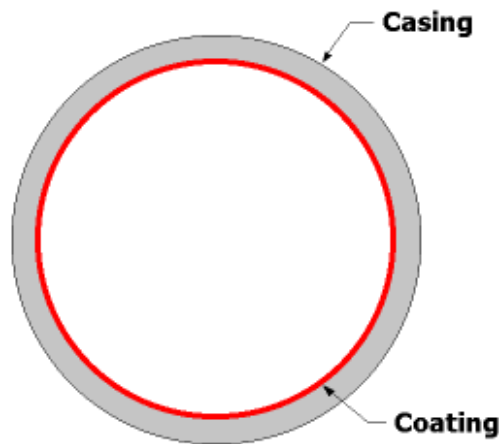
Figure 21. Internally-Coated Casing

In pure water the chrome coating test showed a reduction from 57.2% in the wall thickness of a regular N-80 casing compared to only 5.9% when using the unpolished chrome coating. These, of course, are ideal conditions which are not found in any oil and gas well. The most extensive wear when using a chrome coating was seen when using a 12.5% brine solution which gave a wear of 10.2% which is still better than regular casing. The tests were conducted with a lateral load of 3000 lb/ft over an 8 hour period.

7.2 Non-Rotating Drill Pipe Protectors

Non-rotating drill pipe protectors, NRDPPs, reduce the casing wear and torque by preventing the drill pipe tool joint contacting the casing wall. The NRDPP consists of three main parts as illustrated in Figure 22; a central hinged rubber or plastic protector sleeve which is attached to reinforced metal insert, and two aluminium hinged thrust bearing collars [29]. To allow the sleeve to rotate freely it's positioned between the two collars with sufficient clearance. Passages, or "flutes", along the protector sleeve face ensures sufficient passage for fluid flow.
Since the NRDPP sleeve has a larger outside diameter than the surrounding tool joints and its placement is in close proximity, it comes in contact with the casing before the tool joint does. This hinders wear of occurring at points where there is only contact between the protector sleeve and casing since rotational wear is eliminated. But this implies that there is a need to install NRDPPs evenly throughout the string which is highly impractical. Therefore its use is focused in the build sections of the well.
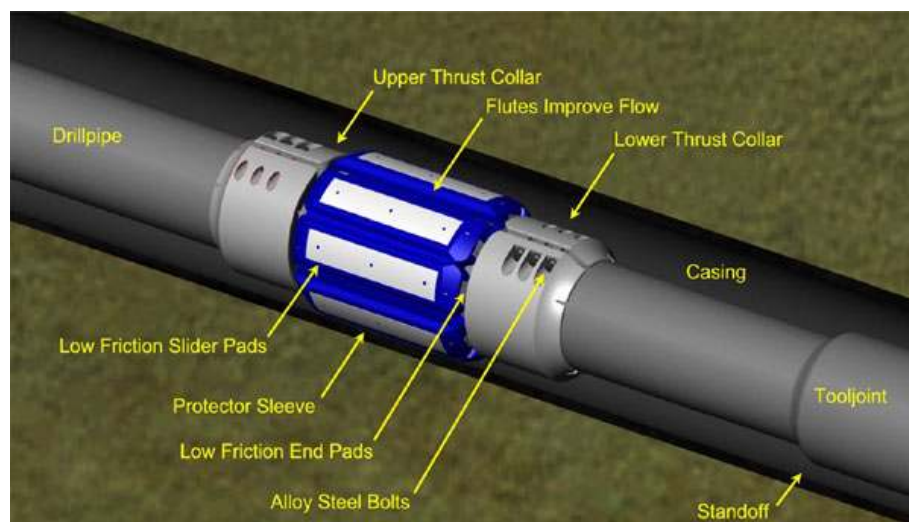
Figure 22. Non-Rotating Drill Pipe Protector [30]

In ERD wells torque is often a limiting factor when deciding a target depth. Two mechanisms which help reduce the drillstring torque by 10-30% include [29]:

- Fluid "lift" of the drill pipe from the protector
- Reduction of the effective size of the drill pipe

The protector sleeve is specially designed to act like a fluid bearing to create hydraulic lift which effectively separates the sleeve from the casing wall. This phenomenon happens because

of the drilling fluid, which is forced along the sleeve, and the relative motion of the drill pipe. NRDPPs are specifically designed to allow drilling fluid to easily pass the protectors by introducing flutes in the sleeve which are passages that allow fluid flow. The inside diameter of these passages are specially designed to act like a fluid bearing by using the drilling fluid and the relative motion of the drill pipe to the sleeve to create hydraulic "lift". The two interfacing surfaces are effectively "jacked" apart and experience extremely low frictional contact since the friction at the point of contact is reduced to the friction between the drill pipe and the drilling fluid. Depending on which type of drilling fluid being used, the remaining friction may typically be around 10% of that of steel against steel [29].

Since the effective dimension of the drill pipe is reduced from the normal outside diameter of the tool joint point (old contact point) to the inner radius of the protector sleeve (new contact point), it also reduces the drillstring torque. This is evident when considering that torque is directly proportional to the effective radius of the drillstring. For example, the NRDPP will reduce the torque of a 5" drill pipe with a 6 5/8" tool joint diameter by more than 20% because of the change in the point of relative rotation [29]. A 5" drill pipe with an effective tool joint diameter of 6 5/8" would use a NRDPP with an outside diameter of 7 1/4". Problems were encountered with collars slipping and wearing of early versions of these tools utilizing a 2 bolt collar system. The use of a longer 3 bolt system increased the axial slippage loads to more than 2700 kilos and eliminated this slippage problem. During the last few years of usage involving several thousand protectors, only a hand full have been lost in wellbores. All of the major components are either millable or have specific gravities which make them recoverable with viscous sweep techniques.

8 Remedial Actions for Casing Wear

After all casing has been cemented in place, with all drilling and completion completed, it is difficult to predict how the well will keep its integrity throughout its productive life. But one thing we do know; the casing will leak if it's kept in production long enough. This time span, from the casing is lowered into the well and until its starts to leak, is highly affected by all kinds of casing wear which reduces its intended strength in any way. If the casing integrity is lost it must be repaired or replaced immediately which is an economical burden often approaching 15% of the cost of drilling a replacement well [31]. The question of whether to repair or replace the casing depends on its condition which will be discussed in the following sections.

8.1 Repairing Techniques

There are many ways of repairing a casing but common for them all are that they are applied inside the existing casing which is damaged. This means that the repair mechanism exists as a patch of casing length having a smaller outer diameter than the inner diameter of the damaged casing. This patch of casing may be designed to expand so that it makes a seal against the damaged area which then creates a relatively small inner diameter restriction. The metal patch is stressed to its limit to yield against the casing. If it's not designed to expand it will be placed over the damaged zone and there will be an inner diameter restriction equivalent to the inner diameter of the patch. Regardless of design, the ideal casing patch should [32]:

- Provide economic selection of weight, grade and threaded connections to meet well requirements
- Be able to pass through minor restrictions such as nipple profiles and heavier-wall casing
- Ensure seal reliably with the seal mechanism equally strong as the rest of the system
- Provide an internally flush bore (same ID) with tieback capability

In most types of patches the pressure ratings in both burst and collapse mode are high which ensures that the casings burst and collapse values are maintained as original after setting the patch. However, in a report prepared by Maurer Engineering [5] there are experimental data, delivered by casing patch producer Homco, which estimated the burst and collapse pressure ratings of a patch set in casing sizes varying from 2 7/8" to 10 ¾". These tests indicate that the burst loading of a casing with a diameter less than 7 inches is preserved with the patch in place. Any casing size above 7 inches will have reduced burst strength. Tests performed on collapse loading showed a reduction in every scenario. This shows that it's important to evaluate how a patch affects the integrity of the well depending on the design of the patch.

The internal casing patch is limited to damaged areas that have a small leakage, leaking connection or a tear along the casing and of course areas with reduced wall thickness. If the pipe is parted, has a large tear or is collapsed, a replacement might be necessary.

The biggest benefit of using a repair method is the economical aspect when considering the cost of rig time, equipment and service costs. The obvious drawback of such a technique is the internal diameter reduction which consequently reduces any production if there is fluid flowing through the affected area and it also limits what kind of equipment that can be run into the well.

8.2 Replacement Techniques

There are several replacement techniques that can be used if the operator detects casing damage and the type of technique used depends on the extent and severity of the damage. The first main category of replacement is the complete replacement which is preferred when there are multiple leak areas or areas of damaged casing. The second main category involves partial replacement which is preferred when the leakage or damage is limited to one or two joints of casing. These two categories along with a squeeze cementing technique will be discussed in the forthcoming sections.

8.2.1 Complete Replacement

A complete replacement of the leaking or damaged casing is often the most simple approach but also the most expensive. If a wellbore is in such a bad physical condition that it could not withstand the severe pressure requirements the installation of a new inner string of casing is the most viable option. When such a string, with a smaller diameter, is cemented in place the well will be completely isolated from the old well where the leak is, as illustrated in Figure 23.
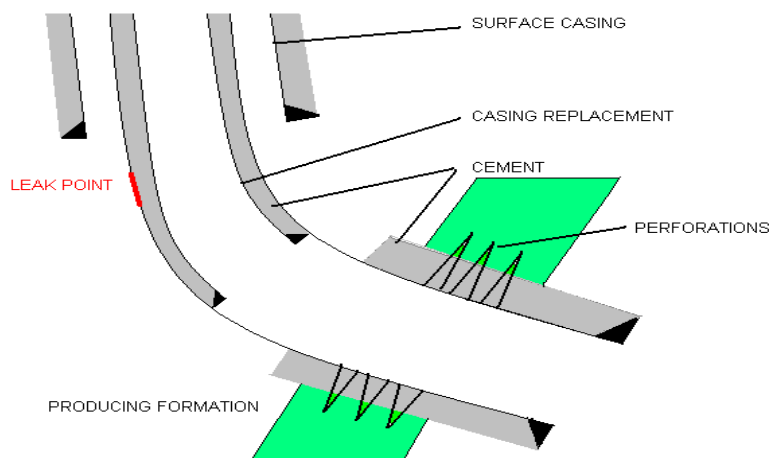
Figure 23. Complete Casing Replacement [5]

The procedure for installing an inner string in a well is straightforward. One must be careful not to have to much overbalance and possibly damage the formation with wellbore fluid by using an incorrect mud weight. Before the replacement casing is run a junk basket and scraper is run to remove potential obstructions. The replacement casing is run with centralizers and it is rotated and reciprocated while cementing. After sufficient time for the cement to set, a bit and a scraper is usually run to clean up the wellbore before the next operation commences [5].

The benefit of running a complete replacement is that it's not a complicated operation and that a casing which is new, uncorroded and free of any stress cycling, greatly increases the life of the well. The biggest drawback of such a method is the cost involved and the reduction of internal diameter, possibly compromising future well interventions. Compared to a patch or a partial replacement operation, the cost is extremely high [5]

8.2.2 Partial Replacement

The partial replacement option is considered when the damage to the casing is relatively isolated and where there isn't any cement behind the casing or where there is any formation collapse present. There exist two partial replacement methods, either a rethreading or an overshot technique. Common for both methods is that the existing casing string must be intact with regards to burst, collapse and tensile strength except in the affected area of damage.

The rethreading method makes it possible to unscrew the damaged part of the casing and replacing it with a new joint, thereby avoiding the cost of replacing a large section of casing. But because the rethreading takes place down hole it's not always an easy task to perform. When the damaged joint is retrieved, the insertion of a new one, called stabbing in, and making up the connection, can create problems due to the harsh down hole conditions. This rethreading method is preferred when there is a bad section of casing since it's the least expensive method [5]

Sometimes there will be a need to cut out the damaged part of the casing, including everything above, instead of unscrewing it. When the casing is cut and retrieved the cut area has to be properly conditioned in order for the overshot to seal properly around the remaining casing in the well. The overshot has a slightly larger inner diameter than the outer diameter of the existing casing so that the new casing can attach itself onto the old one. This method will obviously be more expensive than the rethreading option due to the cost involved with cutting and preparing for the actual overshot and the extra casing required. But the overshot is widely recognized in the oil and gas industry as a proven method for replacing damaged casing.

8.2.3 Squeeze Cementing

If the previous options of remedial actions aren't applicable to a given situation, there is a third option called squeeze cementing which involves hydraulically placing a volume of cement adjacent to the leak and then forcing the cement into the leak by pressure. If correctly placed, the cement will create a seal between the inside of the casing and the formation or steel. This method is favoured when the casing is parted or ruptured or when previous columns of set cement are inadequate or damaged.

The design of the cement is an important factor in ensuring a successful operation and the crucial parameter is often the setting time of the cement along with a correct displacement. It's also important to avoid down hole movement of the cement after placement by using a correct density.

After the cement slurry is designed the placement methods may vary depending on the down hole conditions. Bullheading is the most common method where the cement is pumped as a slurry under pressure from surface and thereby forcing the contents of the casing through the leak. This can either be done through the casing itself or down the tubing if it's in place. The use of a packer to direct the cement slurry is optional. For shallow, low-pressure squeeze jobs a retrievable packer is commonly used. The benefit of squeeze cementing, compared to the other methods, includes cost and strength. A drawback lies in the time required to perform such job and the fact that multiple jobs may be required to gain sufficient strength [5].

9 Casing Wear Logging Tools

The tools used to check for casing wear are mainly the ultra-sonic imaging tool, the multifinger calliper tool and the multi-frequency electromagnetic tool. The wells discussed in this thesis will only make use of the results of the ultra-sonic imaging tool which are verified by the cement bond log tool/variable density log.

9.1 Ultra-Sonic Imaging Tool

The ultra-sonic imaging tool, USIT, is classified as an acoustic tool and has a 360 degree view of the well as it spins around its axis and produces a high-level resolution casing inspection which allows for identification of casing wear caused by drilling operations [33]. It uses a single transducer (a device that converts one type of energy to another) mounted on an Ultrasonic Rotating Sub (USRS) on the bottom of the tool, is shown in Figure 20. A transmitter emits short ultrasonic pulses between 200 and 700 Khz and measures the received ultrasonic waveforms reflected from the internal and external casing interfaces [34]. Depending upon the objectives of the survey, either 5 degree or 10 degree radial/azimuthal sampling can be employed. The transducer rotates at approximately 7.5 rps and pulses are fired 18 times (every 20 degrees) per revolution. The pulses creates echo's which are reflected back to the tool after hitting any interface on its path and are analyzed. The result is four measurements; Acoustic impedance, cement bonding to casing, internal radius and casing thickness. The rate at which the reflected cement interface waveforms receives decay gives a picture of how the cement has set and if there is good bonding between the casing and the cement. A measure of the casing thickness is given by an interpretation of the resonant frequency of the echo.
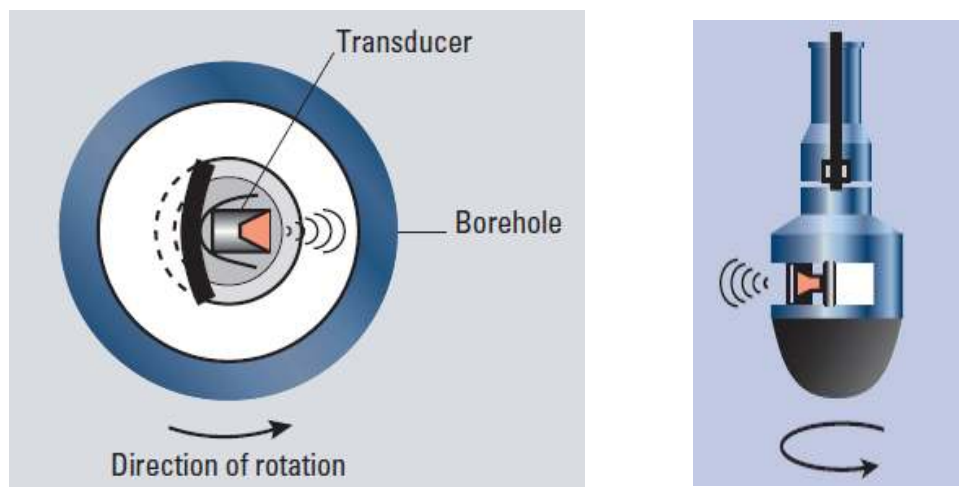
Figure 24. Tool configuration and measurement position [35].

The ultrasonic pulse between 200 and 700 KHz excites the casing into its thickness resonance mode, which is detected as an exponential decay in the reflected echo. This decay rate is controlled by the acoustic impedance of the mud in which the tool is in and the cement behind the casing. The fluid in which the sonde operates in is important with regards to signal to noise ratio, therefore it's important to select the most suitable transducer subassembly to reduce attenuation in heavy fluids. Because of the 360 degree rotation of the transducer the tool can provide full azimuthal coverage of the casing circumference allowing for detection of local defects such as channels as the acoustic impedance is displayed as a map.

The information gathered from the USIT will be processed and presented as a log with the different measurements represented graphically as shown in Figure 21. The log is corrected for wellbore orientation with the low side of the hole displayed in the middle of the track.
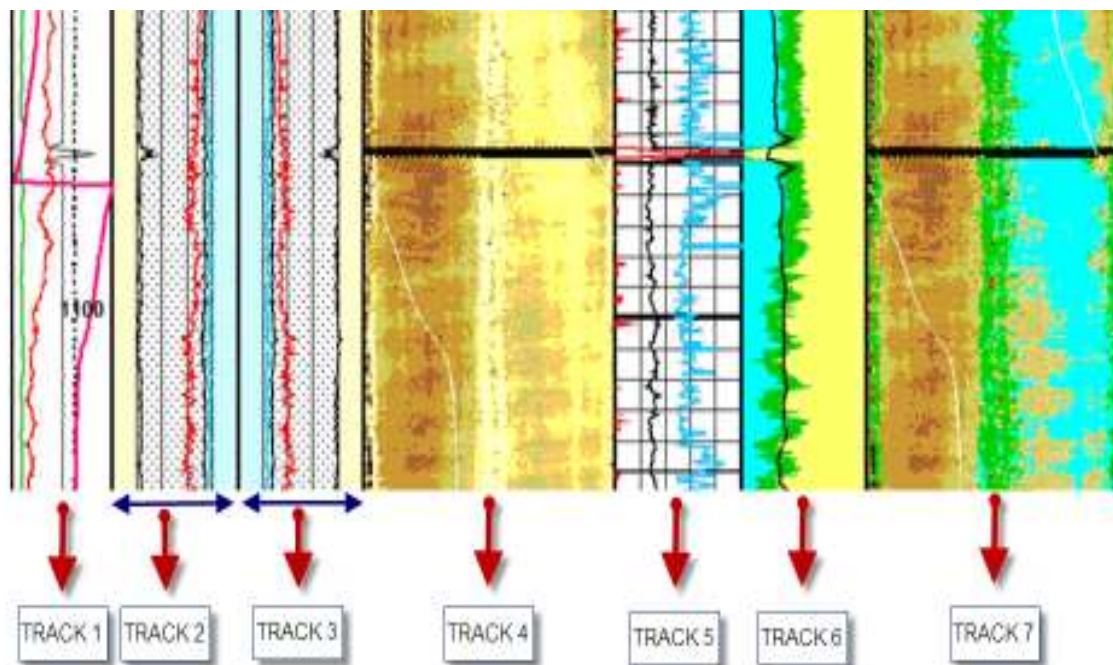
Figure 25. USIT Log – Example tracks [36].

As one can see from Figure 21, the log is colour coded for easier interpretation. The different colours are explained below in Table 2 along with the different tracks. There are many different tracks that can be displayed, this is of course governed by what information one is seeking. The tracks which are chosen in Figure 25 often accompany the casing thickness measurements which are displayed in Figure 26.

Table 2: USIT Log Track Numbering

TRACK #	MEASUREMENT	COLOUR CODE WITHIN TRACK	Note
1	Eccentering [Inch] Gamma Ray Image Rotation [Deg] Cable Speed [m/h]		
2	Minimum of Internal Radius [Inch] External Radius Average [Inch] Internal Radius Maximum [Inch] Internal Radius Avergae [Inch]		
3	Minimum of Internal Radius [Inch] Internal Radius Maximum [Inch] Internal Radius Average [Inch] External Radius Avergae [Inch]		
4	Raw Acoustic Impedance [mRay]	-500.0000 0.5000 1.0000 1.5000 2.0000 2.5000 3.0000 3.5000 4.0000 4.5000 5.0000 5.5000 6.0000 6.5000 7.0000 7.5000 8.0000	Zero is equal to air. The harder the material the higher the Impedance value will be.
5	Maximum Acoustic Impedance Average Acoustic Impedance Minimum Acoustic Impedance		
6	Fluid Compensated CBL Amplitude Micro-debonding Liquid Content Gas or Dry Micro Annulus Bonded Casing		
7	Cement Map with Impedance [mRay]	-1000.0000 -500.0000 0.2000 2.8000 3.0000 3.5000 4.0000 4.5000 5.0000 5.5000 6.0000 6.5000 7.0000 7.5000 8.0000	Zero is equal to air. The harder the material the higher the accustic impedance value will be.

The two tracks of interest with regards to casing wear are the casing thickness measurements which are depicted below in Figure 26.
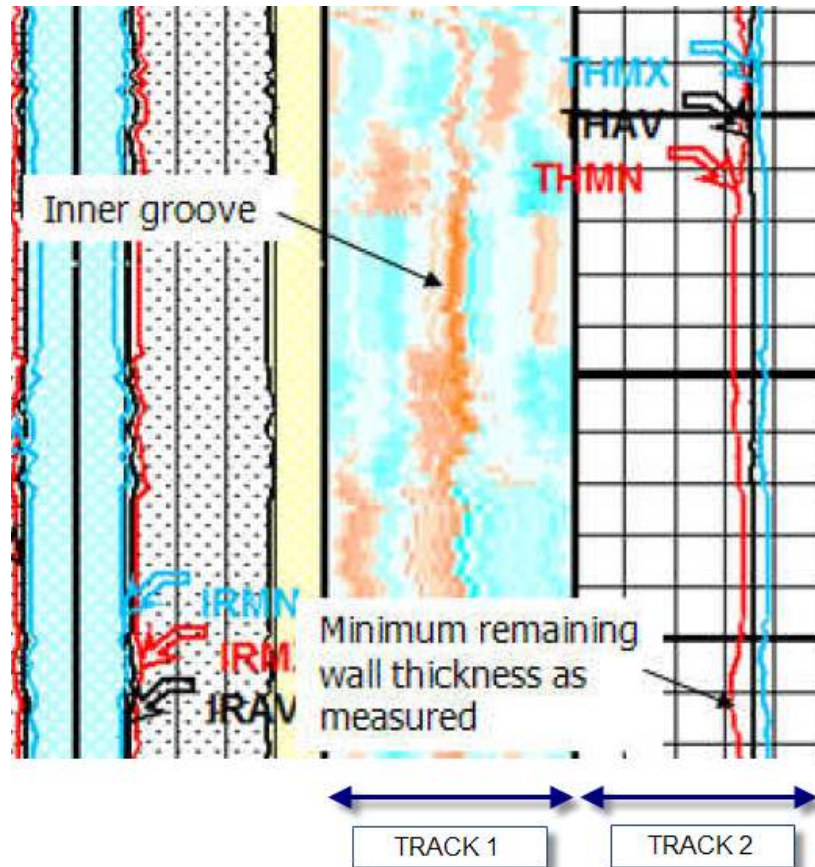
Figure 26. USIT log - Casing thickness measurement tracks

Table 3. USIT log: Casing thickness measurement tracks

TRACK #	MEASUREMENT	Color code within track		Note
1	THMX - Maximum thickness			One row equals 1 inch and the scale is from left to right. It's the minimum thickness value which is of interest in this thesis.
	THAV - Average thickness			
	THMN - Minimum thickness			
2	Wear map	Lighter color - No/little wear		Shows the thickness around the circumference of the pipe, middle is lowside and edges are highside.
		Darker color - More significant wear		

Since a good log is dependent on the accuracy of the mud velocity measurement, it's important to know what kind of fluid that's in the well and adjust the tool and measurements accordingly. As the tool is run into the well it continuously measures the acoustic impedance and borehole

fluid slowness so that any change in fluid properties won't affect the measurements since changing parameters are monitored and reacted upon. A measurement of the acoustic velocity in mud is done by orienting the transducer towards a built in plate with known thickness and distance between plate and transducer. While in this mode, Fluid Properties Measurement (FPM), a continuous record of the velocity in mud is recorded using the simple equation of distance equals speed divided by the time used to travel the distance. This measurement is used to calibrate the interpretation.

One of the USIT's outputs is the internal casing diameter which can be used to calculate the amount of wear, compared to the nominal diameter, which is defined as:

Measured Wear = Nominal Thickness – Measured Thickness   Eq. 9.31

As previously mentioned (5.4.1) there is an API tolerance of 12.5 percent less than the nominal wall thickness which means that there is an error incorporated into the calculations by this tolerance.

When using light-weight cement recipes with densities less than 1 g/cm^3 the impedance, which is a product of the density and the acoustic velocity, can be lowered to about 2.5 MRayls for uncontaminated fully set cement. If the mud impedance reaches 1.5 MRayls or more, the interpreter will have a problem of differencing the mud and the light weight cement. So, if there is a bad displacement of mud when placing cement in the annulus, because of a loss or mud/cement channels created along the casing, it may not be easy to distinguish it on the log. A drawback in the use of the USIT is in the limitation of the penetration depth in the radial direction. The tool can say whether or not there is cement immediately behind the casing but it cannot probe the annulus width for defects within the cement sheath or at the cement-rock interface [37]. The maximum recommended degree of tool eccentralization for a USIT is 2% of the pipe OD, this corresponds to 0.21 inches in a 10 3/4" casing.

The radius measurements can become affected by the centralization of the USIT so good centralization of casing wear logging tools is essential, especially in higher angle holes. The logging companies have the capability of using centralizer tools but may be a bit apprehensive whether to use them or not. The high forces acting on the centralizer, which is required to maintain centralization, increase the probability of getting stuck or breaking the tools. If centralizers are run they are usually of the spring loaded stabilizer type which will give best centralization compared to a fixed stabilizer type. Even though the effect of decentralization is likely to be as large as the casing defect being measured, the implementation of centralizers will reduce this error along with the interpretation software which takes this into account.

9.2 Cement Bond Log & Variable Density Log

The cement bond log, CBL, is usually combined with the variable density log, VBL. This combination, CBL and VDL, is normally run together with the USIT to get a better picture of the down hole condition of the casing and the cement behind it. The discussion of this tool will be kept limited due to the fact that it isn't involved in casing wear.
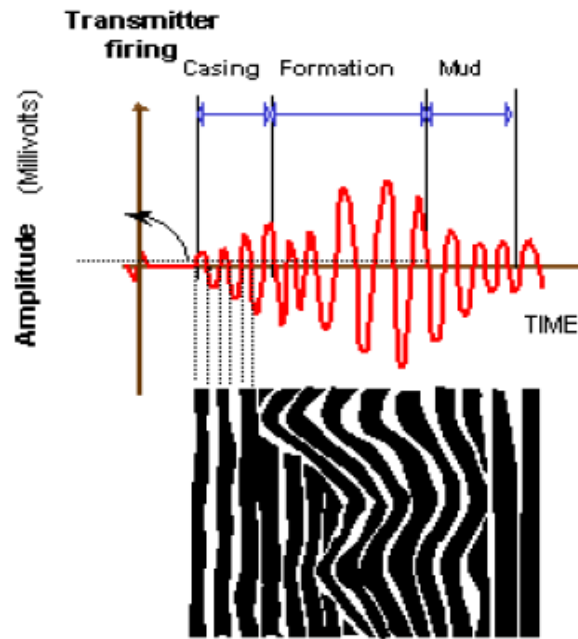
Figure 27. CBL Measurement Theory [38].

The principle of the CBL measurement is the recording of the transit time and attenuation of an acoustic wave after propagation through the borehole fluid and along the casing wall. The tool usually comprises a transmitter and two receivers which are placed at a distance of 3 and 5 feet below. When the transmitter sends out a sonic pulse it travels through the medium it hits, the borehole fluid, casing, cement and further into the formation behind as depicted in Figure 27.

At each interface, between each medium, there will be a reflection of some of the initial energy in the sonic pulse. This energy hits the receivers and is registered in a log and is usually displayed in millivolt units, decibel attenuation, or both. Reduction of the reading in millivolts or an increase of the decibel attenuation is an indication of a good bond between the casing and the cement. The theory behind this is that the wave loses energy mainly through the
shear coupling to the surrounding cement, so that well-bonded cement attenuates more quickly than a fluid [37].

The VDL measurement is in effect highlighting the peaks and troughs of the sinusoidal wave presented in Figure 23, which are acquired by the 5 ft receiver. This receiver registers the reflected acoustic waves which have penetrated deeper than the 3 ft receiver and because of this; VDL is the only measurement that provides information in terms of the cement to formation bond.

10 Grane Field

Figure 28. Location of Grane [39], [40]

Grane oilfield was discovered in 1991 by Hydro and is located approximately 185 kilometres west of Haugesund which is illustrated on the map in Figure 28. It has been developed with an integrated accommodation, processing and drilling platform on top of a fixed steel jacket in a water depth of 127 meters. The facility has 40 well slots.

On the 23'rd of September 2003 production started and Grane was thereby the first field on the Norwegian continental shelf to produce heavy crude oil. The sandstone reservoir rock at Grane is much younger compared to the rest of the shelf and was deposited around 60 million years ago in the Tertiary period. Pulses of submarine turbidity currents have made up the Palaeocene sandstone deposits which are mostly massive and homogenous and characterized by their uniform grain size and excellent reservoir quality. The oil has accumulated in an elongated structure defined by a combination of depositional and structural processed. Top reservoir is located approximately 1720 meters below mean sea level, and the maximum thickness of the oil column is 80 meters.

The field contains insignificant amounts of gas and since the heavy crude oil is hard and demanding to extract, gas from the Heimdal Gas Centre is transported 50 km by pipeline to Grane and down into injection wells to keep the reservoir pressure stable. A reservoir assessment at the start of production concluded with a recoverable reserves volume of approximately 700 million barrels. Since then the production has stabilized at around 150-200 000 barrels of oil per day [39]. The Norwegian Petroleum Directorate, NPD, reserve estimates as of 31.12.2009 are 334 million Sm^3 [41].

To secure an effective sweep of the reservoir and maximize the oil recovery, a total of 35 wells have been planned, 27 oil producers, three gas injectors, four water injectors and one

slop/cuttings injector. The option to drill more wells on the field and thus utilize all template slots will be exercised.

Since there has been an increase in the number of technical sidetracks needed to reach a specific target, and the fact that an MLT well already has a high number of drillstring rotation hours in the reservoir (inside the 9 5/8 x 10 3/4"), there's a concern regarding the issue of wear factors in DrillNET correlating poorly with actual wear seen in the well after it's been logged with the USIT. To get a better understanding of the simulation workflow an introduction to the casing wear section of DrillNET and the pre-simulation work required, is presented in the next two chapters.

11 Pre-Simulation Work

There are many different programs within DrillNET; one of them is Casing Wear. Casing Wear represents a unique, powerful engineering model to calculate and monitor the progression of wear caused by rotary contact of drill pipe with down hole elements such as the casing. This module was originally developed under the sponsorship of the joint industry project known as DEA-42 – Casing Wear Technology. In addition to wear calculations Casing Wear also determines the impact it has on burst and collapse.

An MLT well has multiple lateral trajectories and possibly several sidetracks within one lateral which complicates the simulation process. There is no definite answer on how to simulate a MLT well in DrillNET [1], therefore different methods have been discussed. The method chosen in this thesis will be explained along with how it has shaped the workflow.

A lot of work is put into gathering the information required to do a complete casing wear simulation of a well. Since the purpose is to find an appropriate wear factor based on wells that have been drilled by comparing the result in DrillNET with the actual wear that has been logged, the information has to be extracted from different sources and fed into the casing wear input pages of DrillNET which includes survey data, tubular data, wellbore data, and operation parameters with their different attributes as displayed in Table 1 below;

Table 3: Cwear Input Parameters

Survey Data	Tubular data	Wellbore Data	Operational
MD - Measured Depth [ft]	Section Length [ft]	Bottom MD [ft]	Last Survey MD [ft]
Inclination [degrees]	Pipe Outer Diameter [in.]	Outer Diameter [in.]	Start/end depth [ft]
Azimuth [degrees]	Pipe Inner Diameter [in.]	Inner Diameter [in.]	Mud Interval [ft]
TVD - True Vertical Depth [ft]	Adjusted Weight [lb/ft]	Yield Strength [PSI]	Mud Weight [ppg]
Dogleg [degrees per 100 ft]	Density [lb/ft3]	Density [lb/ft3]	Bottom of Interval [ft]
	Tool Joint Outer Diameter [in.]		ROP [meters/hour]
	Tool Joint Contact Length [in.]		RPM
	Drill Pipe Tool Joint Length [ft]		Weight On Bit [lbf]

Recent wells on Grane are logged by the USIT before running the top completion and a huge amount of data is created with many different kinds of use. For this thesis it's mostly track 4, the casing condition in terms of thickness, in Figure 21 which is of interest. To be able to make use of this track and compare it with the simulated wear it is necessary to retrieve the raw data which is in a number format. This means that one can make a graph of the raw data and

incorporate any other information, like the simulated wear, into the same graph for comparison. The following wells will be processed in this manner;

Table 4: Simulated Wells

WELL	COMPLETION READY	SECTION	TYPE OF WELL	NUMBER OF LATERALS
G-3	17.03.2010	9 5/8" x 10 ¾"	Producer, MLT	3
G-7	13.11.2010	9 5/8" x 10 ¾"	Producer, MLT	3
G-13	21.09.2009	9 5/8" x 10 ¾"	Producer, MLT	3
G-15	25.02.2009	9 5/8" x 10 ¾"	Producer, MLT	3
G-16	25.10.2008	9 5/8" x 10 ¾"	Producer, MLT	3

In order to simulate the wells effectively, with regards to time spent, the information required by the simulation program DrillNET was set up in Excel identically as it appears in DrillNET so that a simple and swift copy/paste action can be utilized, thereby minimizing the time spent on filling in the required DrillNET input parameters and also minimizing the risk of punching in the wrong value in DrillNET if doing it manually.

Since the input parameters now have been established the next step is to gather the information in Excel and setting it up so that it can be copied and pasted directly into DrillNET.

11.1 Creating the Actual Wear Graph

The minimum remaining thickness data was retrieved from the DLIS files which the USIT data is stored as along with many other measurements. In order for the data to be useful it had to be made manageable in Excel where it could be processed and graphically displayed. This was done by opening the DLIS file in a Schlumberger program called "DLIS to ASCII" which is a part of the "Toolbox" download retrieved from their website. The "Toolbox" download contains 7 smaller programs and one of them is the "DLIS to ASCII" application. This application allows for the creation of LAS files that can be opened by Excel. Some adjustments had to be made when arranging the data in the Excel sheet as everything is initially sorted as text is one column when opening it. The minimum remaining wall thickness was converted to a percentage of the nominal thickness to make it easier to view a graph. To get the percentage the minimum remaining wall thickness had to be subtracted from the nominal wall thickness value which gives the wear thickness value. Then the wear thickness value was divided by the nominal thickness value;

$$Wear\% = \frac{THMN - THN}{THN}$$

Eq. 11.31

Where;

THMN   = Minimum remaining wall thickness
THN   = Nominal thickness

When the Wear% column was organized the next step was to generate the graph as a scatter plot with smoothed lines and without markers. The result of this plot was be very spiky due to the sensitivity of the USIT when measuring the thickness along a connection between two casing joints. The USIT used to log the wells on Grane has an upper thickness limit measurement of 0,59" and any measurement above this value will only result in unrealistically high values which aren't relevant. The wall thickness at a connection point is considerably higher than along the rest of the tubular so every connection with a wear value higher than the given trend must be examined and compared with track number 1 and 2 in Figure 26. If there exists a peak in the USIT plot but no sign of wear appears in tracks 1 and 2, the peak in the plot must be eliminated. This is a very time consuming process which is essential for the comparison of measured and simulated wear. The difference of an unprocessed and processed plot can be seen in Figure 29.
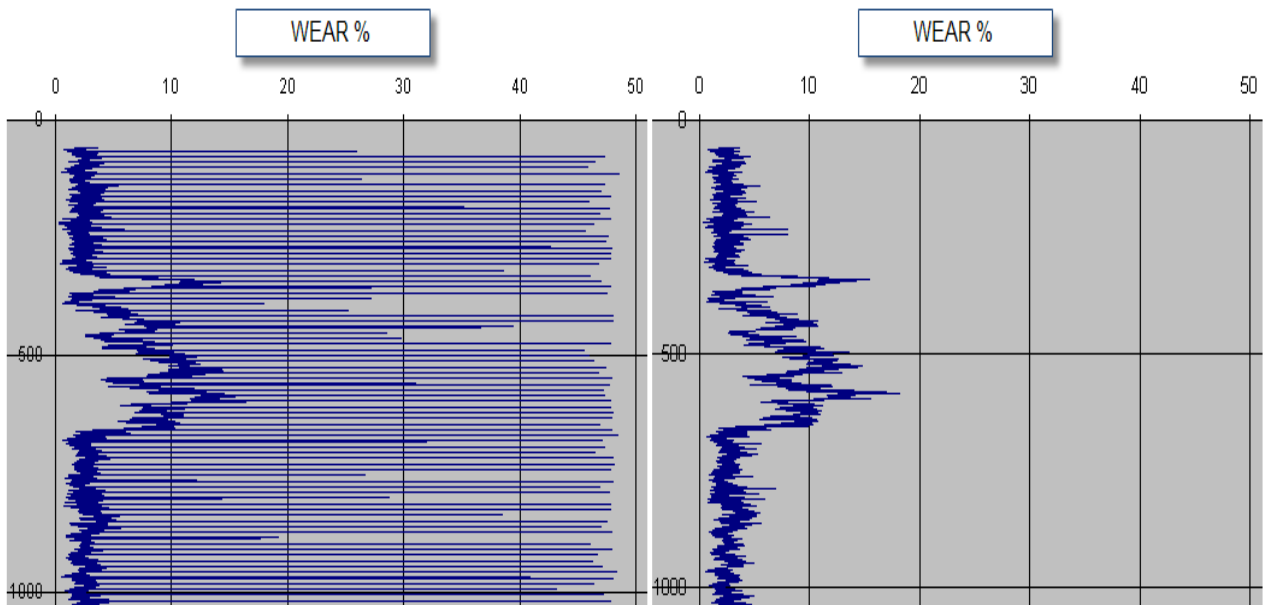

Figure 29. Unprocessed vs Processed USIT log

11.2 Survey Data

The trajectories of the wells in this thesis are gathered from an EDM Landmark program called Compass and pasted into an excel sheet so that they were easy to access at a later stage during the simulation work. To reduce the number of simulations required and at the same time having a realistic approach, it was decided to do one simulation for each lateral including any timedrilling and failed hole meters caused by pulling back and sidetracking areas which create an impossible drilling environment. This extends the trajectory beyond the actual path since any timedrilling and failed hole meters are kept in a straight line after the successful drilled lateral. These terms, along with an explanation to Figure 30 which illustrates the simulation method, will be explained in this section.

End of 9 5/8 x 10 3/4 liner and tieback

| Lateral | Timedrilling | Failed hole |
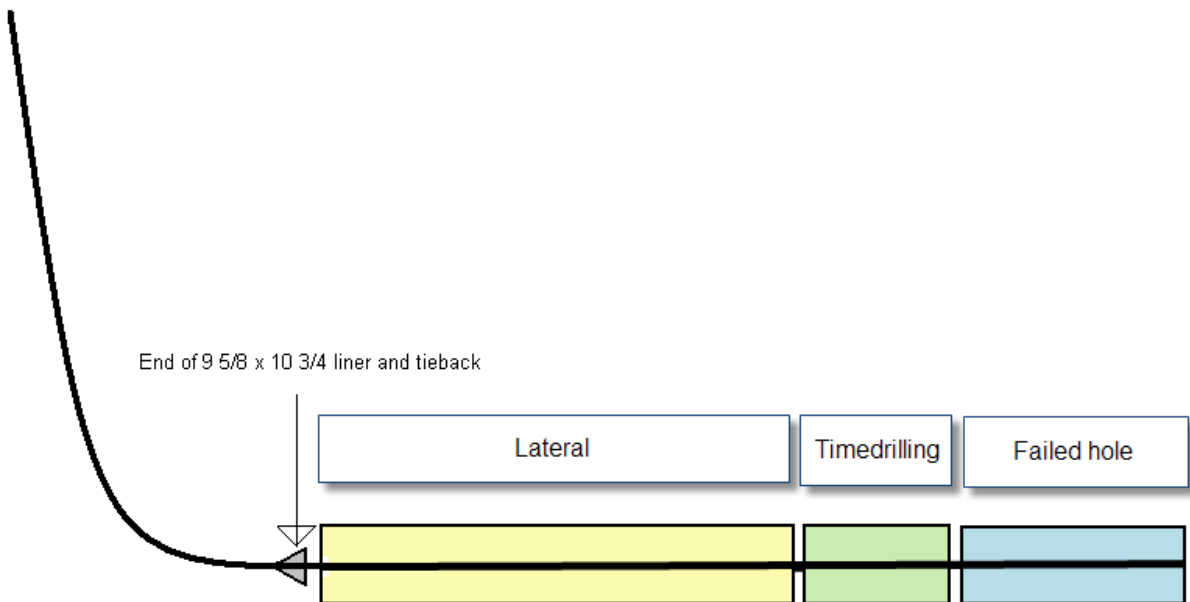
Figure 30. Survey configuration

When extending beyond the actual well path, which starts at the green area called "Timedrilling" in Figure 30, the trajectory maintains the same course as the last point in the successful lateral, which is the yellow area. This is only an issue when there are any sidetracks involved which usually means timedrilling and some abandoned hole meters. However, this depends on what kind of sidetrack that is utilized, either an open hole sidetrack or setting a cement plug and deflecting off of it. When drilling the 8 1/2" section below the 9 5/8 x 10 3/4" liner and tieback it's the open hole sidetrack alternative which is the preferred option besides cases that involve loss of drilling fluid to the surrounding formation which necessitates the use of a cement plug. There are different reasons for abandoning a hole which creates "failed hole meters" and performing a sidetrack, on Grane it's almost always due to shale layers which swell and/or cave inn and creates an impossible drilling environment.

When pulling back and performing an open hole sidetrack there is period of "timedrilling" involved along with creating a ledge that kicks off the well in a new direction, thereby separating the old trajectory from the new one. In order for the bit to get a hold of sufficient area to lay weight on while lying on the low side of the hole, it's necessary to reciprocate the drillstring over the same area, known as reaming, so the low side of the borehole wall gets scraped away. During this reaming period there is almost no weight on the bit and the effective rate of penetration is very low, only a few meters per hour. As the bit creates an area in front of it which it can attack, weight can be applied and the timedrilling part begins. This period is characterized by applying minimum WOB while ensuring that distance is created between the old and new well path. Even though this gives a very low ROP it's important not to apply to much WOB as this will cause the bit to slip off the newly created ledge and into the old hole. This process is time consuming, hence the name "timedrilling".

The whole process of sidetracking needs special attention when simulation it in DrillNET. Since the drillstring is reciprocated up and down several times while reaming the same area, it's important to include this distance, the total distance moved up and down while rotating the drillstring, as "distance drilled" in the simulation. It is therefore important to include every reciprocation with regards to the time being spent on it and dividing the timedrilled distance by this value, giving the effective ROP. The time spent on the timedrilling was found in the individual daily drilling reports.

11.3 Wellbore

The geometry of the wellbore must be specified, either being casing or open hole. Depending on if it's casing or open hole that is selected, the input parameters will vary accordingly. The different properties required by DrillNet for the wellbore can be found in Table 3. It's important to note that the total length of casing and/or open hole cannot exceed the well trajectory input.

Information about the casing type and setting depths is extracted from the casing tally which can be found in the daily drilling report, DBR (Daglig Borerapport). The remaining information, casing specific attributes, can be found in the Statoil Casing & Tubing Database which is a part of the DBR web version.

There are three models in Casing Wear provided to calculate the burst and collapse strength of the casing after it's been subjected to wear; Biaxial stress, API equation, OTS equation [5]. It's also possible to use the DrillNET database here.

11.4 Operations and Tubulars

The Operations page in DrillNET includes both operations and tubulars. Earlier versions of DrillNET split these two subjects apart into two different pages. Each operation needs to be specified with its own tubular configuration.

11.4.1 Operations

Each meter of drilling is specified with the following drilling parameters:

- Mud Weight [sg]
- ROP [m/hr]
- RPM
- WOB [tonnes]

The most important operational parameter, with regards to casing wear, is RPM. Besides the lateral load which isn't an operational parameter (and mostly defined by the string weight), the RPM has a huge impact on the amount of wear seen, and can be controlled. This can be seen by studying Eq. 1.7. The other parameters are either pre-defined or uncontrollable. So the natural boundary, when dividing all the operations of the 8 1/2" hole into different sections, is the variation of the RPM. Since every RPM reading has a ROP, MW and WOB reading at the same depth, it's simple to divide the operations into sections with the same value of RPM and use an average of the remaining operations parameters. To better illustrate this, an example is used in Table 5:

Table 5. Sorting of the Operational Parameters

MD [m]	RPM	ROP [m/hr]	Average ROP [m/hr]	WOB [tonnes]	Average WOB [tonnes]	MW [sg]	Average MW [sg]
1210	120	24.75		3.38		1.2	
1220	120	24.68		3.49		1.2	
1230	120	24.61		3.46		1.2	
1240	120	24.53		3.77		1.2	
1250	120	26.85		3.51		1.2	
1260	120	29.08	25.8	3.77	3.56	1.2	1.2
1270	140	25.61		4.11		1.2	
1280	140	24.99		4.11		1.2	
1290	140	24.18		4.09		1.2	
1300	140	24.26		4.29		1.2	
1310	140	25.19		4.38		1.4	
1320	140	25.42		4.46		1.4	
1330	140	25.11	25	4.53	4.28	1.4	1.29
1340	160	26.23		4.22		1.4	
1350	160	26.93		4.33		1.4	
1360	160	26.42		4.12		1.4	
1370	160	26.37		4.11		1.4	
1380	160	26.32		4.12		1.4	
1390	160	26.37	26.4	4.45	4.23	1.4	1.4

This is the first stage of sorting the operations into representative and manageable lines that can be copied and pasted into DrillNET. The second stage is to finalize the organization of the different lines in a copy/paste format like illustrated in Table 6 below:

Table 6. Input Ready Operational Parameters

Bottom of Interval	RPM	ROP [m/hr]	WOB [tonnes]	MW [sg]
1260	120	25.75	3.56	1.2
1330	140	24.97	4.28	1.29
1390	160	26.44	4.23	1.4

11.4.2 Tubulars

The geometry of the drillstring has to be specified from the bit and all the way up to the surface. Depending on the circumstances in the well at the time of entry with the 8 1/2" drilling assembly, the bottom hole assembly, BHA, is fitted accordingly. To limit the time spent on configuring the different simulations, only one BHA is chosen to be included in all the simulations. The BHA chosen is the one with the largest average O.D so that the worst case scenario is simulated. 5 1/2" drill pipe is used above the BHA. This gives the following list of tubulars with their respective properties as shown in Table 7;

Table 7. Drill String Input.

Item	Joint Length [ft]	O.D [in.]	I.D [in.]	Adjusted Weight [kg/m]	Density [kg/m3]	Youngs Modolus [kPa]
Bit	0,35	8,5	0,546	106,25	7 850	200 000 000
Autotrack	2,17	6,938	2,25	106,25	7 850	200 000 000
Mod stab	1,3	6,938	2,25	106,25	7 850	200 000 000
Deeptrack	2,11	7	2,25	106,25	7 850	200 000 000
Azitrack	7,01	7	2,25	106,25	7 850	200 000 000
BCPM	3,22	7	2,25	106,25	7 850	200 000 000
Deeptrack	6,8	7,25	2,299	106,25	7 850	200 000 000
Mod stab	1,28	6,938	2,299	106,25	7 850	200 000 000
Stop sub	0,71	6,938	2,25	106,25	7 850	200 000 000
Float sub	0,98	6,75	2,25	106,25	7 850	200 000 000
HW DP 5"	9,75	5	3	106,25	7 850	200 000 000
Jar	9,85	6,438	2,75	106,25	7 850	200 000 000
HW DP 5"	9,77	5	3	106,25	7 850	200 000 000
HW DP 5"	9,72	5	3	106,25	7 850	200 000 000
Accelerator	10,66	6,563	2,5	106,25	7 850	200 000 000
Sub	3,27	5	3	106,25	7 850	200 000 000
HW DP 5"	37,6	5	3	106,25	7 850	200 000 000

A tool joint specification of the drill pipe used is also required along with the contact length with the casing and the tool joint O.D. It's possible to use the DrillNET database which has an extensive overview over different tubulars, but to be sure of correct dimensions, the specification sheet of the drill pipe used was retrieved and used as basis.

12 DrillNET Workflow

The different input pages and the actual process of simulation in the Casing Wear section of DrillNET is discussed in the forthcoming sections.

12.1 DrillNET

As the previous Cwear editions now are built into DrillNet [1], the original Cwear program has ceased to exist as a single individual program. DrillNet version 1.7.2.2 and Casing Wear version 1.5.4.1 has been used to simulate wear in this thesis. As previously stated, the goal of this thesis is to calibrate a more specific wear factor range in the casing wear simulation program in DrillNET by comparing the output result with the actual wear results retrieved by a USIT log.

Cwear was developed by Maurer Engineering Inc. as part of the "DEA-42 Casing Wear Technology Project" [5] and evolved as a result of a riser failure and the following investigation of the incident. The casing wear model predicts the location and magnitude of wear in the casing string by:

1) Calculating the energy imparted by the rotating tool joint to the casing at multiple positions along the casing and;

2) Dividing this by the amount of energy required to wear away a unit volume of the casing.

The energy which wears away the casing is a result of the lateral force, which presses the tool joint against the casing. The lateral force is a combination of gravity, buoyancy, tension in the drillstring, and the hole trajectory geometry.

An important empirical element in this model involves the usage of a "wear factor", which has been previously described in section 1.5.1. Evaluation and application of this wear factor is the crucial element in the transition of the model from a theoretical exercise to a practical engineering tool. There is a database of wear factors available in the DrillNET program but there are many different factors which defines a specific wear factor, so a general wear factor database may not necessarily fit a specific well.

12.1.1 DrillNET input and workflow

The result of the simulation is, of course, only as good as the input that is entered into the program. In light of this, the time spent on gathering correct and exact input data is substantial.

The input pages of the casing wear section in DrillNET will be discussed in the following sections so that the pre-simulation work is linked with the actual simulation work which will help to both understand the software package and the workflow involved in simulating the amount of wear in a well, posterior to it being drilled. To get a better picture of the workflow there is a flowchart (Figure 38) prepared after all the input data in DrillNET has been discussed.

12.1.2 Survey Data

	MD (m)	Inclination (°)	Azimuth (°)	TVD (m)	NS (m)	EW (m)	HD (m)	VS (m)	DL (°/30m)	BR (°/30m)	TR (°/30m)
1	197,40	0,00	360,00	0,00	0,00	0,00	0,00	0,00	0,00	0,00	0,00
2	200,00	0,23	232,87	2,60	0,00	0,00	0,01	-0,01	2,65	2,65	-1466,96
3	210,00	0,29	332,28	12,60	0,01	-0,03	0,03	-0,02	1,20	0,18	298,24
4	220,00	0,19	331,11	22,60	0,04	-0,05	0,07	-0,01	0,30	-0,30	-3,51
5	230,00	0,22	280,51	32,60	0,06	-0,08	0,10	-0,02	0,53	0,09	-151,81
6	240,00	0,17	286,02	42,60	0,07	-0,11	0,13	-0,04	0,16	-0,15	16,53
7	250,00	0,22	247,36	52,60	0,07	-0,14	0,16	-0,07	0,41	0,15	-115,99
8	260,00	0,41	316,15	62,60	0,08	-0,19	0,20	-0,09	1,17	0,57	206,38
9	270,00	0,07	228,91	72,60	0,11	-0,22	0,24	-0,10	1,24	-1,02	-261,73

Figure 31. Survey Data

A trajectory which includes the measured depth along the well path, the azimuth and the inclination is required so that the program can fill in the remaining information based on these three variables. The remaining information includes:

- TVD – True Vertical Depth [m]
- NS – North South axis [m]
- EW – East West axis [m]
- HD – Horizontal Displacement [m]
- VS – Vertical Section [m]
- DL – Dogleg [°/30 m]
- BR – Build Rate [°/30 m]
- TR – Turn Rate [°/30 m]

There are two main ways of entering this information, either manually by entering each number into its respective cell, or by copying the three required variables from another source and

pasting it into the survey page illustrated in Figure 31. A third option of importing a specific file type is also available, though the format of the imported file has to be arranged. When all required information is entered, a 2D and 3D representation of the well path is available along with two separate graphs displaying measured depth versus dogleg and inclination. It's important to check the dogleg graph in case there are unrealistically high values present.

12.1.4 Wellbore

	Type		Bottom MD (m)	OD (in)	ID (in)	Yield Strength (kPa)	Density (kg/m³)	Wear Limit %
1	Casing/Liner	∨	2478,34	10,750	9,660	758143	7850,0	0,0
2	Casing/Liner	∨	2514,74	10,750	9,660	551858	7850,0	0,0
3	Casing/Liner	∨	2678,70	10,750	9,660	758143	7850,0	0,0
4	Casing/Liner	∨	3101,40	10,750	9,660	758143	7850,0	0,0
5	Casing/Liner	∨	3137,98	10,750	9,660	551858	7850,0	0,0
6	Casing/Liner	∨	3211,56	10,750	9,660	758143	7850,0	0,0
7	Casing/Liner	∨	3323,67	10,750	9,660	551858	7850,0	0,0
8	Casing/Liner	∨	3539,16	9,625	8,535	551480	7850,0	0,0
9	Open Hole	∨	6704,00		8,550			

Figure 32. Wellbore Data

Each meter of the well has to be specified as:
- Riser
- Center of Rotation
- Flex Joint
- Casing/Liner, or
- Open Hole

The column furthest to the right in Figure 32 shows the option of including a specific wear limit percentage which will be shown as a line in the wear graph after the simulation is performed. The purpose of this line is to show where you have exceeded a pre-determined wear value along the graph. Since this is not of interest in this thesis it has not been added.
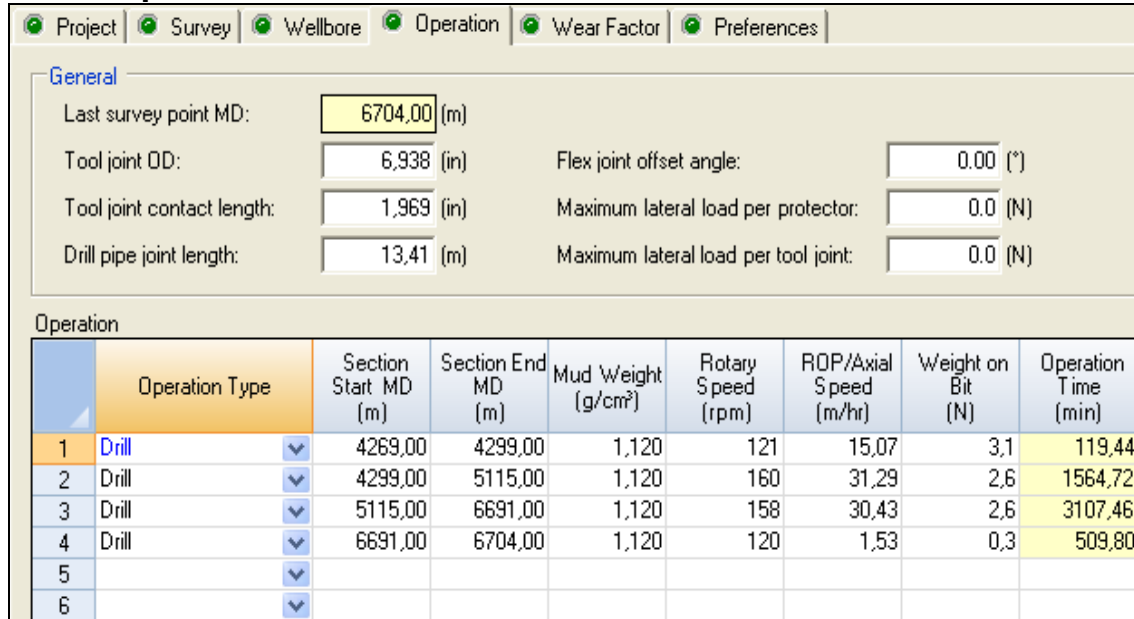
12.1.5 Operation and Tubulars

Figure 33. Operation Data

The Operation page shown in Figure 33 is the most time consuming page when simulating as it includes all the operations along with the tubulars used in each operation. There are three kinds of operations to choose from, these are;

- Drill
- Ream, and
- Rotate Off Bottom

The flex joint offset angle option is mainly for floating rigs that use risers. When the rig isn't directly above the well slot it creates an offset angle which must be compensated for. The flex joint compensates for this but creates an inevitable wear point with the increased dog leg angle. There is also an option of setting a maximum lateral load value to any protectors connected to the drillstring. If the protectors can withstand a certain lateral load value it's important to know if this value is exceeded, possibly rendering the device useless. The same principle applies to the box below which sets a value for the maximum lateral load per tool joint.

When filling in the different operation parameters it's important to keep in mind that the units can be customized to allow for non SI units.

Tubulars (from downhole to surface) - for operation row: 1						
	Length (m)	OD (in)	ID (in)	Adjusted Weight (kg/m)	Density (kg/m³)	Young's Modulus (kPa)
1	0,35	8,500	0,546	106,250	7850,0	200000000
2	2,17	6,938	2,250	106,250	7850,0	200000000
3	1,30	6,938	2,250	106,250	7850,0	200000000
4	2,11	7,000	2,250	106,250	7850,0	200000000
5	7,01	7,000	2,250	106,250	7850,0	200000000
6	3,22	7,000	2,250	106,250	7850,0	200000000
7	6,80	7,250	2,299	106,250	7850,0	200000000
8	1,28	6,938	2,299	106,250	7850,0	200000000
9	0,71	6,938	2,250	106,250	7850,0	200000000
10	0,98	6,750	2,250	106,250	7850,0	200000000
11	9,75	5,000	3,000	106,250	7850,0	200000000
12	9,85	6,438	2,750	106,250	7850,0	200000000
13	9,77	5,000	3,000	106,250	7850,0	200000000
14	9,72	5,000	3,000	106,250	7850,0	200000000
15	10,66	6,563	2,500	106,250	7850,0	200000000
16	3,27	5,000	3,000	106,250	7850,0	200000000
17	37,60	5,000	3,000	106,250	7850,0	200000000

Figure 34. Tubular Data

When the different operations are filled in, each line has to be connected to a drillstring assembly which is shown in Figure 34. As there is only one drillstring assembly used the configuration in Figure 29 will apply for every operation line in Figure 28.
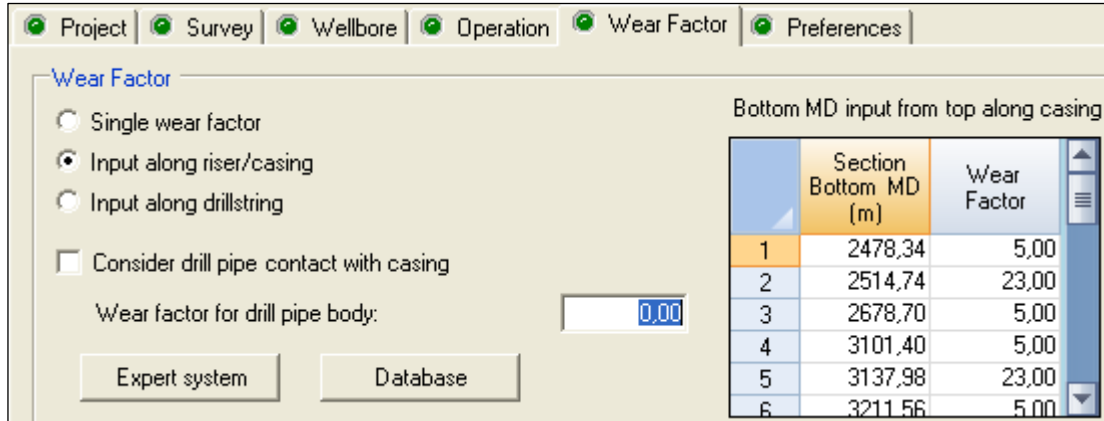
12.1.6 Wear Factor

Figure 35. Wear Factor

Trying to calibrate a wear factor according to the measured wear that is observed is a trial and error based process. Different wear factors have to be tried and the simulated wear curve which is created based on the wear factor chosen has to be compared to the actual wear curve. This process is repeated until a satisfactory wear factor that covers the worst case scenario is found. The worst case scenario simulation is when the simulated curve covers the highest peaks seen on the actual wear plot, as illustrated in Figure 36. This figure also shows how a trend case is adjusted to fit with the actual wear curve which is called the base case scenario. The wear factor chosen for the base cases are determined by the best trend fit that illustrates a moving average of the entire well.
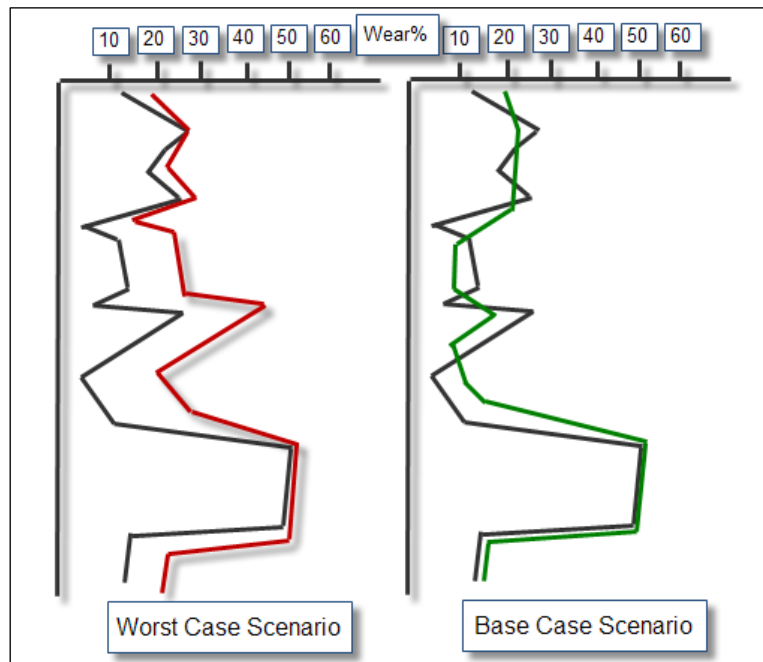

Figure 36. Worst Case Scenario vs. Base Case Scenario

Before choosing a wear factor, the different casing materials have to be split into sections to allow for differentiation with respect to the applied wear factor, shown in the table in Figure 35. This option is located in the Wear factor menu as "Input along riser/casing".

The wells simulated in this thesis all have sections of 13% chrome alloy in steel. The option of considering drill pipe contact with the casing means that the body of the drill pipe, the section between the tool joints, contacts the casing wall and thereby induces additional wear. This may only be considered when the drill pipe is under a high tensional load and passes through a section of the well path that is sufficiently sharply curved, so that the drill pipe body can contact the convex side of the casing. Thus, the resultant wear rate of the casing will be affected not only by the characteristics of the tool joints, but by the wear characteristics of the drill pipe body as well. This issue is more relevant for floating installations which have flex-joints above the BOP that compensates for doglegs which are created by the moving rig. The "Expert system" and the "Database" is an aid in the selection of a wear factor and incorporate results from the DEA-42 laboratory testing.

As previously mentioned there is one simulation for each of the laterals, including the main bore. When a wear factor has been chosen and there is a green sign in all of the input pages which indicates that everything has been addressed, the actual simulation can take place by pressing the play button in the menu. This generates the wear log data which is shown in Figure 36 and is visible after pressing the rewind button that says "Go to input page" directly to the left of the play button that starts the simulation. Immediately after pressing the play button the output data pops up which contains a summary of the simulation results along with different graphs and tables. Coming back to the wear factor page shown in Figure 35, the first simulation will appear as shown in Figure 37 with no "current wear".

Before the second simulation of lateral number two can begin this has to be updated by pressing "update to previous wear" so that the different simulation results builds on top of each other. When the last lateral is simulated the Wear% column in the output data in Figure 37 is compared to the USIT log data. This is done by plotting them both in the same graph which allows for easy comparison. The two cases which are focused on in this thesis are the worst case scenarios which are called the max cases, and the trend cases which are called the base cases. When a wear factor that represents these two scenarios has been found, the simulation is considered satisfactory. If the simulated case doesn't match the USIT log data the entire process has to be repeated with a new wear factor.

Figure 37. Wear Log Data

12.1.7 Preferences

Figure 38. Preferences

There are a few preferences to choose from when setting up each simulation. When it comes to the buckling model options shown in Figure 37 the Dawson/Paslay (sinusoidal) and Chen/Cheatham (helical) criteria were chosen. The reason for this choice is that it's the most conservative approach thereby displaying the worst case scenario. In a curved hole this criteria doesn't take into account that the drillstring is resting on the low side of the hole which reduces the required axial load that initiates buckling.

The preferred burst and collapse strength option are the OTS (Oil Technology Services) equations which take into account that it's a crescent shaped wear groove and not uniformly shaped wear with a representative minimum wall thickness for the entire circumference. This approach gives a more realistic determination of the burst and collapse strength because of the pressure reinforcement from the remaining unworn casing wall which isn't considered when using biaxial or API equations.

Since helical buckling isn't an issue on Grane it's not been used in the simulation. The "bending stiffness considered" box has been checked to allow for the added wear of a stiff drilling assembly. The stiffer the drilling assembly the higher the normal force is on the casing/bore hole wall, thereby increasing the amount of wear.

To get a better understanding of the workflow Figure 34 illustrates the sequence in which the simulation has been approached.
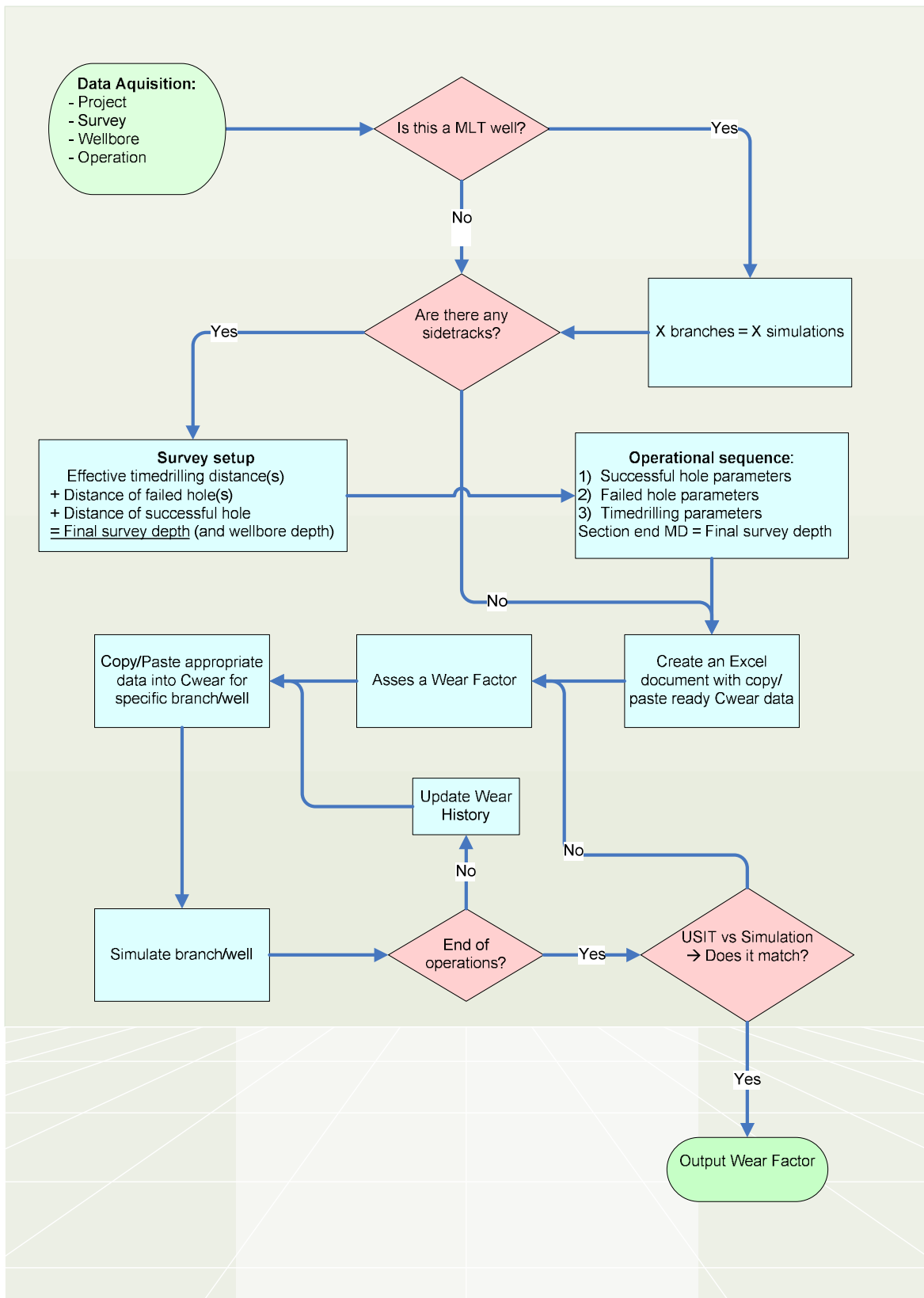
Figure 39. Flowchart of Simulation Workflow

13 Simulation Results

The forthcoming sections include the simulation results for the wells simulated in this thesis and a discussion of the USIT results and the wear factors used to create the simulation results in each individual well. A deeper discussion of the simulation results compared with the actual wear seen in the well can be found in chapter 13.

13.1 Grane Well 25/11 - G-3

G-3 consists of three laterals Y1, Y2 and Y3 which are drilled in the north-east direction. A steady production is ensured by the use of gas lift.

When including all the sidetracking involved in reaching the target depths, TD, of the different laterals, the well consists of the following 8,5" drilled distance:

Table 8: G-3 – Accumulated 8,5" drilled distance

Section	Distance drilled (m)
AY1	1393
AY1 T2	866
Timedrilling AY1 to AY1 T2	22
AY2	1222
AY2 T2	953
Timedrilling AY2 to AY2 T2	26
AY3	1576
AY3 T2	846
Timedrilling AY3 to AY3 T2	13
TOTAL	6917

The liner and tie-back program for the well is as follows:

Table 9: G-3 – Casing program

Casing dimension	Type	Grade	Bottom MD [m]	Top MD [m]	Weight [lbs/ft]
9 ⅝"	Liner	L80 13 Cr	3539,16	3323,67	53,5
10 ¾"	Liner	L80 13 Cr	3323,67	3211,56	60,7
10 ¾"	Liner	P-110	3211,56	3137,98	60,7
10 ¾"	Liner	L80 13 Cr	3137,98	3101,40	60,7
10 ¾"	Liner	P-110	3101,4	2678,70	60,7
10 ¾"	Tieback	P-110	2 678,70	2514,78	60,7
10 ¾"	Tieback	L80 13 Cr	2514,74	2478,34	60,7
10 ¾"	Tieback	P-110	2478,34	0	60,7

13.1.2 G-3 USIT

A USIT/CBL dataset was recorded in well 25/11-G-03 on 18th Mar 2010 in the 10 ¾" liner and tie back from Surface-3293mMD. The objectives for the 10 3/4" logging were to check for casing wear and cement bond so that a suitable depth for setting the production packer could be found.

The USIT log was recorded at a 5 degree, 3" resolution. The tool eccentralization was generally within specification (0.215in) throughout the log, where it is not it does not appear to degrade the data quality. The first reflected arrival from the inside of the casing was strong, indicating that the liner and tieback was clean and smooth (no rugosity). The USIT signal was therefore good for processing the casing thickness and cement information, and consequently there were no processing flags present on the log which would indicate signal disturbance. For some reason not understood the measured radius was "noisy" which could indicate some kind of sub movement while it is rotating. This disturbance does not affect the interpretation since the more robust casing thickness measurement is the primary tool used for assessing the degree of casing wear. In general, the USIT log quality was good.

13.1.3 G-3 Wear Factor

The wear factors which makes the simulation plot fit locally with the maximum peaks measured are tabulated in Table 10 below and illustrated in Figure 40;

Table 10. G-3 - Wear Factors

Base Case		Max Case	
P-110	Chrome	P-110	Chrome
0,05	7	6	7

Even though the wear in the G-03 well as seen in Figure 35 doesn't look any different from other wells simulated with respect to the wear values, the wear factor is considerably higher for the P-110 steel and considerably lower for the chrome intervals. Even though the trend is as expected, the peaks in the P-110 section are as high as the chrome section trend which means that there isn't much difference in the simulated trend when comparing the P-110 steel and the chrome intervals, hence the small difference between the wear factor values. It's mainly the peak at 2750 mMD which forces the simulated plot away from the actual wear creating the higher wear factor value.
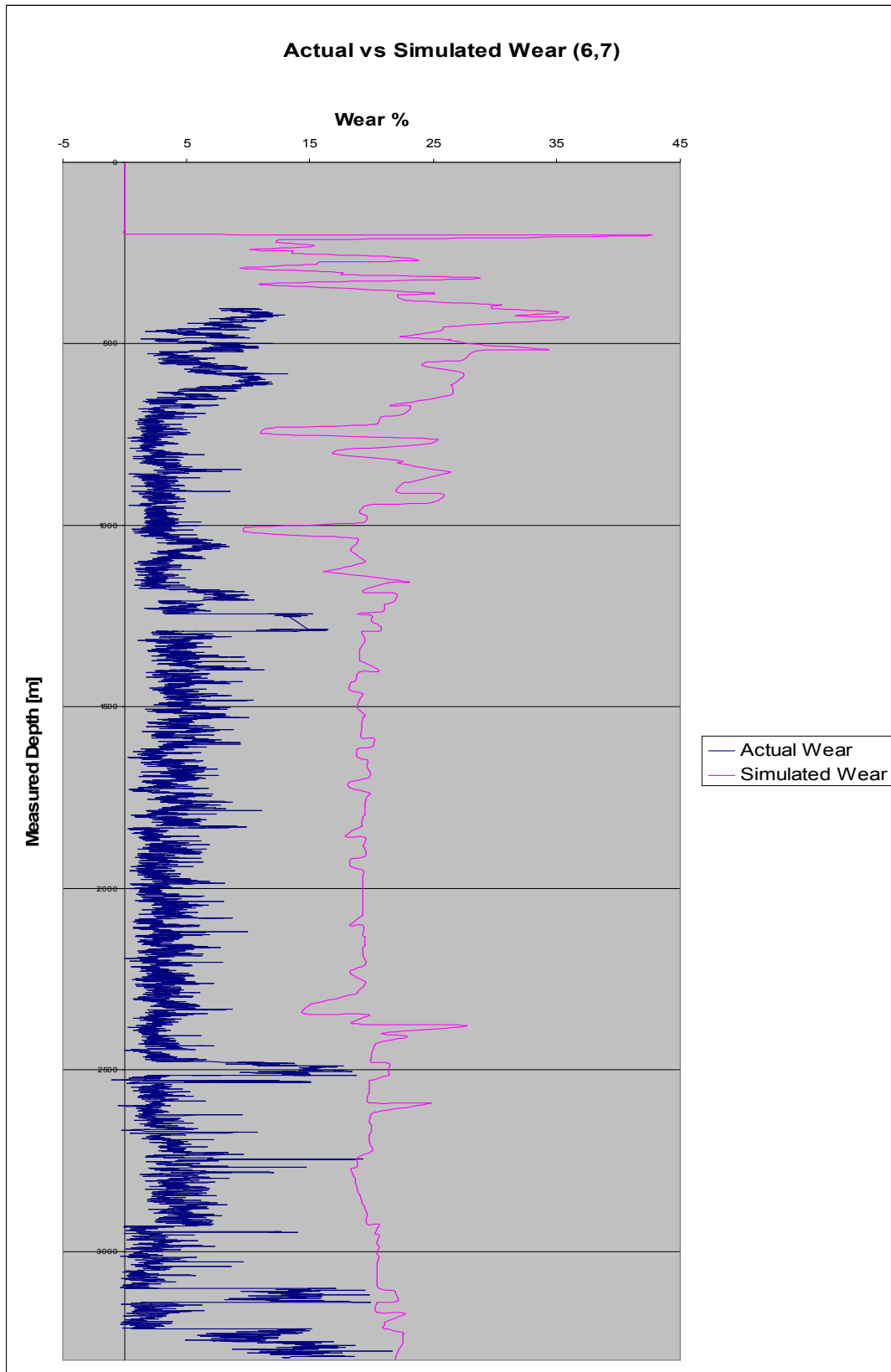
Figure 40. G-3 – Actual vs. Simulated Wear

13.2 Grane Well 25/11 - G-7

G-7 is a 3 branched multilateral oil producer with 2 long branches north and 1 shorter branch towards the east. The objective of this well is to drain the area east and south of well G-13.

When including all the sidetracking involved in reaching the targets depths, TD, of the different laterals, the well consists of the following 8,5" drilled distance:

Table 11: G-7 – Accumulated 8,5" drilled distance

Section	Distance drilled
AY1	374
AY1 T2	2390
Timedrilling AY1 to AY1T2	18
AY2	387
AY2 T2	551
AY2 T3	415
AY2 T4	2184
Timedrilling AY2 to AY2 T2	20
Timedrilling AY2 T2 to AY2 T3	42
Timedrilling AY2 T3 to AY2 T4	21
AY3	435
AY3 T2	347
AY3 T3	1521
Timedrilling AY3 to AY3 T2	21
Timedrilling AY3 T2 to AY3 T3	19
Total	8745

The liner and tie-back program for the well is as follows:

Table 12: G-7 – Casing Program

Casing dimension	Type	Grade	From MD [m]	To MD [m]	Weight [kg/m]
9 ⅝"	Liner	L-80 13 Cr	4249,65	4438,34	79,62
10 ¾"	Liner	P-110	4237,62	4249,65	90,33
10 ¾"	Liner	L-80 13 Cr	4167,01	4237,62	90,33
10 ¾"	Liner	P-110	3482,55	4167,01	90,33
10 ¾"	Tieback	P-110	0	3482,55	90,33

It's important to note that AY1 and AY1 T2 is drilled before the tie-back is installed thereby exerting the wear on the 14" x 13 3/8" casing instead of the 10 3/4" casing. This is adjusted for in the simulation and will reduce the wear observed in the actual wear plot.

13.2.1 G-7 USIT

A USIT/CBL dataset was recorded in well 25/11-G-7 on 15.11.2010 in the 10 ¾" liner & tieback from 4225 mMD RKB to surface. Since the primary cement job in the 9 5/8" x 10 3/4" liner failed the objectives for this USIT and CBL log was to re-evaluate the cement bond quality in the liner part and to determine a setting depth for the production packer which is based on the amount of wear at the setting depth.

The USIT log was recorded at a 5 degree, 3" resolution. The eccentralization is mostly within tolerance, the reflected signal amplitude is strong and therefore there are very few processing flags. Manufacturing patterns are observed on both the radius and the thickness images but the average internal radius and average thickness measurements are close to nominal. To sum up, the log quality is generally good except one short interval at the bottom of the log from 4177-4189 mMD RKB. It appears to be excessive tool eccentralization that has resulted in this reduced log quality.

13.2.2 G-7 Wear Factor

The wear factors which makes the simulation plot fit locally with the maximum peaks measured are tabulated in Table 13 below and illustrated in Figure 41.

Table 13. G-7 - Wear Factors

Base Case		Max Case	
P-110	Chrome	P-110	Chrome
0,04	13,5	3	13

Figure 34 contains a plot of the actual wear together with the simulated wear. The trend of this simulated wear plot is fairly good compared to the actual wear plot even though there are some areas within the first 1500 mMD which doesn't match. Somehow is seems like the simulation results are a bit offset on the y-axis in the increasing measured depth direction even though the chrome interval at 4167 mMD matches. Why this occurs is hard to decide but the important thing is that the trend of the simulated wear plot corresponds to the actual wear plot. Another observation of mismatch is in the interval 1150 to 1180 mMD where there is evidence of a differing trend. Figure 34 clearly shows a drastic reduction with regards to wear in this interval, the difference being approximately 4% between actual and measured. Even though this isn't critical it's hard to come up with a reasonable explanation to this occurrence since the other influencing parameters stay unchanged through this interval.
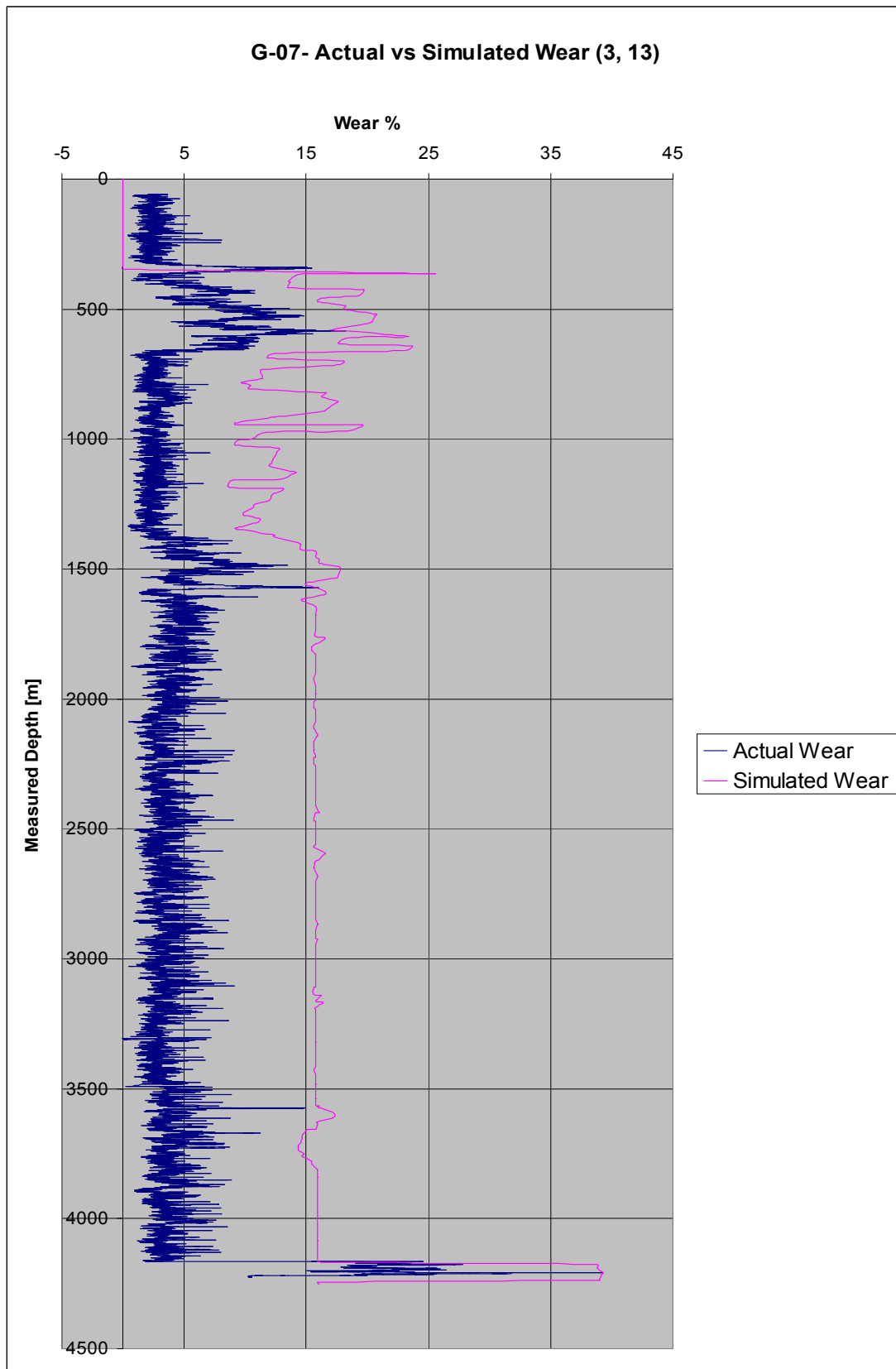
Figure 41. G-7 – Actual vs. Simulated Wear

13.3 Grane Well 25/11 - G-13

Well 25/11 G-13 Y1 was the first branch of planned four branched oil producer in the western part of the northern Heimdal reservoir segment. Due to severe drilling problems caused by unexpected shales, the second branch was converted into an observation well, leaving three branches for oil production.

When including all the sidetracking involved in reaching the targets depths, TD, of the different laterals, the well consists of the following 8,5" drilled distance:

Table 14: G-13 – Accumulated 8.5" drilled distance

Section	Distance drilled
Y1 T3	1472
Timedrilling Y1T2 to Y1 T3	15
Y2	2474
A	347
B	366
Y3	475
Y3 T2	711
Y3 T3	1240
Timedrilling to A	19,6
Timedrilling A to B	17,5
Timedrilling Y3 to Y3 T2	9
Timedrilling Y3 T2 to Y3 T3	20
Total	7166

The liner and tie-back program for the well is as follows:

Table 14: G-13 – Casing program

Casing dimension	Type	Grade	From MD [m]	To MD [m]	Weight [lbs/ft]
9 ⅝"	Liner	L80 13 Cr	4580,19	4777,19	53,5
10 ¾"	Liner	S13Cr-110	4122,47	4580,19	65,7
10 ¾"	Liner	P-110	3931,83	4122,47	60,7
10 ¾"	Liner	S13Cr-110	3810,97	3931,75	65,7
10 ¾"	Tieback	P-110	3426,25	3810,97	60,7
10 ¾"	Tieback	S13Cr-110	3379,56	3426,25	65,7
10 ¾"	Tieback	P-110	1284,87	3379,52	60,7
10 ¾"	Tieback	S13Cr-110	1238,56	1284,87	65,7
10 ¾"	Tieback	P-110	0	1238,56	60,7

13.3.1 G-13 USIT

A USIT/CBL dataset was recorded in well 25/11–G-13 on 23.09.2009 in the 10 3/4" liner & tieback from 4450 to 51 mMD RKB. Like the other wells the purpose of this USIT & CBL run was to find a suitable depth for setting the production packer and checking the general condition of the casing and liner. The max level of tool eccentralization, 0.21 inches in 10 3/4", is exceeded at short intervals throughout the chrome interval from 4552 meters to 3931 meters; however, no data degradation has been detected after reprocessing the logs.

The minimum remaining wall thickness as measured is around 0.3 inches throughout the chrome intervals. This relative reduction is a combination of manufacturing effects, wear and internal corrosion. 0.3 inches corresponds to a wall loss of 49.5% with respect to theoretical nominal dimensions. It should be noted that wear is most serious in absolute terms where it has occurred across areas of pipe which was already relatively thin due to the manufacturing process.

13.3.2 G-13 Wear Factor

The wear factors which makes the simulation plot fit locally with the maximum peaks measured are tabulated in Table 15 below and illustrated in Figure 42.

Table 15. G-13 - Wear Factors

Base Case		Max Case	
P-110	Chrome	P-110	Chrome
0,05	21,5	2,5	21,5

The simulated wear follows the actual wear plot trend throughout the entire interval that was logged but the difference between the trend of the actual wear and the simulated wear plot is approximately 10% when simulating for the maximum observed wear. The peak at around 200 meters is due to an abrupt dogleg of almost 4° in the simulation. The combination of the softer 13% chrome steel interval and a dogleg of about 3,5-4° creates the peak of 68% wear seen at 1250 mMD. Further down along the plot the chrome interval at 3390 mMD shows a simulated value which is about 20% higher than the actual value. This is due to the third and last chrome interval at 3810 mMD which requires the wear factor of 21,5 to stay above the measured wear value.
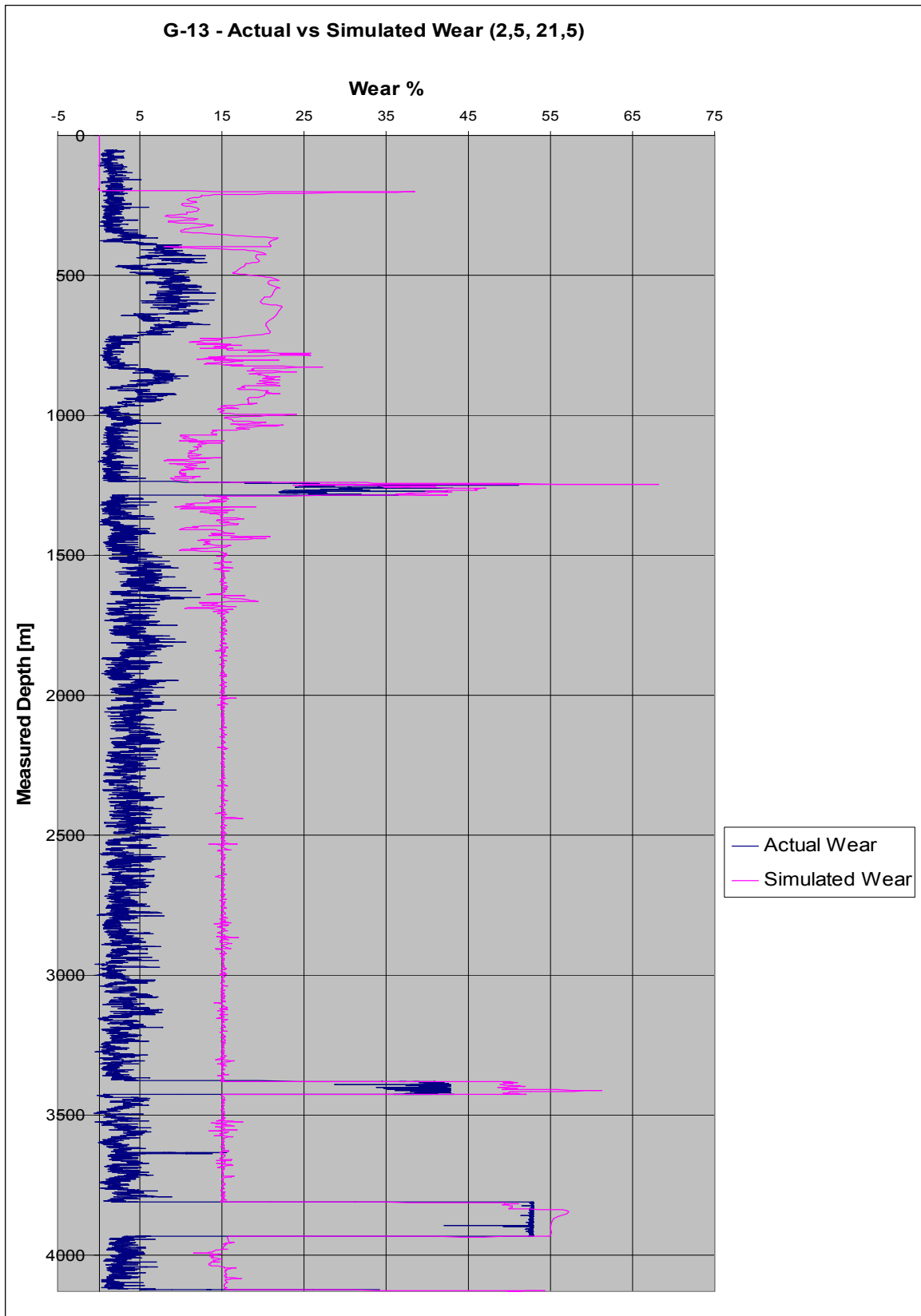
Figure 42. G-13 – Actual vs. Simulated Wear

13.4 Grane Well 25/11 - G-15

Well 25/11 G-15 was planned and executed as a 3 branched multilateral oil producer.

When including all the sidetracking involved in reaching the targets depths, TD, of the different laterals, the well consists of the following 8,5" drilled distance:

Table 16: G-15 – Accumulated 8.5" drilled distance

Section	Distance drilled
AY1	1275
AY1 T2	721
Timedrilling AY1 to AY1 T2	53
AY2	1400
AY2 T2	2975
Timedrilling AY2 to AY2 T2	29
AY3	1206
AY3 T2	320
AY3 T3	1439
AY3 T4	1985
Timedrilling AY3 to AY3 T2	24
Timedrilling AY3 T2 to AY3 T3	23
Timedrilling AY3 T3 to AY3 T4	26
Total	11476

The liner and tie-back program for the well is as follows:

Table 17: G-15 – Casing program

Casing dimension	Type	Grade	From MD [m]	To MD [m]	Weight [lbs/ft]
9 ⅝"	Liner	L80 13 Cr	2028,54	2498	53,5
10 ¾	Liner	L80 13 Cr	1841,59	2028,54	60,7
10 ¾	Tieback	P-110	1824,44	1841,59	60,7
10 ¾	Tieback	L80 13 Cr	1776,13	1824,44	60,7
10 ¾	Tieback	P-110	1727,81	1776,13	60,7
10 ¾	Tieback	L80 13 Cr	1691,95	1727,81	60,7
10 ¾	Tieback	P-110	1621,02	1691,95	60,7
10 ¾	Tieback	L80 13 Cr	1597,15	1621,02	60,7
10 ¾	Tieback	P-110	0	1597,15	60,7

13.4.1 G-15 USIT

A USIT/CBL dataset was recorded in well 25/11–G-15 on 25.02.2009 in the 10 3/4" liner & tieback from 1997 to 107 mMD RKB. Like the other wells the purpose of this USIT & CBL run was to find a suitable depth for setting the production packer and checking the general condition of the casing and liner. Overall data quality is high with manufacturing patterns being clearly identifiable on the thickness and radius images. Even though there are some process flags shown at short intervals, these have been studied in detail and do not appear to degrade the log quality. There is only one very short interval at 1965 meters where the maximum degree of tool eccentralization (2% of pipe OD) is exceeded.

The chrome intervals show a minimum remaining wall thickness of around 0,39 inches, which corresponds to a wall loss of 28%, at several depths and is always associated with an internal groove. The relative reduction is a combination of manufacturing effects, wear and internal corrosion. Above 1597 meters the tieback consists of P-110 steel all the way up to surface and shows no significant sign of wear except at 780 meters where some drill-pipe wear is evident.

13.4.2 G-15 Wear Factor

The wear factors which makes the simulation plot fit locally with the maximum peaks measured are tabulated in Table 18 below and illustrated in Figure 43.

Table 18. G-15 - Wear Factors

Base Case		Max Case	
P-110	Chrome	P-110	Chrome
0,01	21	1,6	21

G-15 has been the most challenging well with regards to matching the actual wear with the simulated wear. The reason for this is the varying dogleg degree down the entire logged interval. Because the simulated wear plot covers the maximum wear case, the peaks and troughs become more exaggerated than the actual wear plot, especially when dealing with such a varying dogleg degree. As with the G-13 well the last chrome interval has a simulated wear value much higher than the actual value. Therefore the first chrome interval is the governing one with regards to setting a wear value for the chrome material. Because of a steady increase in the normal force against the casing along all the chrome intervals, the simulated wear plot increases even though this isn't observed along the actual wear plot. This is probably due to the varying dogleg within the chrome interval (1,25-3).
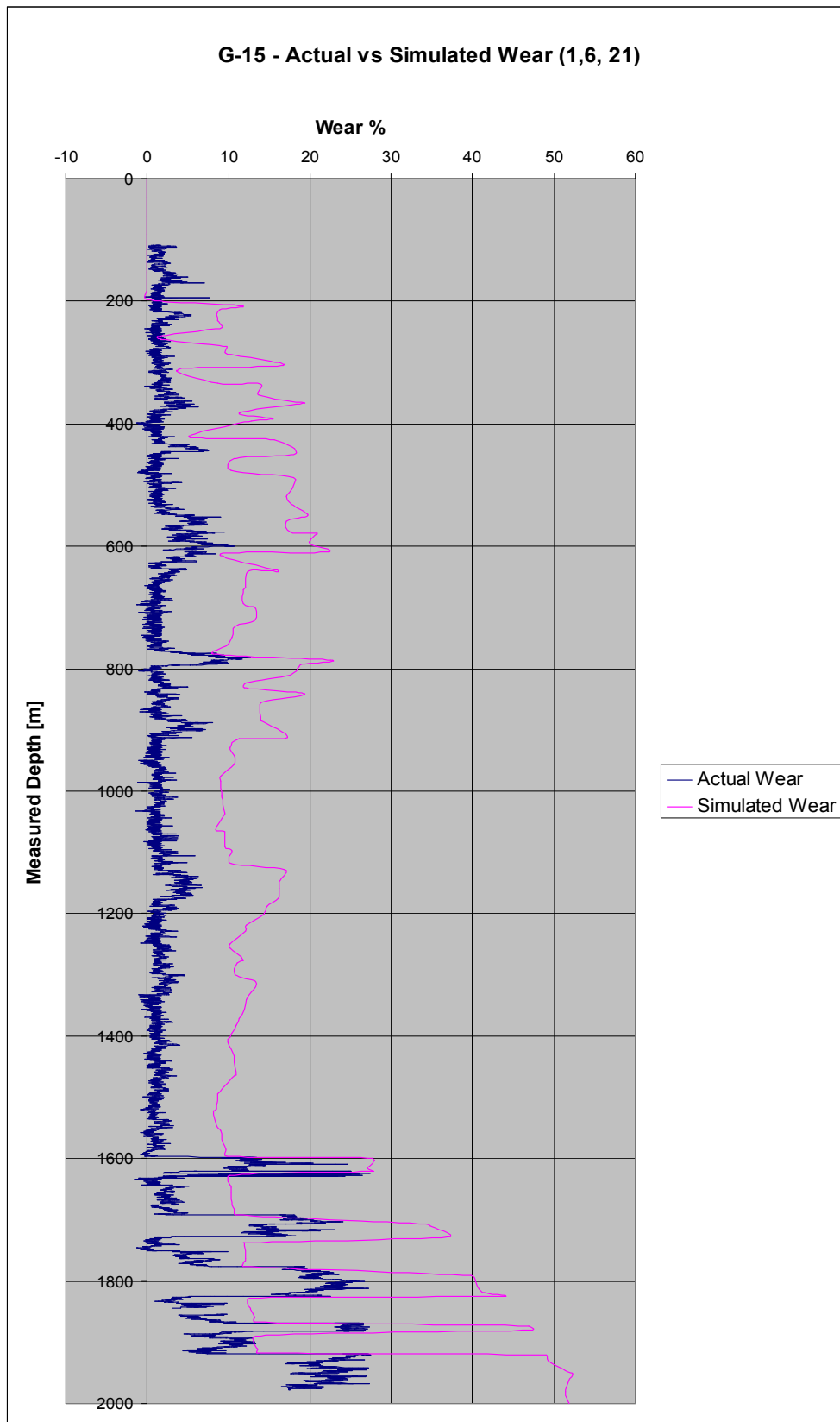
Figure 43. G-15 – Actual vs. Simulated Wear

14 Discussion

When looking at the different actual wear plots for the simulated wells along with Figure 44, it's clear that the wear trend lies in the region of 1-5% for the P-110 steel. Figure 44 shows how different intervals of wear are distributed amongst the total wear. G-15, for example, has around 30% of its wear in the region of 2-2,99% of the wall thickness. The chrome intervals, depending on the number of joints used, will contribute to an increase in the higher wear percentage intervals. But it's the unpredictable peaks which have to be accounted for that dictates what wear factor is to be used and thereby shifting the simulated wear plot away from the trend of the actual wear plot.
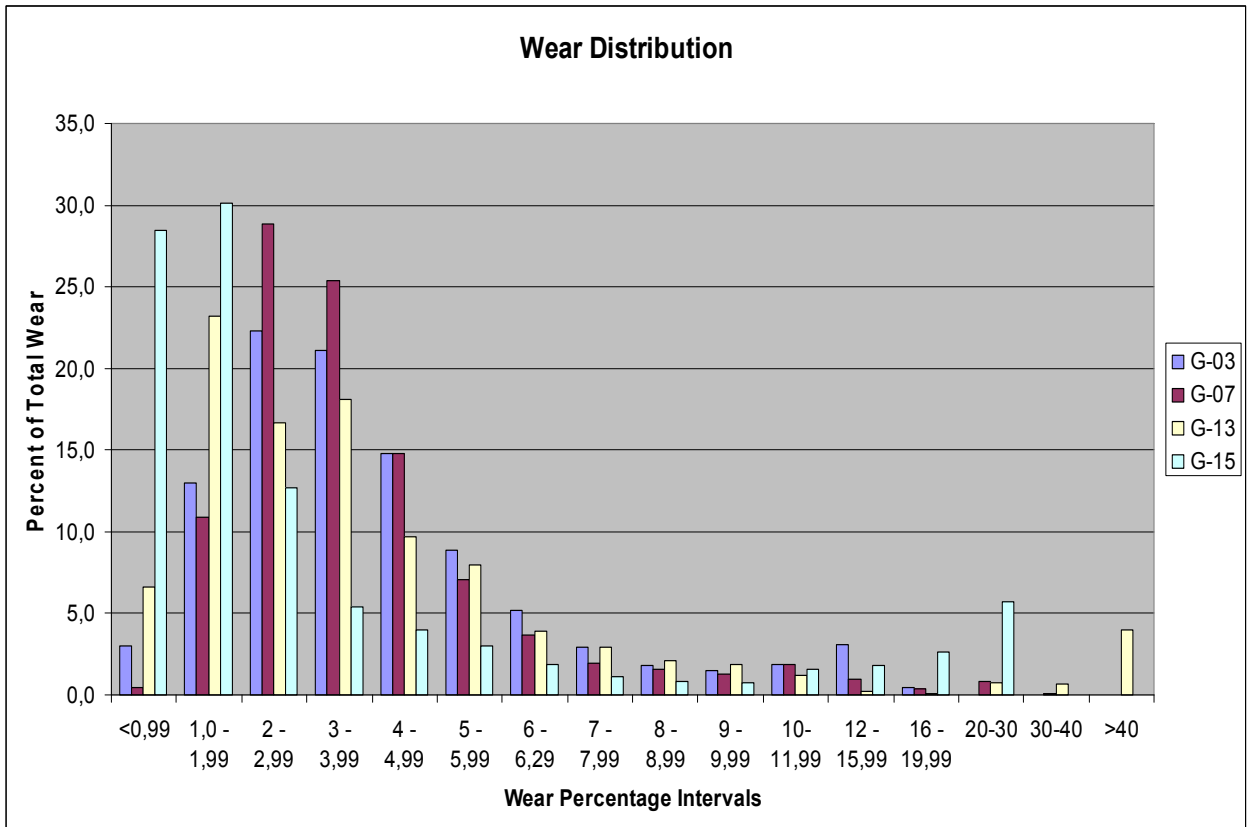
Figure 44. Wear Distribution.

Since it's the maximum wear which is of importance when designing a well with regards to the casing, the base case, which follows the trend of the actual wear plot, has been included in the appendix for reference. This is to illustrate the difference in wear factors when simulating a base case and a max case. It makes it easier to understand how big an impact the unexpected peaks have on the simulations results.

The simulation work done on the wells in this thesis shows that it's the wear peaks that determine the appropriate wear factor for each individual well and that it's hard to accurately predict the value of these peaks before a well is drilled. Therefore some key data has been studied in order to try and find a connection between the level of wear in each well, the predictability of the peaks seen and the wear factors used.

Table 19 gives an overview of the bit rotating time and the amount of bit revolutions which have been registered when drilling the 8 1/2" sections along with the total 8,5" distance drilled and the wear factors chosen to represent the maximum wear case. (Note that G-07 Y1&Y1T2 is drilled before the tie-back is installed → corrected for where appropriate). The wear factor and total wear volume values are based on the maximum wear cases.

Table 19. Well Data and Wear Factors

Measurement	G-03	G-07	G-13	G-15
8,5" Distance Drilled [m]	6917	8745	7166	11476
Total Revolutions	2622452	2687881	6048679	4588097
Bit Rotating Time [Hrs]	392	668	1196	784
WF - Steel	6	3	2,5	1,6
WF - Chrome	7	13	21,5	21

The wear factor for steel in G-03 is with its value of 6 close to two and a half times the value of the wear factor used in G-13. At first this was somewhat puzzling since G-03 is the well with the fewest revolutions and bit rotating hours while G-13 has over double the total revolutions value and triple the bit rotating time, but approximately the same 8,5" drilled distance. After considering the cause for these numbers an explanation is proposed. When the rotating tool joint contacts the casing wall for the first time a line contact occurs which produces high contact pressures since there is a large force against a small area. As the casing wear progresses, the wear groove becomes wider and the contact pressure decreases, resulting in a transition from adhesive wear to abrasive wear [42] , and as a consequence, lower wear.

So, when the amount of wear in the different wells seem to lie in the region of 1-5% and follow a similar trend with respect to the amount of wear seen, the steel must be worn away at a higher rate in G-03 compared to G-13. To compensate for this the wear factor value is, as mentioned above, over two and a half times higher in G-03 compared to G-13. The fact that the total wear volume in G-13 is close to 3 times higher than in G-03 supports this explanation. Since the observation of difference in wear factor is based on the maximum wear plot it might give an unjust approximation towards the actual wear because of the peak severnes and if they are genuine or not.

The chrome sections seem to be worn away at a more even and increasing rate. But as with the steel sections there peaks in the chrome sections which will to some degree determine the wear factor that is to be used. The G-15 plot seen in Figure 43 clearly shows how the simulated trend

in the bottom chrome region deviates with the actual trend which leads to a maximum wear difference of approximately 25 percent.

In appendix C there are plots showing the simulated wear% and the simulated dogleg severity as a function of measured depth. The theory says that with an increase in the dogleg severity the wear will increase as a result of an increase in the normal force against the casing, making the dogleg severity directly proportional to the wear. This can be seen by equation 1.7 (section 1.5.1). The plots in appendix C support this theory to some degree when comparing the two graphs in the same plot. If the plots in appendix C are further compared to the inclination plots in appendix A, it can be observed that the build section in every well simulated have doglegs which are relatively high up in the well. In these shallow dogleg sections where the well is increasing in inclination one can see that the wear% follows the trend of the dogleg severity plot. But when following this comparison further down the well it is evident that this trend weakens.

There are severe peaks in the dogleg severity which doesn't give an increase in the wear%, both in the sail sections and along the horizontal sections. This can to some degree be explained by the fact that the tension of the drillstring is at its highest at the surface and decreases with the decreasing weight of the drillstring down along the well, which makes the effect of a shallow dogleg much more crucial than a deeper one. Even though the trend is expected to weaken as suggested above, the wear% should not be completely unaffected by the dogleg severity.

When the wells were simulated in DrillNET the survey information input was retrieved in the Landmark program called Compass. This program is used to plan the well path and store the directional data for the drilled well where. The distance between every survey point is approximately 28 meters and DrillNET uses this directional data to calculate the dogleg severity per 1 to 30 meters. The USIT, which the wear% is calculated from and the actual wear plot is created by, takes a measurement every 0,15 or 0,30 meters, depending on what is decided when planning the job. This fact, that there is such a large difference in the measured depth between the survey input/output points and the actual wear measurement points, creates a potential deviation between the actual wear curve and the simulation wear curve. It may also help explain some of the wear peaks seen in the actual wear plot and not in the simulated wear plot.

When the dogleg severity is based on survey station input with intervals of 28 meters between them, DrillNET makes a trend based approach to connect these points, effectively masking out any doglegs that appear between them. A rule of thumb says that to obtain an accurate measurement of dogleg severity it is required to have a survey interval that is less than half the length of the dogleg, or else part of the of the survey interval will always fall outside of the dogleg, and the measured dogleg severity will always be smaller than the actual dogleg severity. Casing wear calculations are often made on survey data taken at 30 meter intervals and it has been shown that this may result in dogleg severity and casing wear predictions that are 50 to 75% lower than the actual values [5]. This shows the importance of accurately measuring dogleg severity and explains why casing wear is often much greater than predicted by casing wear models.

Based on the observations pointed out in this discussion there are a few factors that can help to explain why it's hard to make a good fit between the actual wear and the simulated wear. The most important task lies in the pre-simulation work of removing the unreal peaks in the actual wear data. The more accurate the actual wear data is, the better it will fit with the simulated wear curve.

15 Conclusion

Based on the simulations done on the wells in this thesis and the work associated, it can be concluded with;

- The worst case wear factors used (Table 19) gives an interval of 1,6 to 6 for steel and 7 to 21 for chrome.
- The peaks in the actual wear graph dictates the appropriate wear factor to be used. When trying to match the simulation results with the actual wear measured by the USIT log, the wear peaks in the actual wear plot will decide the value of the wear factor. For an untrained eye it can be difficult to distinguish genuine peaks from undesired ones caused by some disturbance in the tool measurement or by the drill pipe connection filtration (see section 11.1).
- Wear peaks occurring at places where there is no registered increase in dogleg severity, or other varying wear parameters, complicates the task of adjusting the measured wear graph to the simulated wear graph.
- By implementing this casing wear analysis to be a part of the post-drilling work associated with MLT wells in the future, it would give a more robust statistical credibility by creating a database of wear factors used to achieve a match between the measured wear and the simulated wear.

16 Future work

There is a need to incorporate additional wells into this investigation for it to be of more value. It's time consuming work to back calculate wear factors but since there now is established a method of conducting the work, the effort of continuing with simulations on the remaining MLT wells on Grane should be reduced.

If the company that supplies the USIT log (in this case Schlumberger) and delivers the associated LAS and DLIS files required to produce the actual wear plot, use their interpretation expertise to eliminate any peaks related to tool disturbance in measurement or drill pipe connection filtration, the wear factor can be back calculated with a higher level of confidence and used as a more precise tool.

This kind of casing wear study should also be implemented at other oil fields/rigs where there is a casing wear concern and the results shared into a common/joint database.

17 References

1. Inc, P.T., *DrillNET*, 2010.
2. Haberer, J., *New Solutions may Ease Hardbanding Controversy* Drilling Contractor, 2000(September/October): p. 49.
3. Bradley, W.B. and J.E. Fontenot, *The Prediction and Control of Casing Wear (includes associated papers 6398 and 6399).* SPE Journal of Petroleum Technology, 1975. **27**(2).
4. Schoenmakers, J.M., *Casing Wear During Drilling-Simulation, Prediction, and Control.* SPE Drilling Engineering, 1987. **2**(4).
5. Engineering, M., *Casing Wear Technology Phase 5.* 2000.
6. Han Yong, J.B., Ouyang Chun, Xiao Guozhang, Tang Jiping, Zhang Bin, and Liang Hongjun, *Experiments illuminate reasons for casing wear* Oil and Gas Journal, 2010.
7. Ali Y. Garkasi, Y.X., Gefei Liu, *Casing Wear in Extended Reach and Multilateral Wells.* World Oil, 2010. **231 No. 6**.
8. Poss, G.T. and R.W. Hall Jr., *Subsea Drilling Riser Wear: A Case History*, in *SPE/IADC Drilling Conference*1995, 1995 Copyright 1995, SPE/IADC Drilling Conference: Amsterdam, Netherlands.
9. Hall, R.W., Jr., et al., *Recent Advances in Casing Wear Technology*, in *SPE/IADC Drilling Conference*1994, 1994: Dallas, Texas.
10. Engineering, M., *Casing Wear Technology, DEA-42 Phase 5.* 2000.
11. Adewuya, O.A. and S.V. Pham, *A Robust Torque and Drag Analysis Approach for Well Planning and Drillstring Design*, in *IADC/SPE Drilling Conference*1998, IADC/SPE Drilling Conference: Dallas, Texas.
12. Bol, G.M., *Effect of Mud Composition on Wear and Friction of Casing and Tool Joints.* SPE Drilling Engineering, 1986. **1**(5).
13. Mobley, J.G., *Finally, the truth about drill string hardbanding.* Drilling Contractor, 2007.
14. Mobley, J.G., *Hardbanding And Its Role in Deepwater Drilling*, in *SPE/IADC Drilling Conference*1999, Copyright 1999, SPE/IADC Drilling Conference: Amsterdam, Netherlands.
15. Eutectic, C., *<OTW 12 Brochure.pdf>*. 2011.
16. Oil Industry Association, F.o.N.M.I., *NORSOK STANDARD - Well integrity in drilling and well operations*, 2004, Standards Norway. p. 28.
17. Akpan, H.O. and S.O. Kwelle, *Efficient Computational Method for Casing String Design*, in *Nigeria Annual International Conference and Exhibition*2005, Society of Petroleum Engineers: Abuja, Nigeria.

18. Wu, J. and M. Zhang, *Casing Burst Strength After Casing Wear*, in *SPE Production Operations Symposium*2005, Society of Petroleum Engineers: Oklahoma City, Oklahoma.

19. P. Magarini, E.M., *Casing Design Manual*, 1999, Eni. p. 46-54.

20. Prentice, C.M., *"Maximum Load" Casing Design.* SPE Journal of Petroleum Technology, 1970. **22**(7).

21. Aadnøy, B., *Modern Well Design*. 2 ed2010. 240.

22. McGraw-Hill, *McGraw-Hill Dictionary of Scientific & Technical Terms* in *McGraw-Hill Dictionary of Scientific & Technical Terms*, T.M.-H. Companies, Editor 2003.

23. Newman, K., *Tubing Limits for Burst and Collapse*, 2002. p. 2-5.

24. Song, J.S., J. Bowen, and F. Klementich, *The Internal Pressure Capacity of Crescent-Shaped Wear Casing*, in *SPE/IADC Drilling Conference*1992: New Orleans, Louisiana.

25. Exprobase. *Exprobase*. 2011 [cited 2011 28.01.2011]; Available from: www.exprobase.com.

26. Chen, Y.-C., Y.-H. Lin, and J.B. Cheatham, *Tubing and Casing Buckling in Horizontal Wells (includes associated papers 21257 and 21308).* SPE Journal of Petroleum Technology, 1990. **42**(2).

27. Mitchell, R.F., *Tubing Buckling--The State of the Art.* SPE Drilling & Completion, 2008. **23**(4).

28. Menand, S., et al., *Axial Force Transfer of Buckled Drill Pipe in Deviated Wells*, in *SPE/IADC Drilling Conference and Exhibition*2009, Society of Petroleum Engineers: Amsterdam, The Netherlands.

29. Moore, N.B., P.W. Mock, and R.E. Krueger, *Reduction of Drill String Torque and Casing Wear in Extended Reach Wells Using Non-Rotating Drill Pipe Protectors*, in *SPE Western Regional Meeting*1996, 1996 Copyright 1996, Society of Petroleum Engineers, Inc.: Anchorage, Alaska.

30. Inc, W.W.T.I. *Non Rotating Protectors*. 2011 [cited 2011 31.01.2011]; Available from: http://www.wwtco.com/protectors.html.

31. Mawford, N., et al., *Beyond the Limits of Drilling and Completion-Expandables*, in *SPE/IADC Indian Drilling Technology Conference and Exhibition*2006, Society of Petroleum Engineers: Mumbai, India.

32. Storaune, A. and W.J. Winters, *Versatile Expandables Technology for Casing Repair*, in *SPE/IADC Drilling Conference*2005, SPE/IADC Drilling Conference: Amsterdam, Netherlands.

33. Bettis, F.E., et al., *Ultrasound Logging in Cased Boreholes Pipe Wear*, in *SPE Annual Technical Conference and Exhibition*1993, 1993 Copyright 1993, Society of Petroleum Engineers, Inc.: Houston, Texas.

34. Schlumberger, *USI Ultrasonic Imager Tool* 2004.

35. Schlumberger, *UBI Ultrasonic Borehole Imager* 2002.

36. Statoil/Schlumberger, *Ultrasonic Imager Log, Cement*, 2010.

37. Kuijk, R.v., et al., *A Novel Ultrasonic Cased-Hole Imager for Enhanced Cement Evaluation*, in *International Petroleum Technology Conference*2005, International Petroleum Technology Conference: Doha, Qatar.

38. Statoil/Schlumberger, *Cement evaluation from USIT, CBL/VDL for Grane*, 2009.

39. Statoil. *Grane*. 2011; Available from: http://www.statoil.com/no/OurOperations/ExplorationProd/ncs/grane/Pages/default.aspx.

40. Hydro. *Supplybåt berørte Grane-plattformen*. 2005 [cited 2011 08.07.]; Available from: http://www.hydro.com/no/Pressesenter/Nyheter/Historisk-nyhetsarkiv/2005/Mai/Supplybat-berorte-Grane-plattformen/.

41. Directorate, N.P. *The NPD's Fact-pages* 2011 [cited 2011 14.02.2011]; Available from: http://www.npd.no/engelsk/cwi/pbl/en/index.htm.

42. Williamson, J.S., *Casing Wear: The Effect of Contact Pressure.* SPE Journal of Petroleum Technology, 1981. **33**(12).

APPENDIX A – Max Case Graphs
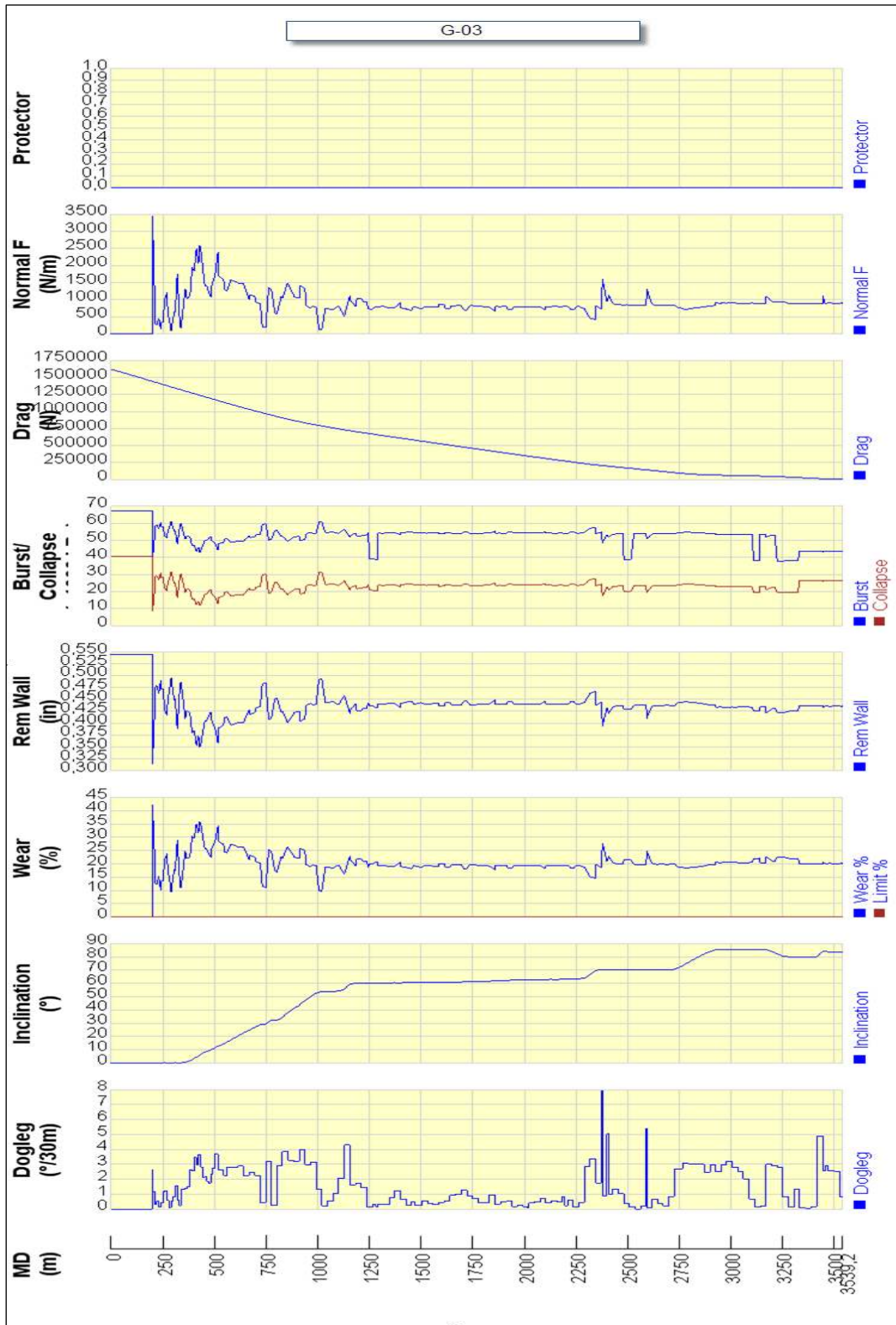
Figure 45. G-03 - Max Simulation Case Graphs
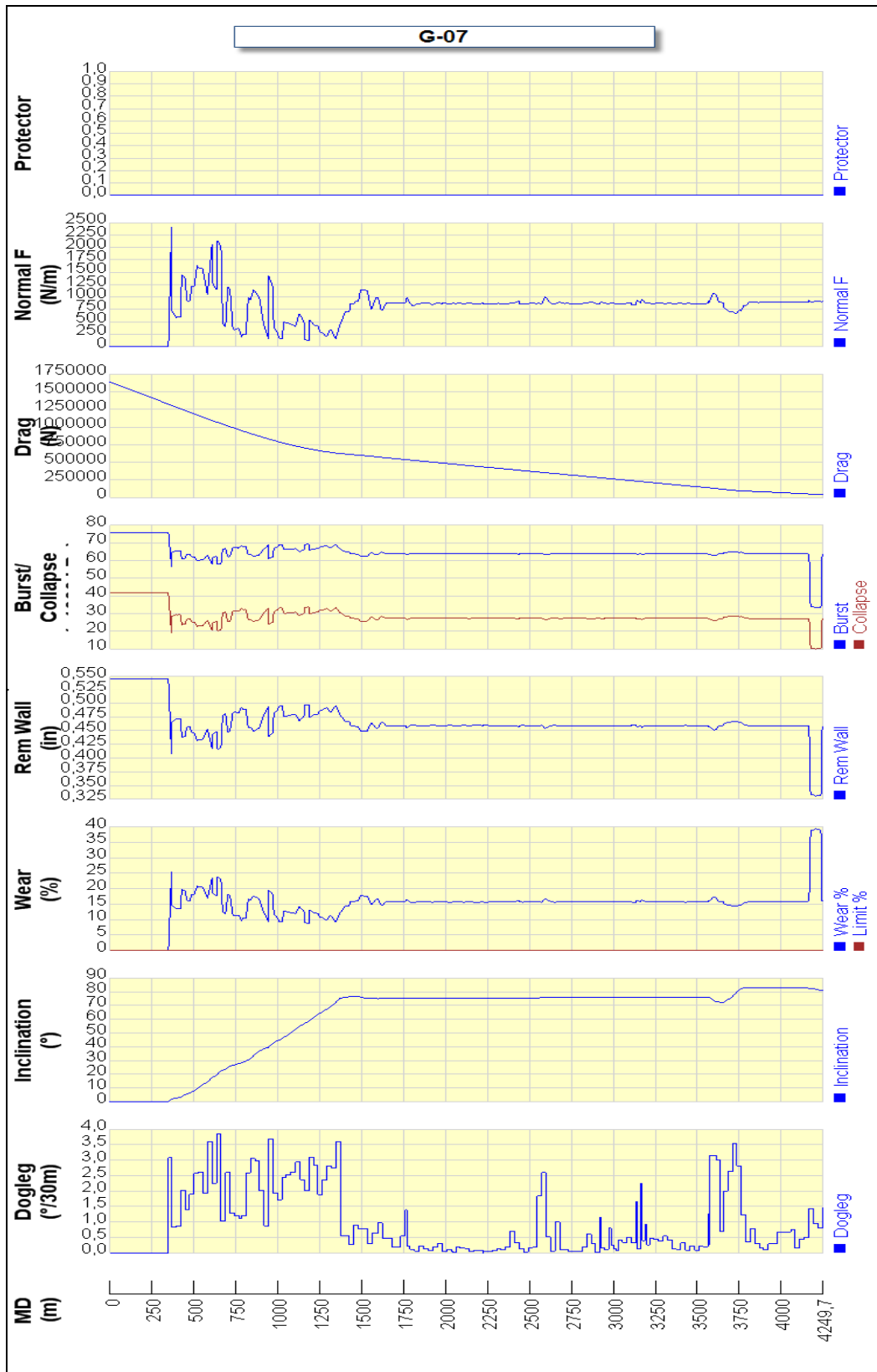
Figure 46. G-07 - Max Simulation Case Graphs
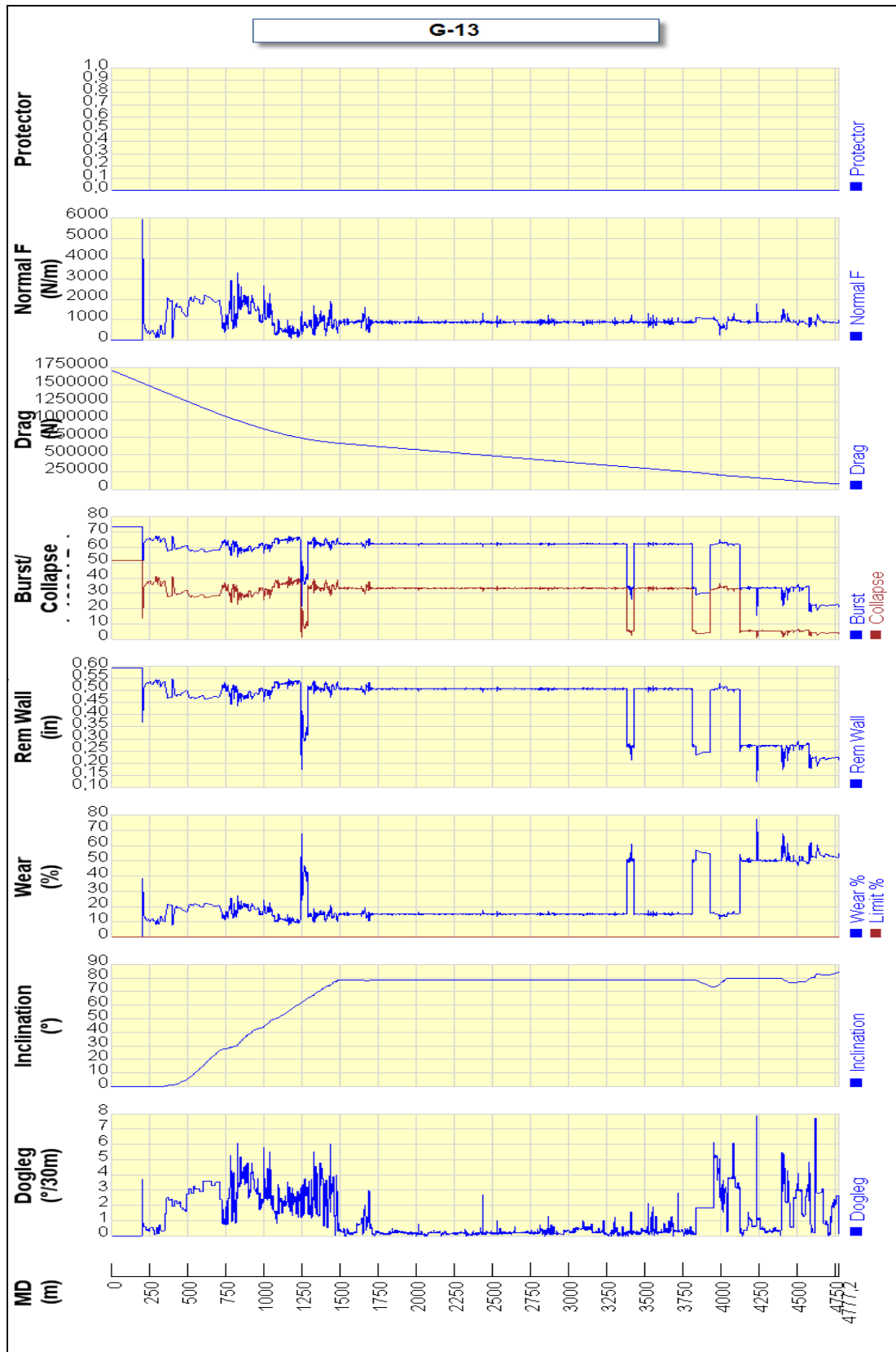
Figure 47. G-13 - Max Simulation Case Graphs
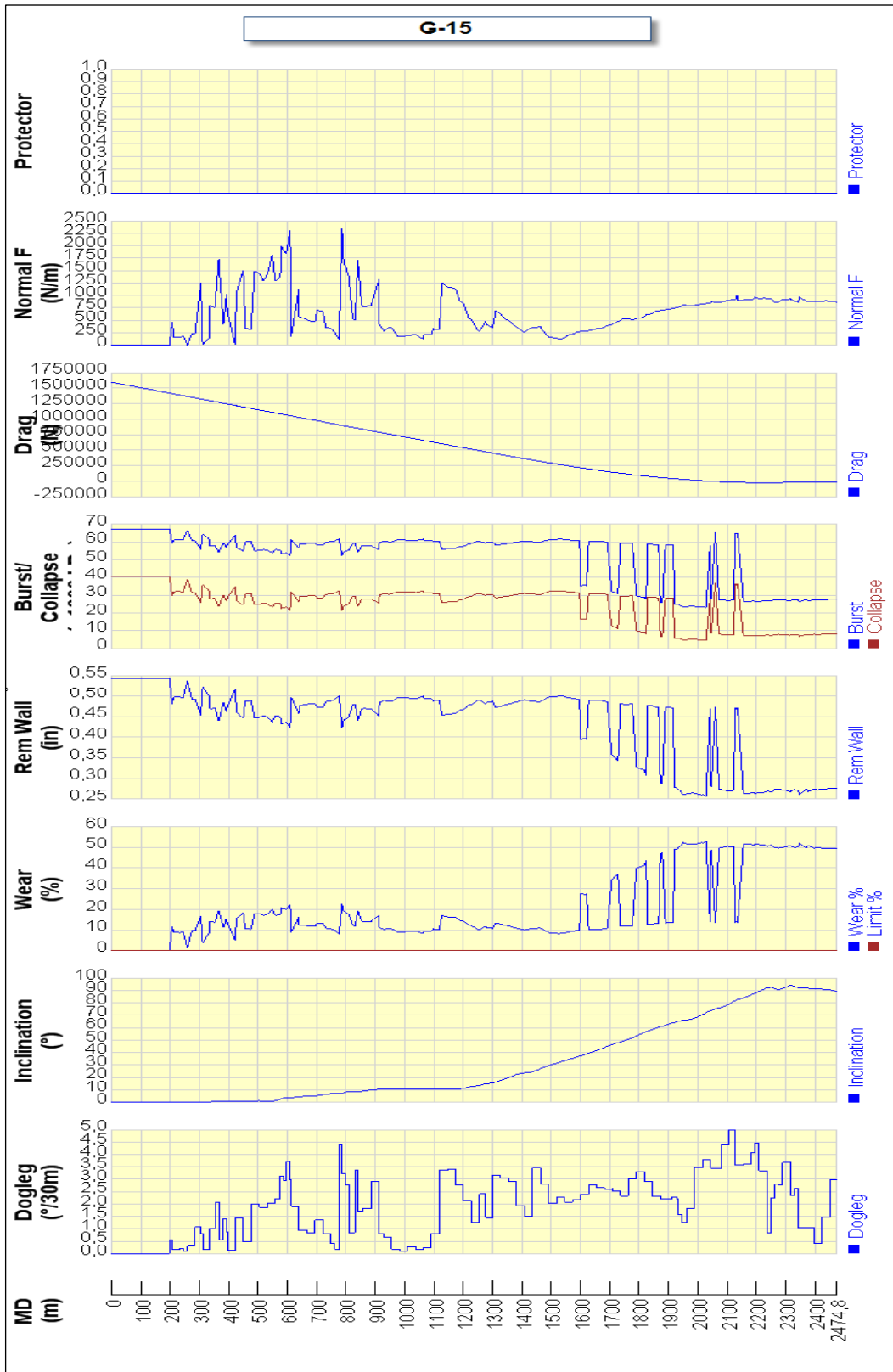
Figure 48. G-15 - Max Simulation Case Graphs
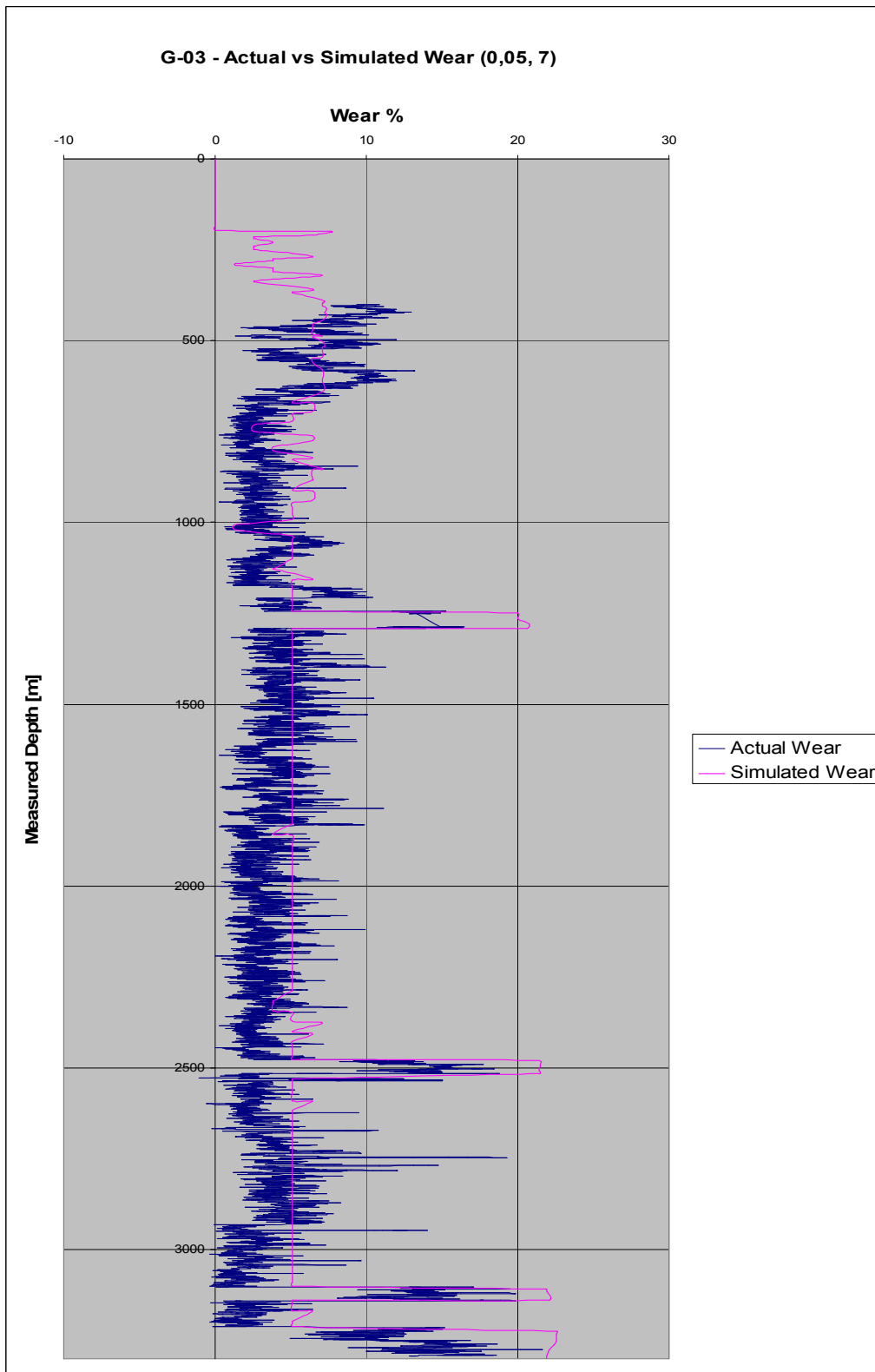
APPENDIX B – Base Case Simulation Plots
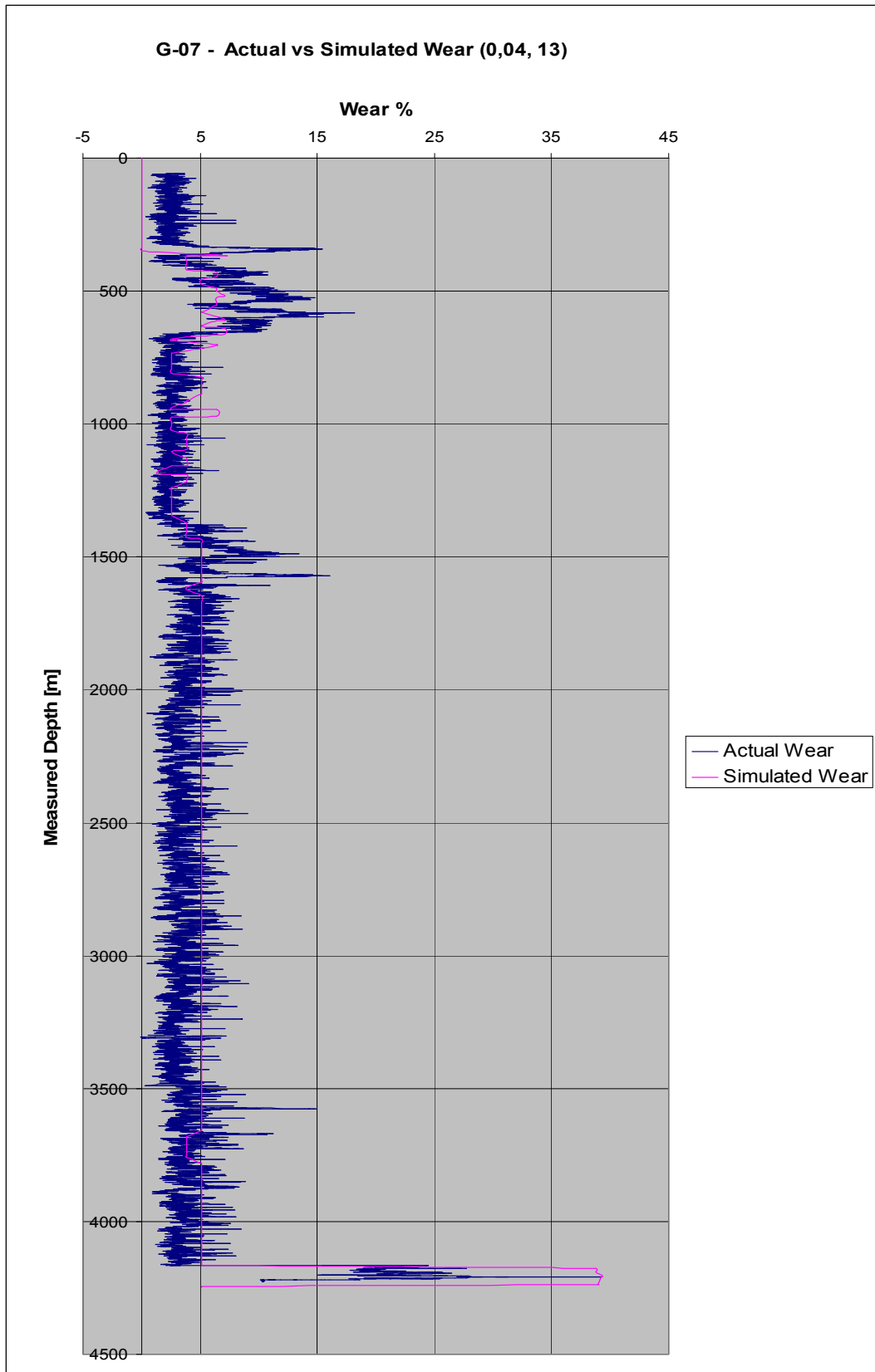

Figure 49. G-03 – Base Case Simulation Plot
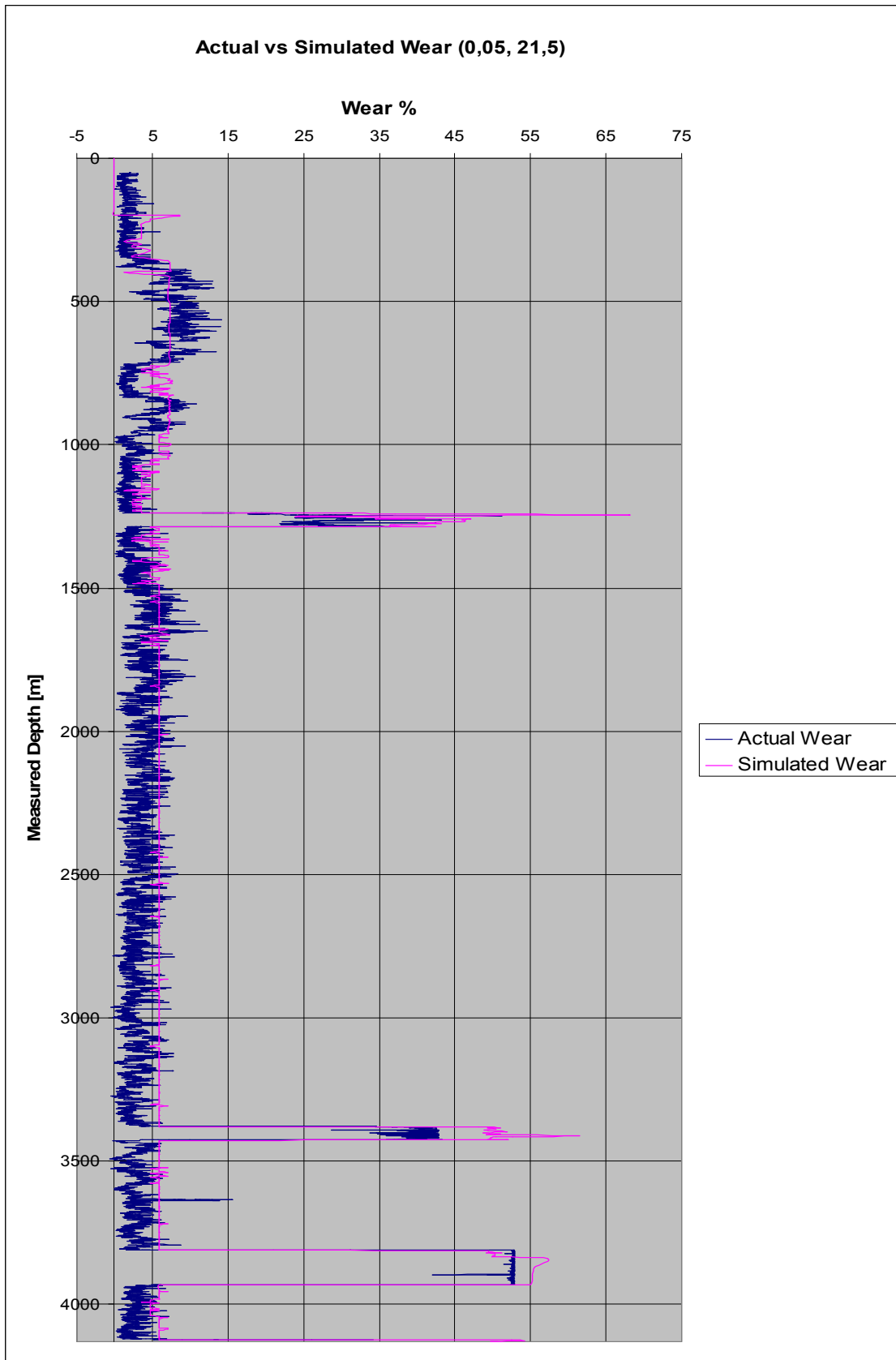
Figure 50. G-07 – Base Case Simulation Plot
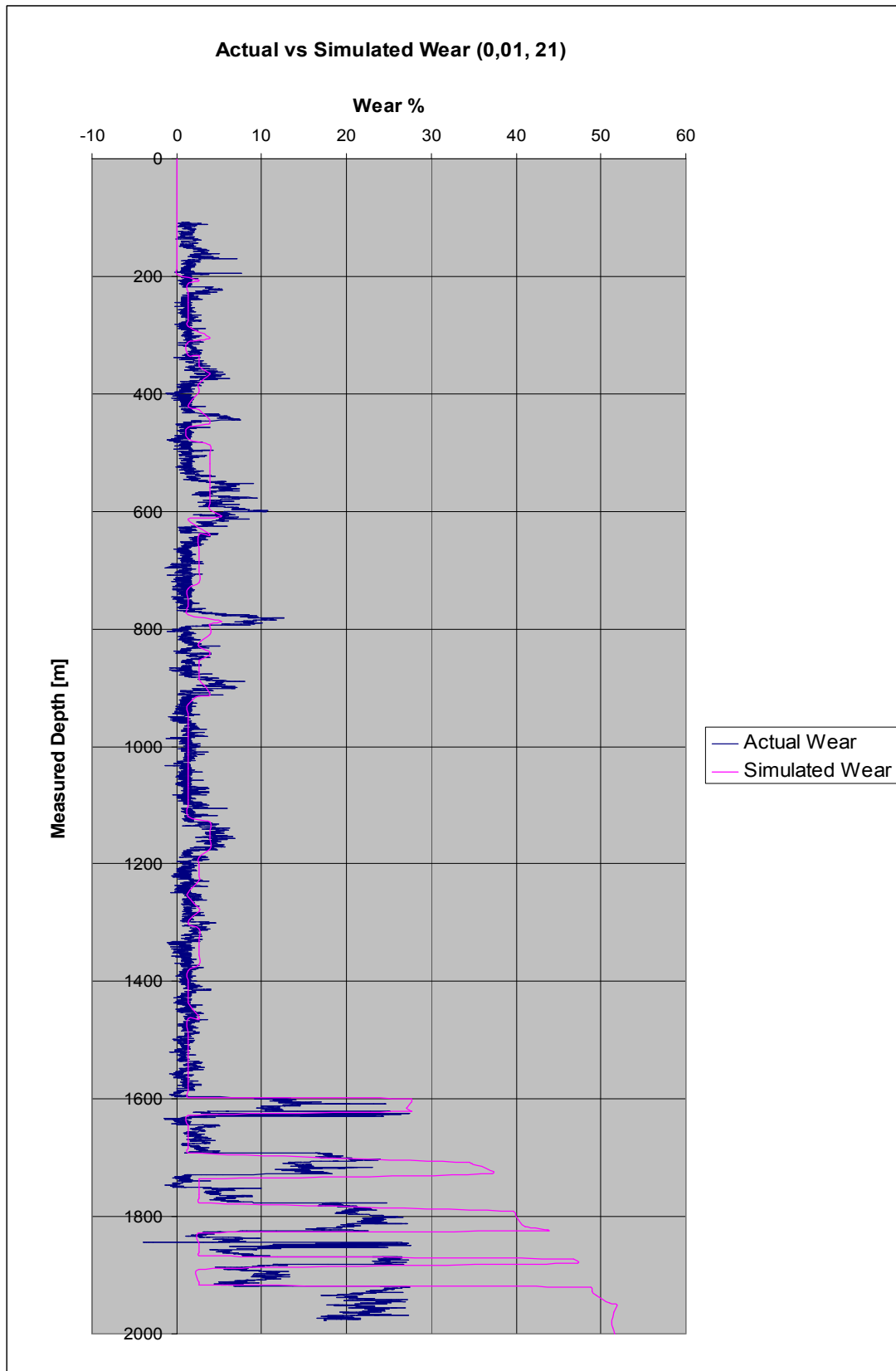
Figure 51. G-13 – Base Case Simulation Plot

Figure 52. G-15 – Base Case Simulation Plot

APPENDIX C – Dogleg Severity vs. Simulated Wear%
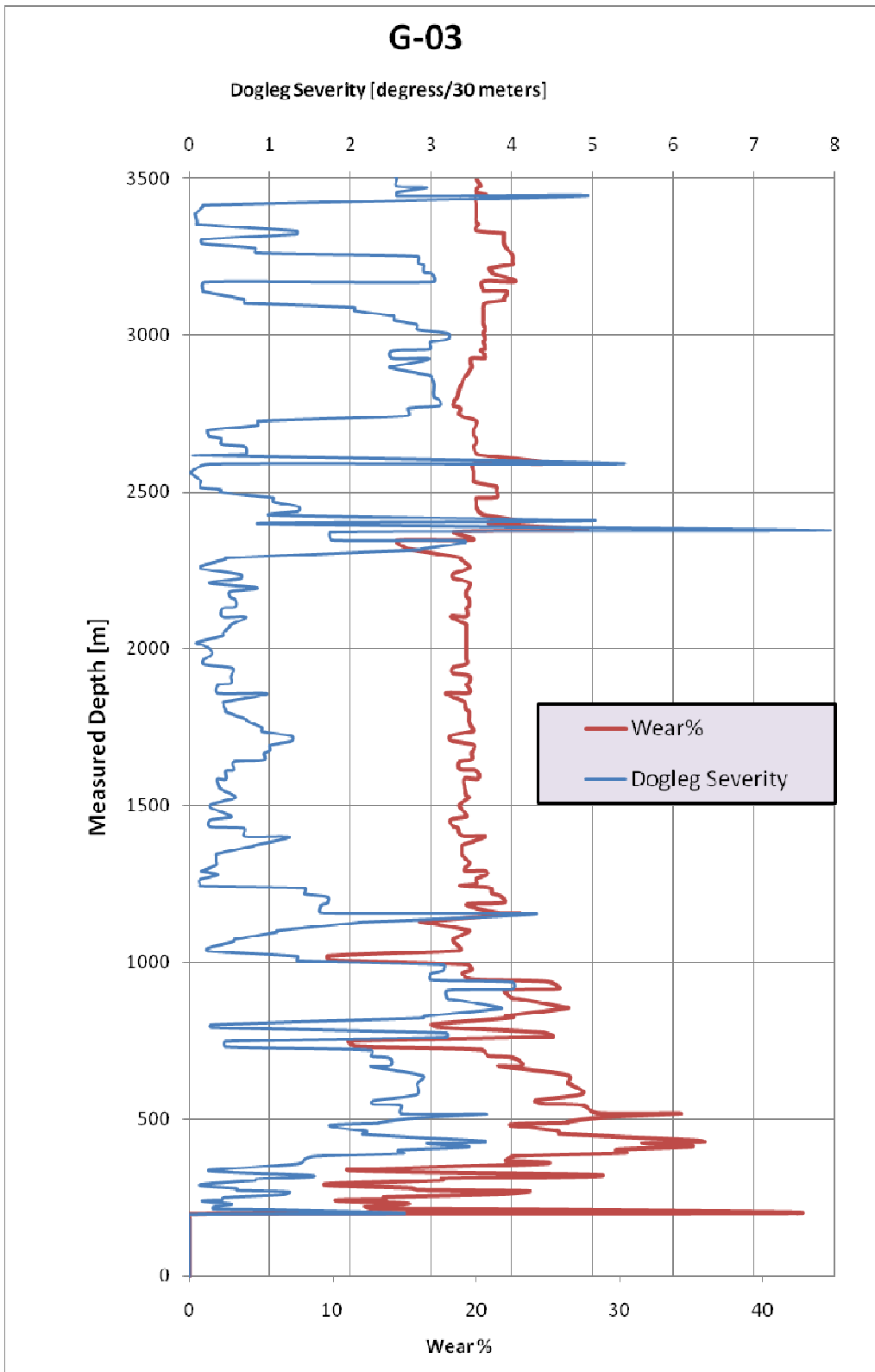
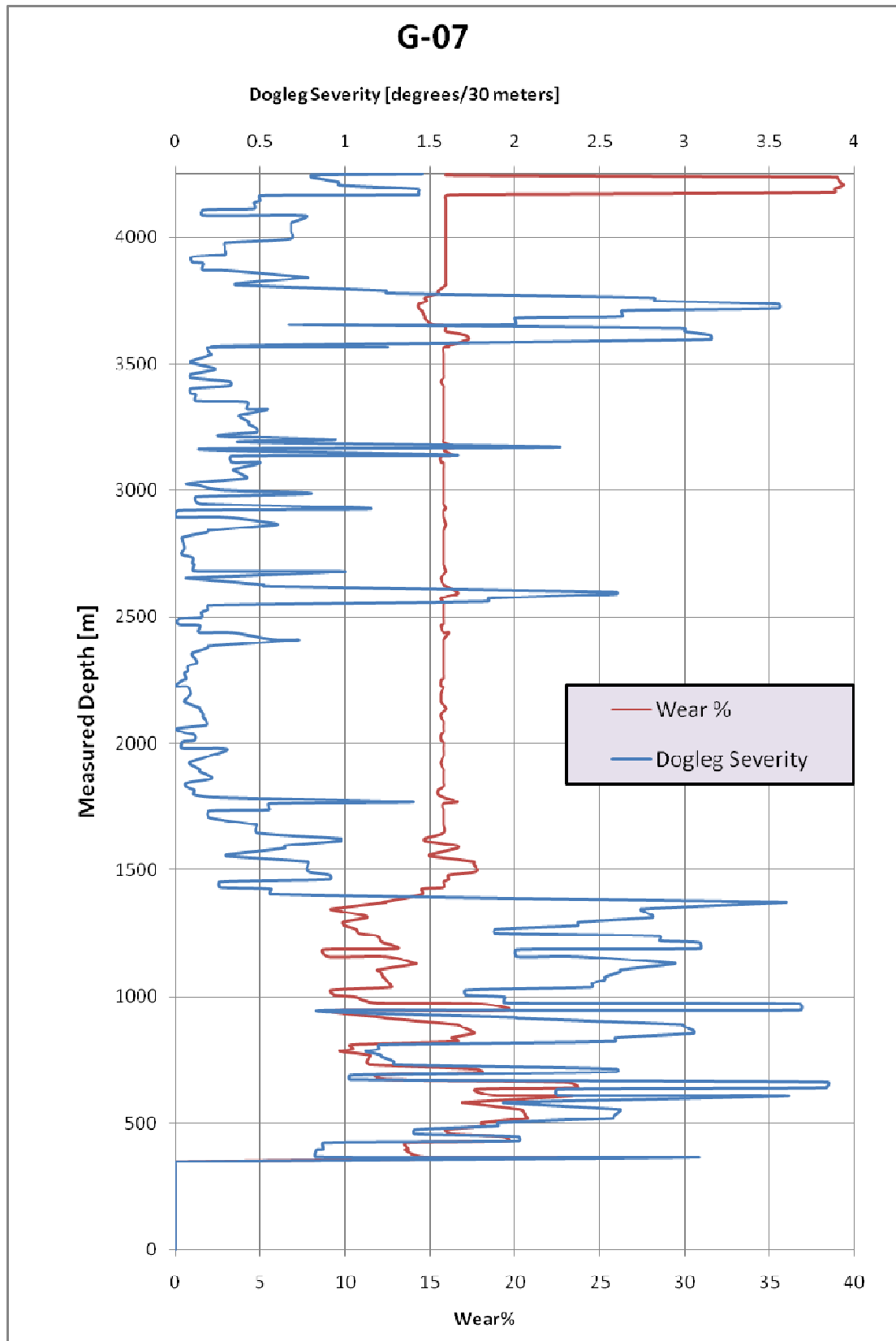
Figure 53. G-03 – Dogleg Severity and Wear% vs. Measured Depth

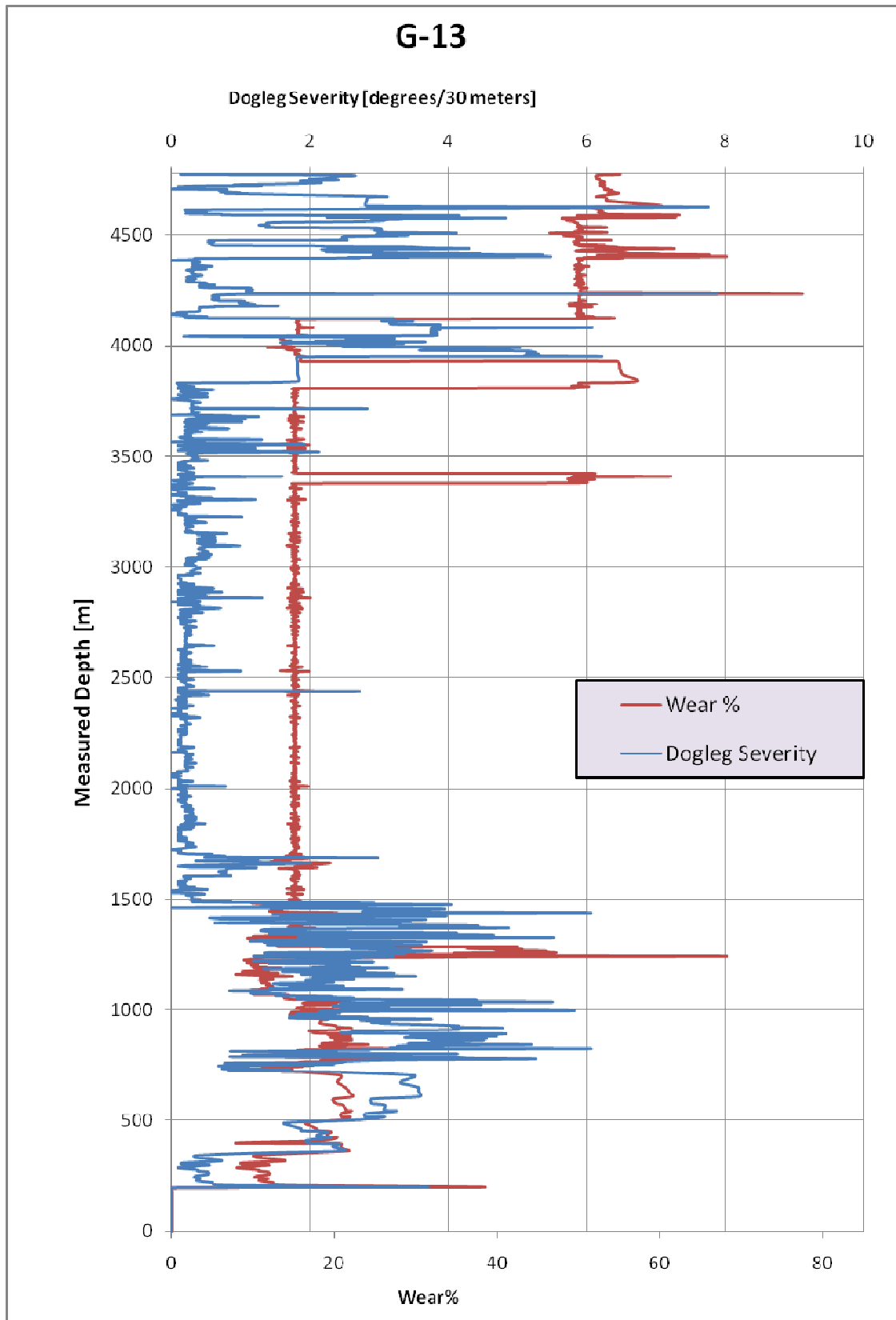**Figure 54. G-07 – Dogleg Severity and Wear% vs. Measured Depth**

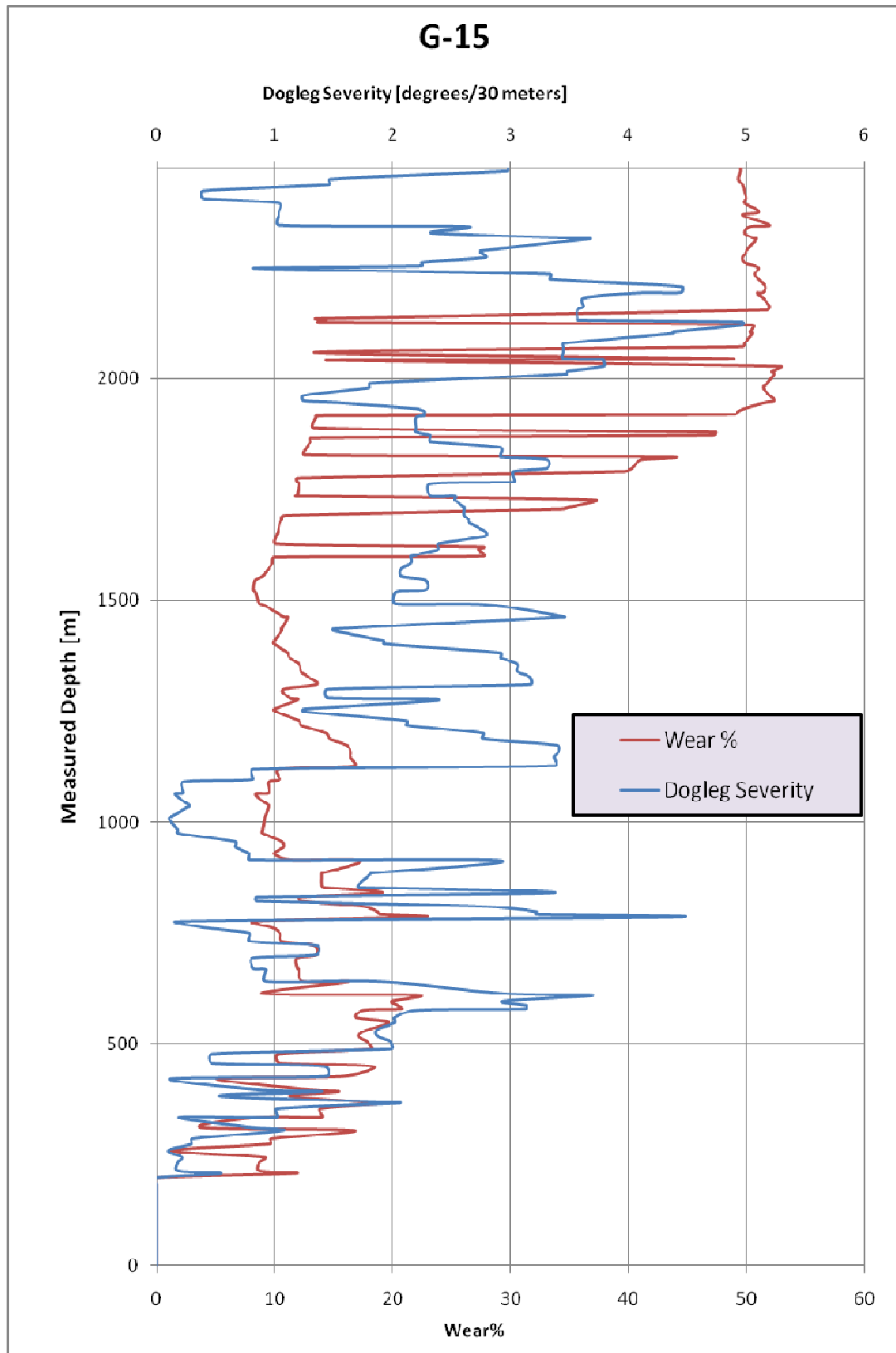**Figure 55. G-13 – Dogleg Severity and Wear% vs. Measured Depth**

Figure 56. G-15 – Dogleg Severity and Wear% vs. Measured Depth